DISSERTATIONES
TECHNOLOGIAE
UNIVERSITATIS
TARTUENSIS
89

INGRID REBANE

Structure-property relationships of moldable silicone foams

DISSERTATIONES TECHNOLOGIAE UNIVERSITATIS TARTUENSIS
89

DISSERTATIONES TECHNOLOGIAE UNIVERSITATIS TARTUENSIS
89

INGRID REBANE

Structure-property relationships of moldable silicone foams

UNIVERSITY OF TARTU
Press
1632

The doctoral studies were carried out at the Institute of Technology, Faculty of Science and Technology, University of Tartu, Estonia.

The dissertation was accepted on 29.10.2024 for the commencement of the Doctor of Philosophy degree in partial fulfillment of the requirements in Physical Engineering by the Joint Council of the Doctoral Program of Engineering and Technology at the University of Tartu.

Supervisor: **Prof. Tarmo Tamm**
Professor of Materials Engineering, Institute of Technology, Faculty of Science and Technology, University of Tartu

Co-supervisor: **Assoc. Prof. Uno Mäeorg**
Chair of Bioorganic Chemistry, Institute of Chemistry, University of Tartu

Reviewer: **Prof. Angela Ivask**
Chair of Genetics**,** Institute of Molecular and Cell Biology, Faculty of Science and Technology, University of Tartu

Opponent: **Prof. Anne Ladegaard Skov**
The Danish Polymer Centre, Department of Chemical and Biochemical Engineering, Technical University of Denmark (DTU), Kgs. Lyngby, Denmark

Commencement: Nov. 20, 2024, 13.15, Auditorium 121, Nooruse 1, Tartu.

This study was partially supported by the Estonian Research Council: Grant No. PRG1084, Grant No. 2014-2020.4.02.19-0155 (Archimedes Foundation projects LLTTI19446 “Low-pressure injection molding technology for pre-foamed non-combustible silicone foam upholstery materials” (8.05.2019−17.07.2023), and LLTTI17205 “Non-combustible mouldable silicone foams for public transportation seat upholstery” (1.03.2017−31.03.2019)).

ISSN 2228-0855 (print)
ISBN 978-9916-27-716-4 (print)

ISSN 2806-2620 (pdf)
ISBN 978-9916-27-717-1 (pdf)

University of Tartu Press
www.tyk.ee

CONTENTS

LIST OF ORIGINAL PUBLICATIONS

This dissertation is based on the following publications (I–III).

I. Kinetics of catalyzed dehydrocondensation of hydrogen functionalized siloxane
Ingrid Rebane, Uno Mäeorg, Urmas Johanson, Mihkel Ilisson, Peeter Piirimägi, and Tarmo Tamm
Journal of Applied Polymer Science ***2022***, 139 (23), 52304
DOI: 10.1002/APP.52304

My contributions to this study include conducting kinetic measurements, formal data analysis, manuscript writing, and handling the correspondence.

II. Enhanced low-density silicone foams blown by water-hydroxyl blends
Ingrid Rebane, Karl Jakob Levin, Uno Mäeorg, Urmas Johanson, Peeter Piirimägi, Tauri Tätte, and Tarmo Tamm *Polymers* ***2023***, 15 (22), 4425
DOI: 10.3390/polym15224425

I conducted the experiments, analyzed the data, performed SEM imaging, and managed the writing and correspondence of the manuscript.

(This article belongs to the Special Issue *Advances in Functional Rubber and Elastomer Composites II*)

III. Microbial growth and adhesion of *Escherichia coli* in elastomeric silicone foams with commonly used additives
Ingrid Rebane, Hans Priks, Karl Jakob Levin, Ismail Sarigül, Uno Mäeorg, Urmas Johanson, Peeter Piirimägi, Tanel Tenson, and Tarmo Tamm
Scientific Reports ***2023***, 13 (1), 8541
DOI: 10.1038/s41598-023-35239-9

I planned and conducted antimicrobial tests, prepared samples for bacterial imaging using supercritical extraction and SEM imaging, analyzed the data, wrote the manuscript, and handled the correspondence.

All articles and their contents were reproduced with permission from the co-authors and publishers, and the corresponding reference is given where necessary (e.g., [**Pub I**] or Publication I).

ACRONYMS AND SYMBOLS

^{1}H-NMR	proton NMR (nuclear magnetic resonance) spectroscopy
c[CFU]	concentration of colony forming units, CFU/mL
CBA/PBA	chemical/physical blowing agent
CFU	colony forming units
C_n	number of carbon atoms in the alkyl chain
d_{cell}	diameter of a cell as a structural unit of porous foams
d_{wall}	cell wall thickness in a cellular foam structure
DMSO	dimethyl sulfoxide
E. coli	*Escherichia coli,* a Gram-negative bacterium
E_s	Taft-Dubois steric effect parameter
f	functionality of a reactant molecule
FIM	foam injection molding
FS	fumed silica (aka pyrogenic silica)
FT-IR	Fourier-transform infrared spectroscopy
iOctOH	2-ethylhexan-1-ol (*isooctanol*)
iPrOH	2-propanol (*isopropanol*)
LB	Lysogeni Broth
LIM	liquid injection molding
logP	log of partition coefficient of a solute between octanol/water
LSR	liquid silicone rubber
MeOH	methanol
OH-PDMS	disilanol-terminated poly(dimethylsiloxane)
PBS	phosphate-buffer saline
PDMS	poly(dimethylsiloxane)
pK_a	negative log of the acid dissociation constant (K_a)
r	the ratio between two types of reactive groups
PMHS	poly(methylhydrosiloxane), hydride-functional polysiloxane
RT	room temperature
RTV	room temperature vulcanization
$scCO_2$	supercritical state of carbon dioxide
secBuOH	2-butanol
SEM/EDX	scanning electron microscopy/energy dispersive X-ray spectroscopy
SIF	silicone foam
tAmOH	2-methylbutan-2-ol *(tert-amyl alcohol*)
Vi-PDMS	vinyl-terminated poly(dimethylsiloxane), divinyl-functional
wt%	weight percentage
WCA	static water contact angle, θ_C, °(degree)
$\boldsymbol{\varepsilon_b}$	elongation at break, %
$\boldsymbol{\varepsilon_r}$	relative permittivity (dielectric constant)
$\boldsymbol{\rho_{app}}$	apparent density, weight (in air) per volume, $kg \cdot m^{-3}$
$\boldsymbol{\sigma_b}$	tensile strength, MPa

TERMINOLOGY AND TECHNICAL SPECIFICATIONS

In this dissertation:

- The term '***siloxane***' describes the repeating unit $–(R_2Si–O)_n–$ in '***polysiloxane***', which is the polymer backbone of silicone materials. Despite '***silicone***' being commonly used, 'polysiloxane' is the correct terminology for siloxane polymers and is the term used in this dissertation.
- '***SIF***', a common abbreviation for silicone foam, refers to polysiloxane-based foams; also '*SiRF*", referring to 'silicone rubber foam' is found in the literature., This dissertation uses '***silicone foam***' or '***SIF***' to ensure consistency with previous work and findings in the literature.
- The terms '***cell***' and '***cellular***' are fundamentally overlapping terms that describe the different constructs.
  - In the context of polymer(ic) foams, '***cellular***' refers to the foam's microscopic structure, while '***cell***' refers to individual voids within the foam (see *Chapter 1.2.2, Important bulk properties of SIFs* for more details).
  - In the context of microorganisms, '***cellular***' refers to the fundamental unit of life, the cell itself.

Apparent density (ρ_{app}) – relationship between the mass and unit volume of the material in natural state, including internal pores; $\rho_{app}=m\cdot V^{-1}$, [$g\cdot cm^{-3}$ or $kg\cdot m^{-3}$];

Fumed silica (**pyrogenic silica**) – synthetic amorphous silica produced via flame pyrolysis;

Specific strength – a measure of strength equivalent; material's (ultimate) tensile strength divided by the material's apparent density, also known as the strength-to-weight ratio; SI unit is $Pa\cdot m^3\cdot kg^{-1}$ or $N\cdot m\cdot kg^{-1}$.

'Mol %' is used to represent the mole percent as a concentration of a component's functional groups in a blowing blend; e.g., "10 mol% alkanol/water" corresponds to a 1:9 molar ratio of alkanol-to-water functional groups.

MarvinSketch was used for drawing, displaying, and characterizing chemical structures and reactions, Marvin version 24.1.2, ChemAxon (https://www.chemaxon.com).

ABSTRACT

Elastomeric silicone foams are cellular polymeric composites created by expanding and crosslinking a polysiloxane framework. Polysiloxanes serve as reliable precursors with a wide range of functionalities and polymerization degrees, facilitating the development of injection-moldable formulas for large-scale industrial applications and, moreover, for producing foams with cushioning properties. Silicone foams and polysiloxanes, in general, offer benefits such as compliance with safety standards and a degree of inherent fire retardancy. There is an ongoing focus on designing silicone foams with densities below 100 $kg \cdot m^{-3}$ for their use in automotive and aviation applications. Maintaining the physical and mechanical properties of elastomeric foams at relatively low apparent densities offers another challenge. Adjusting the blowing process in a crosslinking polymer blend can significantly affect the final physical and mechanical properties of the foam. For this, it is crucial to balance the parallel catalytically activated hydrosilylation and dehydrocondensation reactions in a multicomponent composite blend, as it significantly affects the injectability of the mixture, network formation during foam expansion, and its final cellular structure. However, achieving a homogeneous cellular structure and enhanced mechanical properties simultaneously is less controllable than reinforcing a polymer matrix with fillers and additives. Utilizing the chemistry of polysiloxane elastomers, we show that inherent gas generation combined with cross-linkable blowing blends alone met the reproducibility requirements for controlled elastomeric foam formation. Water, mono- and dialcohols, and glycerol were applied as affordable and sustainable industrial reagents, focusing on their application as simultaneous gas-generating and crosslinking agents, individually and as blends. In a balanced reactive polymer system, these combinations allowed successful tuning of the structure and mechanical properties of the foams, indicating that such alkanol-water blends can be used as cell size adjusters whilst expanding the foams and with improvements in the specific strength of the foams. Additionally, the elastic and open-cellular nature of silicone foams as wound dressings, orthotic supports, seat cushioning, or mattresses would benefit from antimicrobial activity throughout the polymer scaffold. The inclusion of additives to the foam formulation showed that the majority of these particles remain covered by the elastomer layer, thereby limiting their contact with microorganisms. The antimicrobial characteristics of polysiloxane composites, in the case of *Escherichia coli,* are significantly dependent on the elastomer's surface properties and minimally by the addition of additives. However, the porous nature of the silicone elastomer and the foam itself promotes the dissolution of antimicrobials in water-rich environments, which redirects the research towards polymer grafting and soluble additives rather than relying on particulate additives.

Keywords: silicone foams, blowing agents, alcoholysis, crosslinked polymers, low-density composites, Pt catalyst, chemical blowing, bacterial adhesion

INTRODUCTION

Polymer foams can be fabricated using various materials, including synthetic polymers and materials derived from renewable sources. This variety allows for a wide range of properties and functions, which can be tailored to specific needs. Synthetic polymers have significantly advanced the development of processes for addressing complex design challenges. This has also enabled improvements in the performance of cushioning foams, partly due to the lower foam densities and an open-cellular structure. These specialized structures are characterized by polymeric scaffolds with gas-filled cellular voids predominantly filled with air from the surrounding environment. Combined with elasticity, these structures, such as foams, sponges, and membranes, can be used in diverse applications, primarily for vibration dampening and insulation, as structural and cushioning materials for automotive and medical applications.

Selecting polymers with good flexural properties is crucial for higher absorption of mechanical vibrations and impacts, owing to the high elasticity of the resulting material. Additionally, the choice of polymer is fundamental for sufficient fire retardancy, which is particularly important in applications such as transportation and has become a standard safety requirement in recent years [1]. These properties are characteristic of **polysiloxanes**, which are commonly referred to as **silicones**. Polysiloxanes are well-known for their high-temperature resilience, inherent fire-retardant properties, and other beneficial qualities that can mitigate fire-related risks and promote their use in elastomeric foam synthesis as the core polymer [2]. Polysiloxanes possess unique properties that set them apart from other polymers. Ongoing research is expanding their potential applications, focusing on advancements in waste reduction and recycling. Additionally, efforts are being made to enhance their surface properties to prevent degradation in material performance due to biocontamination and the potential spread of infections.

There are **two significant challenges in making polysiloxane-based foams**, that is, **silicone foams** (**SIFs**) viable. First, by lowering the density of the foam, which also decreases consumption (and cost) of polysiloxanes, and second, by enhancing its physical and mechanical properties. The physical and mechanical properties, one tied to another, are significant for the foam to provide cushioning and support, even as a thin layer at low densities. Adopting injection foam molding (FIM) as a routine method to manufacture polymeric products offers both economic and environmental benefits. However, it is still a challenge to consistently obtain uniform foam structures at low densities. Inhomogeneity in cellular structure is a common reason why foams are typically produced as continuous rolls or buns. The proper timing of the nucleation and evolution of gas and the simultaneous crosslinking during foam expansion are the defining processes in cellular structure formation [3]. Consistency in physicomechanical properties necessitates a homogeneous distribution of bubble nucleation sites in the polymer blend.

Additionally, polysiloxane-based cellular materials are subject to microbial contamination in applications such as cushioning in seats and mattresses or as wound dressings [4], [5], prostheses [6], [7], and even medicinal patches. Considering the nature of these applications, contact with body tissues and fluids, food, and liquids is highly probable. It is very common for these materials to have a certain degree of porosity to provide sufficient cushioning and support via facilitated airflow. This also means that fluids can permeate the surface layer and travel into and out of the material. Although the covers on seats or mattresses are often antibacterially treated, they are still permeable to air and atmospheric humidity. As a result of dynamic compression, the liquids carrying microorganisms eventually permeate these breathable materials and reach the inner layers of the polymeric foam.

Under suitable conditions, microorganisms, bacteria, and fungi adhere to these polymeric surfaces and multiply, often producing an unpleasant smell and degrading the material's aesthetic and functional properties [8]. The adhesion of microorganisms and the following biofilm formation also increase the likelihood of infections and pathogen transmission, which is a significant concern [9]. Therefore, understanding how microbial adhesion and biofilm formation occur on polysiloxane materials (or, in general, polymeric materials) is crucial, regardless of their intended use.

Combining these challenges, the ultimate **purpose of this research** was to evaluate the structure-property relationships of the synthesized SIFs. A significant part of the discussion is **dedicated to gas evolution kinetics and its effect on foam formation, specifically on the structural and mechanical properties of the foam.** The use of water, alcohols, and their blends is an environmentally friendly approach, with the only byproduct being hydrogen gas. Introducing these blends at different molar compositions alters the foam formation kinetics, providing a basis for further exploration and foam structure enhancement. The potential applications of elastic SIFs have sparked interest in studying how bacteria interact with foams with and without fillers and additives. **Part of the study aimed to understand whether microorganisms** adhere to and grow within porous elastomeric foams to simulate application-related contamination.

1 BACKGROUND AND CHALLENGES

1.1 Polymer foams for cushioning applications

Cushioning materials are expected to provide support as well as comfort while also being able to restore their original shape and remain resilient under repetitive use. In particular, for bedding and furniture, these foams are designed to be flexible, open-celled, and preferably have a low apparent density (≤ 250 kg·m^{-3}) [10, p. 8]. The selection of the base polymer plays a significant role in the elasticity and resiliency of the final foam, particularly when a foam with flexural properties in the low-density region is desired [11]. The inherent properties of the polymer are the primary factors determining the foam's elasticity rather than the foam's structure, which mainly affects its compressibility. On the other hand, the structure of the foam – how its cells are arranged and interconnected – plays a more significant role in determining how compressible the foam is [12]. As Bernard E. Obi has stated in breve, "Foam's elastic modulus or stiffness is a function of the base polymer modulus and the ratio of the foam to solid polymer densities." [10, p. 375]. Hence, the cushioning abilities of the foam can be altered by adjusting its density.

Elastomers are highly versatile materials for producing polymeric foams that exhibit high deformability under stress. Their low elastic moduli make them well-suited for applications involving repeated compression without compromising their integrity while maintaining a relatively soft nature. The ability to recover their original shape after compression, facilitated by the mobility of their long polymer chains and the formation of crosslinks between the chains, is also advantageous for reducing apparent density during foam expansion and crosslinking, thereby preventing material rupture. Utilizing thermoset polymers as elastomers offers the added benefit of enabling these lightweight porous structures to form and set quickly [13].

Elastomers based on synthetic polymers started to replace heavy natural rubber (latex) when better control over their synthesis was achieved and advanced to an industrial level during the 1940s–1950s [10, p. 19]. Polyurethane (PU or PUR) currently constitutes most of the polymeric foams produced [10]. Although PUR foams can be synthesized with superior physical and structural properties at ultralow densities ($<<100$ kg·m^{-3}), their inherent flammability and fast flame spread in the case of fire have challenged scientists to find a balance between fire retardants, environmental concerns, and affected mechanical properties [14], [15]. Collateral emissions of toxic gases are the leading cause of death in fire incidents [1]. Therefore, the synthesis of an inherently nonflammable PUR or finding an appropriate fire retardant continues to be a significant scientific ordeal [15]. Polyurethane-based foams are utilized not only in bedding and furnishings but also as automotive cushions. The purpose of fire safety standards, e.g., EN 45545-2 and the related tests (UL-94), is to minimize the impact of heat, smoke, and toxic gases from a fire on passengers and staff [1], [16], [17], [18]. In

addition to the general industry standards, all polymeric foams must meet or exceed requirements specific to the automotive, aviation, and rail industries [19]. Owing to the growing population and the use of polymeric foams in everyday items, such as mattresses, soft furniture, seats in theatres, and public transportation, the safety of these materials is more important than ever. Although meeting the safety requirements may seem challenging, some polymers possess many intrinsically favorable properties for elastic foam production. Polysiloxanes have these properties, therefore being excellent base materials for those applications.

The following subsections provide an overview of **polysiloxanes** and **SIFs** and the main characteristics that favor their use in polymer foam composition.

1.2 Silicone foams (SIFs)

1.2.1 Polysiloxanes as the core of elastomeric SIFs

Polysiloxanes are a one-of-a-kind superstar among synthetic polymers. With the general formula $R_3Si(OSiR_2)_nOSiR_3$ (where R is an organic group), polysiloxanes were discovered in Dow Corning during the rise of synthetic rubber in the 1940s [20]. Due to misconceptions about nomenclature, the term 'silicone' has remained in everyday use, referring to a broad range of polymers containing a silicon-oxygen backbone. Polysiloxanes are known for their unique properties, such as thermal stability, low chemical reactivity, and low toxicity, making them a material of interest for research and industrial applications [20]. Their application as core polymers in elastic foam structures has many advantages owing to the physicochemical properties of the siloxane (Si–O) bonds (**Figure 1**).

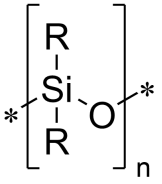

Figure 1. General structure of a Si–O repetitive unit in polysiloxane backbone, where R=H, alkyl, or aryl group.

The structural flexibility of the siloxane backbone is attributed to the large Si–O–Si bond angle, which allows the rotation of the organic groups attached to the silicon atom [21]. Flexible polymer chains enhance the elasticity of the material in the crosslinked state. The long and entangled chains allow this material to recover its initial state after straining during compression (in real-life examples, seats and mattresses [22], [23]), making the material more resilient to repetitive use. Maintaining a material's elasticity over a wide temperature range is especially important in applications where a severe fluctuation in temperature occurs, such as in vehicles in colder climates or materials facing direct sunlight for an

extended duration. This is favored by the low glass transition temperature T_g (–120 °C, [24]) of polysiloxanes. The fairly low liquid surface tension (20.4 $mN \cdot m^{-1}$ [25], 21.3 $mN \cdot m^{-1}$ for PDMS at 20 °C [26]) and critical surface tension of wetting (24 $mN \cdot m^{-1}$) result from siloxane molecule flexibility as well. The methyl groups contribute to moderate hydrophobicity, which is advantageous for cushioning applications because it prevents moisture accumulation in the porous material. However, polysiloxane membranes are reported to be highly permeable to water vapor [27]. Furthermore, polysiloxanes possess only slight temperature dependence on their physical properties. A very high Si–O bond dissociation energy (460 $kJ \cdot mol^{-1}$) results in high thermal stability of polysiloxanes with temperatures ranging from –50 °C to +200 °C, whereas the thermal degradation of polysiloxanes in the presence of oxygen starts near 325 °C [21], [24], [28]. The chemically inert nature of PDMS or crosslinked polysiloxanes is attributed to the electron pairs around oxygen being spatially diffuse and not readily served for electron donation [20]. The Si–O bond provides not only greater thermal and chemical stability but also resistance to oxidative processes and UV light compared to organic polymers [20].

One of the most significant advantages of using polysiloxane for designing new materials is the highly polar covalent nature of the Si–O bond, which makes it possible to functionalize the siloxane chain, providing a variety of reactive polysiloxanes with controlled molecular weights [20], [21].

1.2.2 SIFs as cushioning materials

After decades of research, SIFs are increasingly gaining attention as their use as insulation, vibration dampening, and cushioning materials [29], [30], [31], [32]. The unique molecular structure of siloxanes drives continuous innovation because of their direct relationship with properties that cannot be found in other polymer classes [33]. Inevitably, producing SIFs is more expensive than producing polyurethane foams because of the relatively high cost of precursors [34]. Focusing on decreasing the content of reactive polymers and modifying the composition with low-cost fillers but also aiming for recyclability supports the goal of introducing polysiloxanes among competitive polymers and, thus, products. However, owing to the complexity of the synthesis process and historical-economic reasons, it has taken much longer to compete with other common polymers. Although polysiloxanes became commercial materials after the 1940s [35], the production of foams began in the 1970s when Lee *et al.* from Dow Corning introduced the first flexible polysiloxane RTV foam [36], [37]. Since then, different synthesis methods, catalytic mechanisms, and improvements in mechanical properties have been reported.

SIFs possess far better properties than commonly used foams [34] and, most importantly, higher resilience to mechanical load and vibration-dampening properties than PUR foams [38]. They have higher resilience to weather, UV [24], and ozone [25] and higher chemical stability [38]. SIFs have been shown to be safe for humans and the environment, and possibilities for reusing them as a filler

and recycling (SiO_2, CO_2, and H_2O produced during combustion) are constantly sought [25]. There are numerous advancements in the research on the recyclability of crosslinked polysiloxanes. As this is an extensive and fast-developing field, these advancements are not discussed in the context of this dissertation.

1.2.3 Important bulk properties of SIFs

It is well known that the mechanical behavior of foam is significantly influenced by its structural geometry, the relative density (ratio of foam density to base material density), and the inherent properties of the base material itself. The foam structure is the result of the combined behavior of polymer blends during and after the blowing process.

1.2.3.1 Structural properties

Polymeric foams, in general, consist of a solid part – a polymeric scaffold – and voids, usually termed cells, containing a gaseous phase. The three primary parameters that describe cell structure are cell size (defined as $d_{cell,}$ the diameter of a cellular void of the porous architecture), cell density, and expansion ratio [39]. Based on d_{cell} average values, the fabricated foams are considered nanocellular (0.1–100 nm), ultramicrocellular (0.1–1 μm), microcellular (1–100 μm), and macrocellular foams (>100 μm) [39], [40]. Supported air flow through open-celled and porous structures enhances its fast deformation and recovery, increasing and maintaining the material's cushioning effect. Closed-cell structures, often referred to as sponges, are used as gaskets (mechanical shock absorbers), insulators, and joint sealants, mainly due to their low temperature- and gas-exchange properties [41]. Highly periodic structures are challenging to achieve in chemical foaming; therefore, stochastic architectures are commonly reported (**Figure 2**).

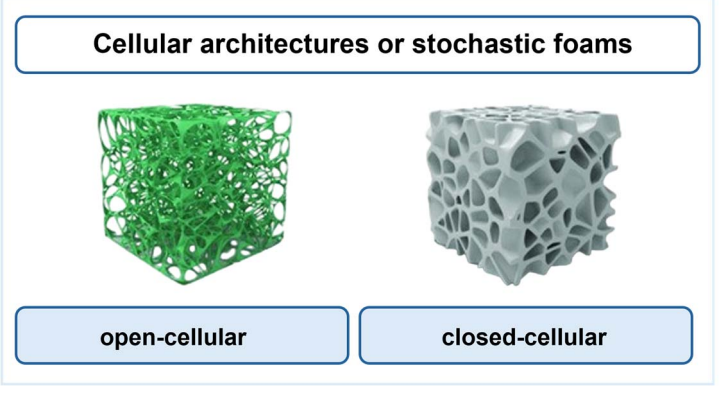

Figure 2. Classification of lightweight cellular materials with irregular pores. 3D structures reproduced from [42], ©2018 WILEY-VCH Verlag GmbH & Co. KGaA, Weinheim.

During the gas evolution and expansion, the cellular wall material is drained to a certain extent until solidification, potentially leading to a decrease in cell wall thickness d_{wall}, increasing the probability of low-density open-cellular structures. Rapid cell growth during blowing can also lead to premature bubble coalescence [40]. To withstand constant loading and unloading, open-cell foams are preferred. Closed cells deform over time under load, leading to softening of the cushioning foam in seatings and bedding mattresses. [10, p. 377]. The mechanical properties of open-cell structures depend on the elastomer composite's strength and flexural properties, as well as the structural characteristics of the elastomeric foam.

1.2.3.2 Apparent density

Whether the polymeric foams will be used for insulation, bedding, seat cushioning, or medical applications, the apparent density (ρ_{app}) is one of the most defining parameters for the material's applicability. The transportation industry generally expects these foams to remain in a low-density region below 250 $kg \cdot m^{-3}$, preferably <100 $kg \cdot m^{-3}$. According to one of the largest SIF cushion producers, the ρ_{app} of seat cushion foams used in aviation is expected to be even lower, 75–80 $kg \cdot m^{-3}$ [43]. For more specific applications, usually, less emphasis is placed on density, and more attention is given to adjusting porosity, d_{cell}, and cell density. For example, lowering ρ_{app} accompanied by a decrease in average d_{cell} (from 485 μm to 185 μm) and an increase in porosity has been shown to improve the thermal insulation properties of SIFs [44].

1.2.3.3 Elasticity and cushioning effect

In order to achieve effective cushioning, it's important to improve or maintain the elastic properties of the polymer scaffold, especially when fillers are used, which could compromise the elastomer's mechanical properties. In cushioning applications, a balance between stiffness (elastic modulus) and toughness (resistance to fracture) is crucial. For this, a variety of polysiloxanes with different functionalities, molecular weights, and crosslinking degrees can be used to enhance the overall elasticity of foamed materials. While a certain degree of stiffness is important to withstand vibration and compression forces, an excessively high modulus can make the foam less deformable and more likely to fracture when subjected to stress. Therefore, maintaining softness, as indicated by the elastic modulus [10, p. 375], is necessary to improve the resilience and cushioning effect of polysiloxane-based foams. According to Obi, achieving adequate softness and comfort for seat cushioning applications is possible when the strain (under average load) falls in the plateau region of the material's stress-strain modulus [10, p. 377]. Foam stiffness or softness can also be adjusted by changing the foam density. For the same elastomer composition, open-celled foams have lower elastic modulus than the respective closed-cell structures [10, p. 375], [42].

1.2.3.4 Fire-retardancy of SIFs

As an alternative material for cushioning, polysiloxanes correspond to the materials' fire-safety requirements used in passenger trains (BS 6853:1999) [45, p. 685]. Lee *et al.* found that the choice of catalysts has a profound effect on the SIF integrity under extreme conditions, avoiding chain-scission of the backbone; therefore, Pt-catalyzed crosslinked network has an enhanced flame retardancy [36], [37]. Typically, this applies to RTV polysiloxanes, room-temperature curable formulations catalyzed via Pt complexes [38]. The inherent flame retardancy of Pt-catalyzed polysiloxane elastomers can be enhanced by introducing a variety of additives that improve barrier properties or by modifying the polymer backbone with specific functional groups that increase thermal degradation temperatures [38], [46]. Fire tests have indicated that these elastomers produce fewer volatile and toxic substances compared to PURs, with only carbon monoxide (CO) and carbon dioxide (CO_2) [28], [28, p. 559], solid SiO_2 and water formed [33]. Additionally, emitting almost negligible concentrations of smoke in the flame [2]. As a fundamental construct of polysiloxanes, the Si–O bond provides an advantage over organic polymers due to its chemical stability and the numerous substitution possibilities on the siloxane chain. The attributed inherent flame retardancy, the formation of isolating layers, and relatively safe degradation products give polysiloxanes a considerable advantage over other commercially used synthetic polymers.

The bulk properties of SIFs mentioned above can be moderately tuned by making modifications in the elastomer composition as well as in the polymer blowing method. The following sections give a constructive overview of SIF fabrication processes and blowing techniques.

1.3 Fabrication of SIFs

One of the most intriguing and challenging tasks is to synthesize an elastomeric foam that is simultaneously low in density and structurally consistent. There are two distinctive parallel processes during the foam expansion – the crosslinking of polymers, which creates an elastomeric network, and the gas evolution and expansion, which creates a porous structure in the gradually crosslinking polymer blend. Control over crosslinking and, therefore, the consolidation of cellular structure is found to be the most crucial factor in enhancing the mechanical properties of engineered foams [47]. Without a doubt, the polymer blend has a profound effect on the elastomer itself and the foam's final properties and performance. But so does the blowing of that blend – selecting a suitable blowing technique will affect the apparent density ρ_{app} and the structural characteristics of the foam, which all determine its cushioning properties [28, p. 542].

In the following sections, conventional SIF fabrication processes and blowing techniques are discussed, narrowing down to the specific method of blowing, which will be at the center of the dissertation.

1.3.1 General fabrication principles and processes

Polysiloxane blends undergo several chemical reactions depending on the curing system and the selected blowing method. The curing system involved usually defines the fabrication process since the polymer blend must be able to expand and solidify during the one-step manufacturing process. Although there are considerable advancements and novelty in polymer product manufacturing (e.g., additive manufacturing or using expandable spheres), the production of SIFs in bulk volumes is still reasonable using processes that allow a continuous fabrication of materials in high volumes. The most common high-volume production processes, extrusion and liquid injection molding (LIM), are designed for different crosslinking chemistry [34], [48]. The well-known extrusion process applies high-consistency rubber (HCR, polysiloxanes of high M_w) in a heat-activated radical-initiated curing reaction (HTV) in which ethylene bridges are formed between polysiloxane chains [49]. The extrusion process, where the parts produced are determined by the extruder die, results in medium- or high-density gaskets or sheets with limited thickness due to the limited uniform expansion or die dimensions [50].

The **LIM** process is an industrially feasible approach for SIF fabrication, as it allows thorough mixing and rapid distribution of the polymer blend, following its free flow and expansion in the mold, thereby minimizing waste. The LIM process uses a metered mechanical mixing and pressurized dispensing to combine predefined liquid silicone rubber (LSR) blends, commonly referred to as parts A and B. The composite blends are cured through Pt-catalyzed crosslinking reactions, which are well-controllable and rapid and result in a reliably crosslinked network at RT (RTV formulations). The addition of reinforcing and inert fillers increases the viscosity of the moldable blend, making it difficult to combine and inject. Therefore, reasonably medium-viscous LSRs are used due to their processability. Foam injection molding (**FIM**) is a variant of LIM, with the only distinction being the incorporation of blowing agent(s), either chemical or physical, into the dispensable polymer blends. The research described in this dissertation is based on the use of LSRs for Foam Injection Molding (FIM) applications. The following sections discuss the core elements of elastic SIFs – polymeric scaffold and cellular voids – and the chemistry involved in their formation.

1.3.2 Elastomeric scaffold formation

1.3.2.1 Crosslinking reactions for network formation

To create a solid structure from LSRs, it's necessary to link the polymer chains into a ternary network. The covalent crosslinks formed between long and flexible chains keep the material from permanent deformation under stress and provide recoverability due to the formed anchor points. Once the intended cross-linkage has occurred, e.g., the material is cured, the material can exhibit elastic properties

[51]. For elastomer synthesis, mainly vinyl- (~$(CH_3)_2$Si–CH=CH_2), silanol- (~$(CH_3)_2$Si–OH), and hydride functionalized (~$(CH_3)_2$Si–H) polysiloxanes are used [24]. Such functional chains can be crosslinked via two well-known reactions: **hydrosilylation** and **dehydrocondensation**, which both require catalytic activation [52], [53] (see **Figure 3**).

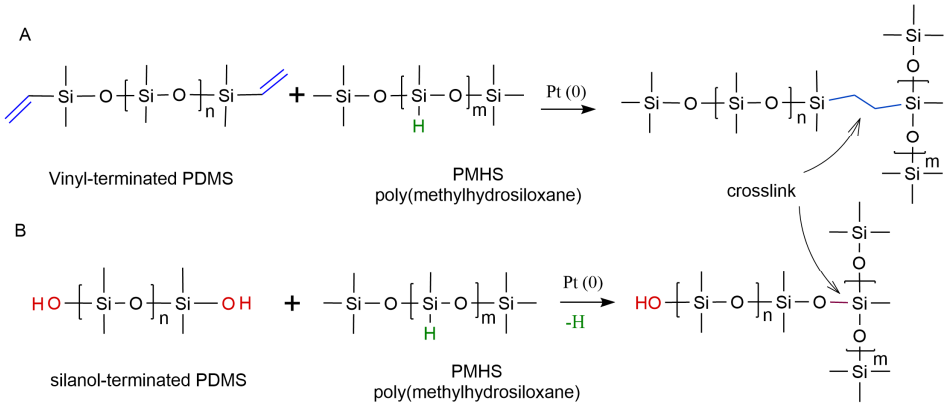

Figure 3. Crosslinking reactions via hydrosilylation (A) and dehydrocondensation (B) in the presence of a catalyst.

Hydrosilylation is the addition of a silicon hydride, Si–H, to a carbon-carbon double (or triple) bond [48]. In polysiloxane chemistry, the hydrosilylation reaction is most utilized between the vinyl-functional PDMS (Vi-PDMS) and hydride-functionalized PDMS (PMHS, or H-PDMS). Similarly, dehydrocondensation reaction (aka dehydrogenative coupling) results in a Si – O – Si crosslink, typically between Si–H and Si–OH functional polymers, and volatile H_2 as a side-product, as the reaction name indicates. The evolving gas from the condensation reaction could be trapped timely, when the polymer blend is sufficiently gelled due to crosslinking, allowing gas pockets or even interconnecting pores to form in the solidifying blend. It is worth noting that such condensation-cured elastomers benefitting from hydrogen evolution were one of the first polysiloxane-based foams presented by Lee and coworkers of Dow Corning aside from hydrosilylation crosslinking [36]. Both reactions can be conducted individually or combined, leading to simultaneous crosslinking and foaming of the material and are the most typical reactions for obtaining crosslinked polysiloxanes. Although terminal group reactions using telechelic polymers are significant [51], polymers with pendant reactivities also hold importance, particularly in SIF synthesis. An illustration of this is poly(methylhydrosiloxane) (PMHS), which is used as a polymeric crosslinker to create a ternary polymer network [33].

In the following **Figure 4**, the condensation between Si–H and R–OH (reaction B) initially results in a silanol group (Si–OH) on the siloxane backbone, which is consumed in a secondary, relatively slower condensation step [53] and a resulting crosslinking either with Si–H groups or in reaction with each other [54].

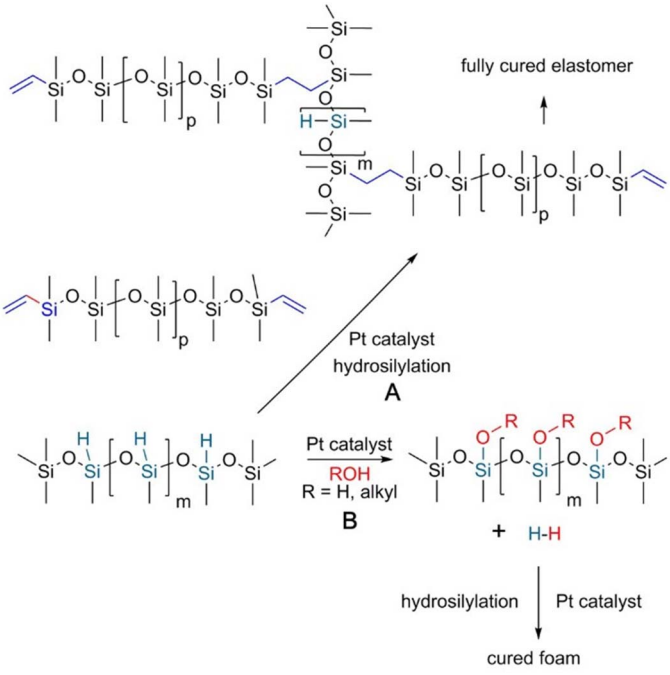

Figure 4. Typical catalytically activated reactions for crosslinking functionalized polysiloxanes can be applied simultaneously for SIF synthesis (R=alkyl, or H). Image obtained from Brook *et al.*, copyright © 2018, John Wiley and Sons. (B) Initial dehydrocondensation follows secondary dehydrocondensation when R=H; (B) can be accompanied by reaction (A) as one option.

It is also reported that such silanol formation occurs catalytically with O_2 upon heating [54]. Simultaneous addition of silicon-hydrogen bond (Si–H) across carbon-carbon double bond (C=C) (reaction A) generates crosslinks and increasingly solidifies the expanding polymer blend. However, secondary condensation is also relevant in the post-cure process, where cured materials are submitted to additional heat treatment. Any remaining reactive Si–H groups follow the condensation path, forming additional crosslinks that contribute to a bimodal distribution of the cross-linkage [54], [55], often referred to as a 'secondary network'. In formulations where R–OH bonds are intentionally introduced, this condensation crosslinking plays a crucial role during simultaneous network formation and polymeric blend expansion. Considering the abovementioned crosslinking mechanisms, some possible combinations of functional polymers for SIF synthesis are discussed in the following section [53].

1.3.2.2 Combining functional polymers

By combining polymers with various lengths and functionalities, we can easily adjust not only the elastic properties of the foam's solid structure but also the foam's ρ_{app} by modifying the expanding blend's viscosity and its change during

the expansion. For practical aspects of preparation procedures, it is common practice to select polymers based on their viscosity or M_w, for example, for the use of LSR in the FIM process [56]. More importantly, the **mechanical properties of the elastomer matrix** will be determined by the combination of polymers of specific functionality, the location, and the mol% of reactive groups. The mol% of these functional groups will determine crosslink density upon full participation in covalent bonding [55]. It is common practice to adjust the elastic properties of the network via stoichiometry ***r***, which is defined by the ratio between two types of reactive groups:

$$r = \frac{[hydride]}{[vinyl]} = \frac{f[crosslinker]}{2[polymer]} \quad (1)$$

Theoretically, an ideal network is formed when the reaction is equimolar, 1:1 in stoichiometry ($r = 1$), and the crosslinker's functionality is $f > 2$ [55]. However, due to the use of fillers and necessary adjustments in elastic properties, the r (**1**) for a reliable elastic network should be 1.1–1.4. Although siloxane chains are flexible, in a crosslinked state shorter chains restrict network mobility and give relatively more rigid networks. For example, adjusting formulations with longer end-reactive**,** telechelic chains (e.g., Vi-PDMS or OH-PDMS) results in softer, more elastic structures [55], partially due to fewer crosslinks formed per material's volume. Pendant polymers with varying mol% of functional groups offer more potential crosslinking sites and impact the resulting crosslinking degree and elastic properties of the elastomer [55]. Such siloxane polymers are applied to elastomer synthesis as **polymeric crosslinkers**. A fine example is the polymeric hydride-functional PDMS with various structures in polymer chemistry (**Figure 5).**

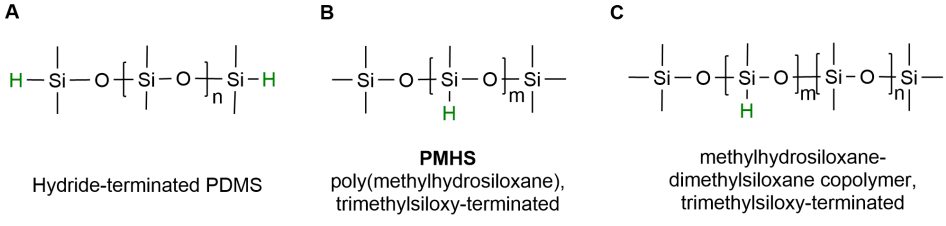

Figure 5. Most common polymeric hydride-functionalized crosslinkers applied in polysiloxane elastomer formulations. (B) PMHS is denoted as 100% H-functional (mol% of methylhydrosiloxane in the polymer), whereas in (C), the Si–H content varies (commonly 1–55 mol%).

From Si-H functional polymers, poly (methylhydrosiloxane) (PMHS) and PMHS-*co*-PDMS are primary crosslinkers used for vinyl-addition polysiloxanes [57]. PMHS-PDMS copolymers are extensively used in soft elastomer synthesis, resulting in fewer crosslinks due to the smaller amount of hydride groups and more sparse cross-linkage. However, the position and mol% of the reactive groups

determine but can also limit the crosslink density due to the increasing steric hindrance of Si–H during the progressive crosslinking. [55]

To facilitate the crosslinking reactions and maximize cure, employing effective catalysts in effective concentrations is necessary. The catalytic activation of the aforementioned crosslinking reactions is relevant; therefore, many suitable catalysts are known. The following subchapter will discuss the most common catalysts used in polysiloxane crosslinking.

1.3.3 Catalysts in SIF synthesis

The cure of LSR-based blends is expected to be rapid and controlled for efficient blowing due to the evolving gas, especially in producing foam in bulk. The hydrosilylation and dehydrocondensation reactions necessitate catalytic activation for effective network formation via crosslinking [58]. In hydrosilylation, the reaction rate depends on the type and molecular structure of the catalytic complex, the vinyl groups of the PDMS, and the number of Si–H groups on the crosslinker, as well as on their concentration [54]. In polysiloxane chemistry, catalysts employed are often effective in both catalytic processes. That said, the formulation of the SIF blend is fundamental in adjusting the rates of parallel processes during foam formation.

In the early years of SIF synthesis, in 1977, Lee *et al.* of Dow Corning employed a platinum catalyst (unspecified) to facilitate the dehydrocondensation reaction between OH-PDMS and PMHS as a crosslinking agent [36]. Replacing the organotin catalyst with platinum led to significant improvements in the thermal stability, fire retardancy, and physical properties of the resulting foams. These improvements were achieved through precise control over gas evolution and curing rates. Lee and coworkers also stated that proper adjustments of reaction kinetics can lead to either open or closed-cell foam structure [36].

Karstedt's catalyst is currently the most widely utilized Pt catalyst due to its exceptional efficiency [16]. Before Karstedt's, other Pt-based catalytic systems, such as Speier's and Lamoreaux's [59], have been successfully used in hydrosilylation and continue to find application [52], [60]. Based on the context of this thesis, two Pt species catalysts, Lamoreaux and Karstedt, are presented. Karstedt's catalyst is a Pt^0 complex containing **divinyl tetramethyl disiloxane** ligands (**Figure 6**).

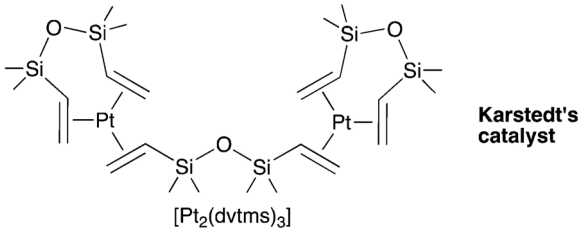

Figure 6. Proposed structure of Karstedt's catalyst [61]. Copyright © 2011 Elsevier B.V.

Lamoreaux catalyst (2.0%–2.5% Pt in octanol) is a mixed Pt^{II} and Pt^{IV} complex in octanol; its exact molecular structure is yet unknown [62]. The advantage of using the Lamoreaux catalyst is its simplicity and ease of use, as it can be accurately and consistently introduced into the reaction mixtures via a syringe, for example, in kinetic measurements, which are sensitive to any smallest deviations. Lamoreaux catalyst is found to exhibit greater stability compared to Karstedt's catalyst [63]. On the other hand, divinyl siloxane as a carrier in Karstedt's enhances the catalyst's miscibility in the polysiloxane blends, minimizing colloid formation in polymer blends.

A comparison of the effectivity of these Pt-based catalysts in hydrosilylation reactions was conducted at 65 °C in toluene by grafting PMHS-*co*-PDMS with polyoxyethylene. At [Pt]<40 ppm, distinct differences were observed between catalytic systems, Lamoreaux catalyst showing slightly lower reactivity. However, a nearly complete conversion of Si–H above 40 ppm of Pt takes place for all catalysts [60]. The same study also stresses that catalyst concentration (Speier's) has a more significant effect on the conversion than *T* in the 45–75 °C range.

Platinum-catalyzed reactions are comparatively rapid and are used in two-component RTV (RTV2) formulations, especially for producing RTV2 foams. Besides faster cure, some other benefits have been reported. Based on Mazurek *et al.* [31], polymer chains disentangle and release minute stresses when the slow setting of elastomer is allowed, eventually forming a softer elastomer. Fast cure times necessitate high-speed and thorough combining of the components, which in turn encourages polymer chain entanglement, leading to more resilient elastomers. Currently, recent reviews report that only a few [33], 10 [48], or 5 to 20 ppm of Pt is needed to cure polysiloxane in a matter of minutes at RT [56]. In general, when looking at the economic aspect of using catalysts based on rare metals, low concentrations are desired, and their regeneration is needed. To ensure optimal catalytic activity of Pt catalysts, it is crucial to minimize the presence of electron-dense atoms like sulfur and nitrogen, which can adversely affect the coordinative ligand and the efficiency of the Pt catalyst.

Although Karstedt's catalyst is highly efficient, its use in producing elastomers that will ultimately end up in landfills is stated as not being a sustainable approach [24]. In a recent review, Brook stressed that other hydrosilylation catalysts should be revised to avoid the use of expensive and non-recoverable platinum [24]. Optional catalysts are based on Ru, Ir, Co, Pd, and Fe but may require controlled conditions [64]. Although they are not commercially used in elastic SIF production, advancements in the research of sustainable catalysts are important for future perspectives.

1.3.4 Elastomer reinforcement

Fillers comprise a relatively large portion of the polymer matrix for economic and property enhancement reasons. Besides lowering the polymer content in the composition, fillers can be functional, for example, improving the material's mechanical properties (fumed silica, mica), supporting the nucleation of gas

bubbles (activated carbon, mica), and enhancing fire retardancy [65]. Low-density elastomeric foams are relatively soft, and their compressive properties depend not only on their architectural properties but also on the properties of composite elastomers. For polysiloxanes to be economically and mechanically sustainable, a significant amount of fillers used in polysiloxane blends makes them colloidal mixtures and are often treated as emulsions [30] that need stabilization with emulsifying agents [31]–[33]. Although such fine-tuning can benefit enhanced particle distribution, additional organic molecules contribute to flammability.

1.3.4.1 Surface-modified fumed silica

Fumed silica (FS) serves as a reinforcing filler for polysiloxane elastomers, significantly enhancing their elastic modulus, stiffness, and tear strength [55], [66]. Without FS, the polysiloxane elastomers have poor physical properties and tend to be very brittle due to poor intermolecular forces between the polymer chains [24], [57], [67].

FS is an amorphous silicon dioxide (SiO_2) produced in flame pyrolysis with inherently hydrophilic surfaces due to the formation of silanols in the post-synthesis hydroxylation process [67], [68]. These silanols contribute to the reinforcing effect of hydrophilic FS with extensive hydrogen bonding between the silanols and polysiloxane backbone [55], leading to reversible physical aggregation and often unwanted high adsorption of polysiloxanes [51] (**Figure 7**).

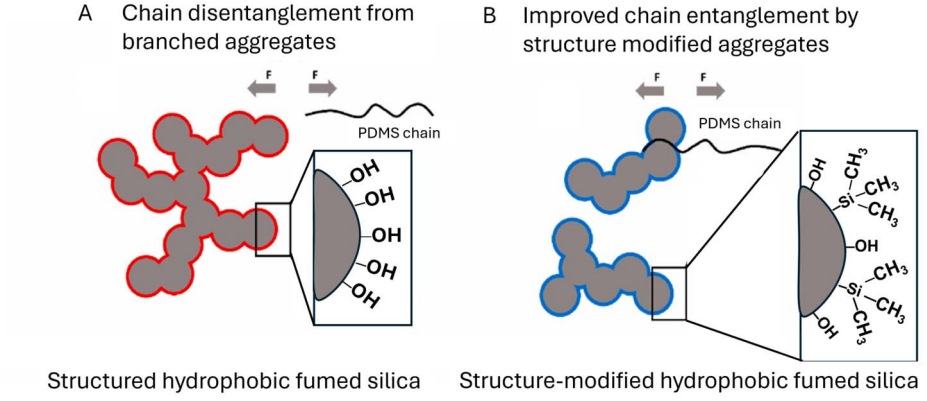

Figure 7. Schematic illustration of hydrophobic fumed silica agglomerates and surfaces and their interaction with polymer chain upon applying tensile force F in polysiloxane elastomer. Adapted from Allen *et al*. [67], CC BY 4.0.

In addition to the size of primary particle agglomerates and their Brunauer-Emmett-Teller (BET) surface area, the extent of interactions between FS particles and polymer depends on surface functionalization, namely the degree of hydrophobization. Hydrophobizing structure modification by partially protecting silanols diminishes hydrogen bonding and van der Waals interactions between

the FS particles and the polymer matrix [67]. By weakening these interactions, the FS particles become less likely to form strong, rigid networks within the polymer, which can contribute to increased brittleness [67] and permanent set [67]. As a result, using FS in a hydrophobized form improves the material's performance during and recovery after compression. The most common FS for this purpose is hexamethyldisilazane (HMDZ) treated FS. Moreover, silica nanoparticle agglomerates are shown to enhance the polymer foam structure by acting as nucleating agents; increasing the silica content also increases cell density [69].

1.3.4.2 MICA

Silicates and other mineral additives are common additives for improving polymeric materials' strength, insulation, and fire performance, including foams. Micas are high-density (2.8–2.9 $g \cdot cm^{-3}$) aluminosilicate compounds (ideal formula $K_2Al_4(Al_2Si_6O_{20})(OH_4)$, splittable into thin, ~1 nm thick and tenths of microns in size elastic plates referred to as silicate layers [65, p. 180], [70]. Due to their relatively high density and particle's high aspect ratio [71], their applicable volume fraction in low-density polymeric foams is limited in terms of final foam density and polymer blend viscosity [71]. However, even in low concentrations, they are reported to significantly enhance the polysiloxane elastomer's tensile strength [70], [71], fire barrier properties (the high aspect ratio of flakes), and thermal insulation while decreasing polymers' permeability to gases (membranes) [65], [72].

Micas' ability to absorb water can be used as a possible nucleation and crosslinking site. The high aspect ratio of plateous mica particles offers increased surface area for gas adsorption, point of nucleation, and polymer-filler interactions. Surface-silanols enhance mechanical properties due to the crosslinks formed with Si–H in PMHS. In combination with silica glass frit, mica is shown to significantly improve fireproofing properties and tensile strength ($\boldsymbol{\sigma_b}$, MPa), however decreasing elongation at break ($\boldsymbol{\varepsilon_b}$, %) and increasing density [70], [71]. In comparison with HMDZ-modified silica, mica's effect in improving PDMS-elastomer tensile properties is lower [71].

1.3.5 Blowing techniques

Independent of the immense number of variations in the polysiloxane elastomer composition, the blowing techniques are divided into two main categories**:** physical and chemical. Both blowing methods can be employed on small and large scales, independently or in combination, depending on the cure system.

Physical blowing is termed foaming via gases (incl. air and other gases) and low-boiling volatile liquids, such as alkanes [73]. A recent trend in blowing SIFs, an environmentally friendly method, is to control the expansion of saturated gas, providing low-cost and relatively robust fabrication. Although saturated physical blowing agents (PBAs), *i.e.,* CO_2 or intense mixing of the polymer blend to incorporate air bubbles is often applied, it is difficult to maintain a homogeneous

structure at low densities [74]. Due to the poor affinity of air towards highly hydrophobic polysiloxane, carbon dioxide (CO_2) is used instead, which is highly soluble although highly diffusive in polysiloxanes [34]. For effective blowing with supercritical CO_2 ($scCO_2$), pre-vulcanization, *i.e.*, partial crosslinking of the foamable blend to increase blend viscosity, is often reported to retain the gas [74]. Additionally, supersaturation of gas and modifications in composition give a premise for bubble nucleation [3], [74].

Chemical foaming, on the other hand, can be more controllable and result in uniformly blown foam if gas bubble nucleation sites (chemical or physical, homogeneous or heterogenous are evenly distributed [3], [47]. The blowing typically arises from the gaseous decomposition product(s) of CBAs or a chemical reaction between CBAs, reactive polysiloxanes, or both. CBAs, once widely used, are being replaced by more environmentally friendly blowing agents to avoid potential reaction by-products that could contribute to material degradation and deterioration of properties over time. Following the principle of energy efficiency, additional heating required for the decomposition of CBAs is frowned upon, so CBAs that react at RT are preferred.

There are various sub-techniques reported to create porous polysiloxane scaffolds [34]. A sacrificial templating, in which porogen crystals (e.g., NaCl [5], sugar [15–17]) are washed away from the polymer scaffold, or emulsion templating (e.g., with water [75], [76]) with subsequent evaporation. In specific applications, some porogens are intended to function as an impregnation (*i.e.*, glycerol [77]). Although such techniques are applicable for enhancing foam density and offer valuable insights into SIF synthesis, these will not be discussed further in this dissertation due to the restricted formation of low-density SIFs ($<<250\ kg \cdot m^{-3}$) and impracticality for effective bulk foam production.

It is important to note that all the blowing techniques summarized above can be combined, whether in lab-scale mixing or an up-scaled FIM process. It requires careful timing and optimization of conditions to overcome the complexity of controlling parallel physical and chemical processes governing the cure and expansion. Further discussions on the extent and applicability of chemical blowing in elastomeric SIF synthesis focus on generating blowing gas utilizing existing functional groups on polysiloxane chains.

1.4 Chemical blowing via inherent dehydrocondensation

One of the possible variants of chemical blowing is utilizing the existing reactivities of polysiloxanes from catalyzed polymer-polymer interactions or in combination with environmentally friendly CBAs. In theory, every molecule can potentially act as a nucleation site, leading to the most optimal nucleation density and cell radius in homogeneous nucleation [78].

1.4.1 Polymer-polymer blowing

As previously shown in **Figure 3**, crosslinking PMHS and OH-PMDS is one possibility to give the polymer a porous nature without additional blowing agents. One of the first reports on SIFs using dehydrocondensation reaction between polysiloxanes was by Lee *et al.* [36] without additional CBAs. Although no additional information regarding the structure or density of the foams was published, these SIFs were reported to be suitable for sealing/caulking, insulation, or acoustic applications [36], [37]. Despite the presence of hydroxyl groups, using dehydrocondensation of OH-PDMS and PMHS as a primary (or only) gas source for producing low-density and, more importantly, elastomeric SIFs is insufficient. On the one hand, the volume of H_2 from polymer-polymer condensation reactions can be maximized using shorter telechelic chains, so the concentration of reactive groups in the blend is higher. More H_2 and crosslinks are generated theoretically, although the resulting structure is more brittle due to shorter crosslinks. While less hydrogen is produced in a reaction using longer telechelic chains, lower crosslinking density, and longer crosslinked chains improve the network mobility and elasticity. Considering the importance of both elasticity and the low-density aspiration, introducing additional gas or gas sources is relevant without compromising the material's elasticity.

1.4.4.1 PMHS as a Si–H source

The polymeric siloxanes with Si–H functional groups are excellent base materials for enhancing SIFs. By introducing excess Si–H along the siloxane polymer, both the mechanical and structural properties of SIFs can be improved. In addition to the hydrosilylation and dehydrocondensation reactions with polymeric siloxanes (Vi-PDMS and OH-PDMS), the additional hydride in PMHS can be applied in H_2 generation, provided there is a sufficient ratio of hydroxyl groups for Si–H conversion.

For a hydrosilylation reaction with tetra-functional silane in the presence of Pt^{II}, it was demonstrated that when the ***r***, as the ratio of [hydride]/[vinyl], is increased above 1.0, the vinyl double bonds are more rapidly reacted. However, higher ***r*** significantly decreases the percentage of non-bonded (extractable) species, and the residual Si–H continues to participate in secondary reactions, forming Si–O–Si crosslinks in the presence of atmospheric humidity [54]. The previous statements create conditions where the hydrosilylation reaction proceeds faster, which is especially advantageous when the blowable polymer blend consists of polysiloxanes with various functionalities. Using Vi-PDMS in blends with OH-PDMS and PMHS induces a faster increase in viscosity, which helps to maintain the gaseous phase in the expanding blend. An excess of Si–H groups remaining in the elastomer causes it to harden over time due to additional crosslinking from oxidation/hydrolysis processes [53].

The general idea of using polymeric hydride-functional polysiloxanes (≡Si–H) is to lower the foam's density while maintaining its flexural properties. Whereas increasing the excess of Si–H and Si–OH functionalities in the polymer blend would produce increased volumes of H_2, it is equally important to balance

the parallel reactions during polymer foaming to capture the evolving gas and secure desired cross-linkage timely.

The Si–H functionalized polysiloxanes have different structures, with hydride groups situated at the ends, sides, or both, and with varying degrees of functionalization (from a few mol% to 100 mol%). These variations in mol% and location on the siloxane backbone allow for tuning the crosslinking degree and also the volume of hydrogen generated from the reaction. To maximize hydrogen volume, a 100 mol% PMHS homopolymer can be used in reactions with the hydroxyl group containing molecules. However, using a dense cross-linking of the PMHS may cause elastomers to become brittle, potentially reducing the elasticity of the foam. This effect will depend on the molecules that act as cross-linkers and the final cross-linking density. Adjusting the chain length and substitution of functionalized polymers can be intentionally used to enhance the elasticity of the material. In addition to oligomeric and polymeric hydroxy-functional polysiloxanes (≡Si–OH), other hydroxyl group-containing molecules can be used to crosslink and blow SIFs simultaneously. The following section discusses the selection, applicability, and properties of suitable reactants.

1.4.4.2 Polymer-alkanol blowing

While the Si–H bond in PMHS reacts with silanols in the OH-PDMS, it is also very eager to take part in dehydrocondensation reactions with alkanols (e.g., alcohols of alkane) and water and its vapor as humidity in the reaction environment [34].

The following **Figure 8** represents the reaction between PMHS as a Si–H source and molecules containing hydroxyl groups. In the case of compounds containing at least two hydroxyl groups, the concurrent formation of additional cross-links gradually increases the viscosity of the polymer mixture and affects both the mechanical properties of the elastomer and the developing foam structure.

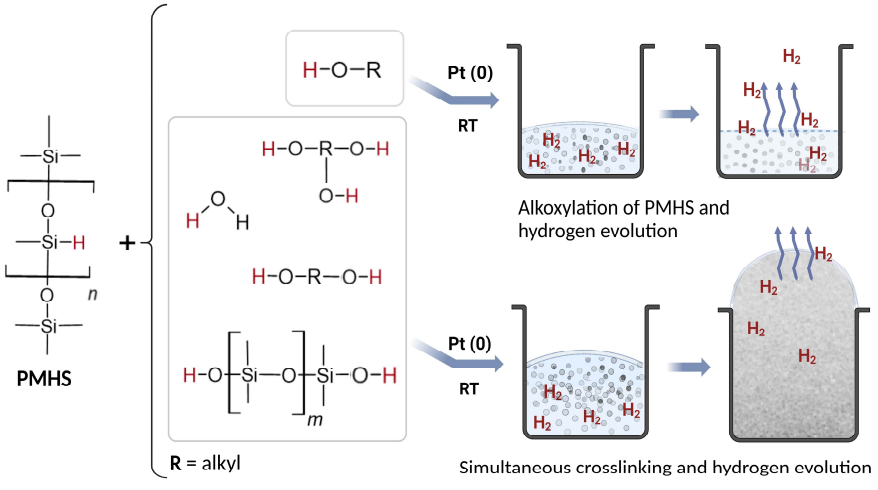

Figure 8. The coupling process involving PMHS and OH-functionalities can lead to either condensation without the formation of chemical cross-linkage (hence, polymer grafting) or condensation with the formation of cross-linkage due to the conversion of Si–H.

The use of alkanols can be considered favorable since it leaves an opportunity to use low-molecular reagents and their mixtures as blowing agents without significantly altering the viscosity of the blowable blend. These compounds are easily accessible low-cost reactants and some often industrial side-products (as wastes).

1.4.2 Concluding summary on chemical blowing

Different approaches to chemical blowing are used, and not all are intended for achieving low-density foams specifically. A significant part of previous research seeks to blow the fixed formulations intended to cure into solid elastomers (e.g., the Sylgard line by Dow) [79]. These commercial formulations are the result of carefully balancing reactive moieties, and adding reactive components that consume existing functional groups can lead to imbalance and insufficient cure [55], making the interpretations less reliable.

However, **using either water or alcohol as blowing agents** is gaining more interest and has been tested in various specifically tailored polysiloxane blends. It is interesting that dialcohols (diols) have not been used for SIF-blowing purposes. Some of the recent findings, focusing on the period of 2019–2022, on synthesized SIFs and their selected characteristics, are summarized in '***Table A1***. *Comparative data on the physicomechanical properties of silicone-based foams produced by applying additional blowing agents or techniques*.' as an appendix for **Publication II**. The represented range of ρ_{app} (100–250 kg·m^{-3}) and missing data on tensile and structural properties make it difficult to compare and evaluate the effectiveness of chemical blowing. In addition, the available discussion on catalytic alcoholysis focuses on selectivity and product yields rather than on describing the first stages of chemical-blowing reactions. However, the first minutes of the reaction are decisive, during which the reactants' performance and stoichiometric balancing determine the overall foam structure. Therefore, the chemical blowing and processes involved should be examined in more detail to enhance the blowing of the SIFs.

1.5 Bacterial adhesion to polymeric surfaces

The adhesion of microorganisms is found to be dependent on the biological properties of the microorganism and the physicochemical properties of the material surface. These properties include electrostatic and steric interactions, van der Waals forces, surface chemistry, and topography, as well as the size, shape, and mechanical properties [80], [81], [82]. Moreover, the temperature and properties of the surrounding medium can also impact the strength and nature of these interactions, as well as the changes in the bacterial envelope during different growth stages often complicate drawing solid conclusions about its hydrophobic interactions with the material's surface [83].It is generally understood that the adhesion of microorganisms depends on hydrophobic interactions between the bacterial cell wall and the polymer surface Further bacterial growth and colonization eventually lead to biofilm formation (**Figure 9**).

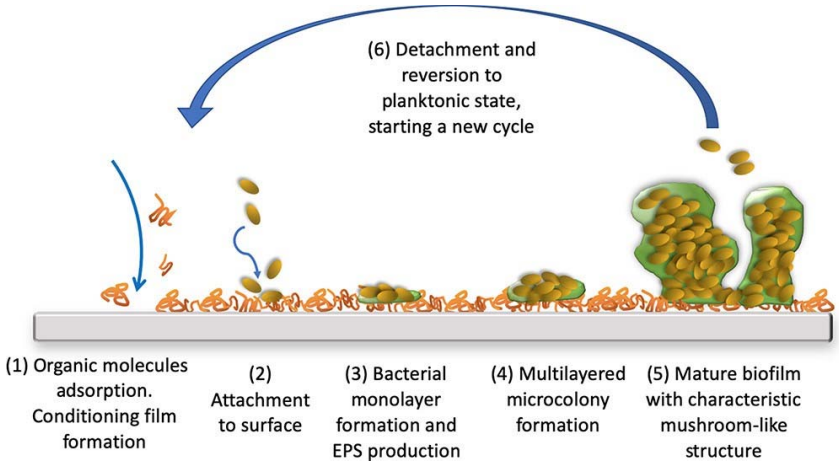

Figure 9. "Steps involved in biofilm formation". The initial adsorption of organic matter (1) promotes the attachment (2) of microorganisms, leading to further biofilm development (3–5). Reprinted with permission from Ghilini *et al*. [84], ©2019 American Chemical Society.

The initial adhesion of bacteria to a surface is influenced by physicochemical and electrostatic interactions between the bacterial envelope and the conditioned substrate (**Figure 9** (1)), which can be impacted by surrounding fluids [83], [85]. Shortly after adhesion to the surface (**Figure 9** (3)–(4)), singular bacterial cells start to divide and grow into structured communities (microcolonies), producing extracellular polymeric substances (EPS), which is a vital attribute for the biofilm lifecycle [86]. The matured biofilm is a source for singular cells starting new colonizations and may lead to infections, which complicates decontamination due to the protective layer.

In a previous study of polymer membranes, it was found that microorganisms' attachment is higher to more hydrophobic surfaces than to hydrophilic ones [85].

Studying ***Escherichia coli*** adhesion on polystyrene surfaces with different roughnesses and hydrophilicity concluded that "an extremely hydrophobic or an extremely hydrophilic surface reduces *E. coli* adhesion" [87]. On the other hand, the bacterial adhesion peak on polystyrene was found to be highest near moderate hydrophobicity with WCA of θ_C=95° (**Figure 10**).

Studies on the adhesion of yeast organisms, specifically *Candida albicans* and *C. tropicalis*, have revealed that the hydrophobicity of the microorganisms' surface is directly proportional to their tendency to attach to polysiloxane surfaces [88]. For example, among the Gram-negative bacterium species *E. coli*, *Pseudomonas putida* (soil bacterium), and *Acinetobacter calcoaceticus* (soil bacterium), the adhesion of relatively more hydrophilic *E. coli* is found to be lower compared to more hydrophobic species [85]. It has also been suggested that in aqueous environments, the hydrophilic surfaces are covered with a surface hydration layer, which deters the microorganisms from adhering to the surface [89].

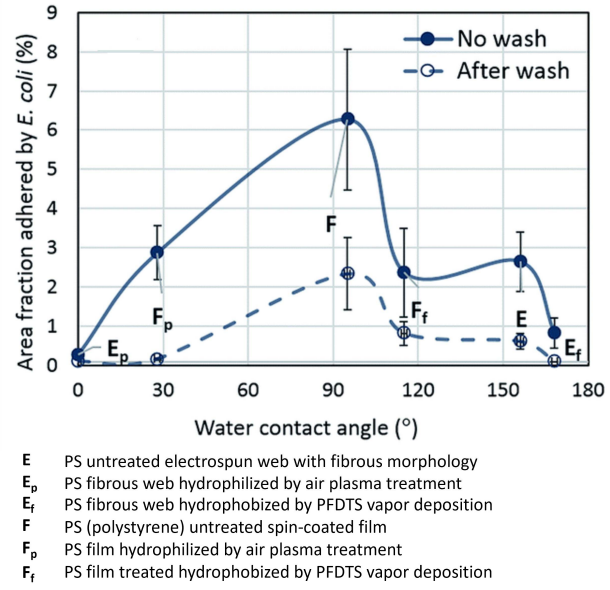

Figure 10. Average area fraction adhered *E. coli* with respect to water contact angle with and without wash on polystyrene surfaces; E and F are polystyrene substrates with modified surface roughness. Image obtained from ©2017 by Yuan *et al.* [87], licensed under CC BY.

1.6 Biofouling quality of polysiloxane elastomers

As a core structural component **in SIFs**, polysiloxane elastomers do not possess intrinsic antibacterial properties or provide growth-supporting nutrients [90]. However, in conditions where polysiloxane is in contact with aqueous media, such as beverages, blood, urine, and saliva, the availability of nutrients favors bacterial contamination. Polysiloxanes are essential in creating medical devices such as catheters [90], [91], [92], intravenous tubing, and increasingly applied as a porous elastic layer in wound care applications [4], [5], [93]. In addition to wound dressings, SIFs for orthopedic and non-orthopedic cushioning needs must prevent the further spread of infections.

The primary reason why the surface of **polysiloxane** elastomer is susceptible to bacterial adhesion and protein adsorption is thought to be due to its low surface tension and, consequently, high hydrophobicity [94], [95]. Earlier research shows that increasing hydrophilicity of polysiloxane elastomer has a considerable anti-microbial effect, particularly against *E. coli, Staphylococcus aureus,* and *Pseudomonas aeruginosa* [94].

The hydrophobic nature of both the outer lipid layer of microorganisms and the **surface of polysiloxane** means they tend to adhere to each other through hydrophobic-hydrophobic interactions. This phenomenon is part of why nonpolar substances, in general, tend to aggregate in aqueous environments – to minimize

their contact with water. This principle is observed in various biological and synthetic systems, where the compatibility of different substances in aqueous environments can significantly influence their behavior and interaction.

Without specific surface functionalization, **polysiloxanes** have a moderately **hydrophobic surface** (static water contact angle, WCA, $\theta_C \approx 105°$ [79], 107.1° [90]) and intrinsically repel aqueous medium. The Gram-negative ***E. coli,*** as a ubiquitous species in the gastrointestinal tract [83], can be found on contaminated polysiloxane-based medical devices and prostheses, as well as mattresses. *E. coli*'s outer membrane is reported to be hydrophilic (WCA, $\theta_C \approx 29.8° \pm 2.6°$ [96], $\theta_C \approx 28°$ [97]), with a bilayer membrane considered less susceptible to antimicrobials than Gram-positive bacteria. Gomes *et al*. reported that polysiloxane with the highest $\theta_C \approx 115°$ showed the highest level of *E. coli* adhesion, concluding that both the adhesion and the extent of adhesion on surfaces are related to substrate hydrophobicity [97]. It is suggested that the hydrophobic interactions are favored due to the hydrophobic lipopolysaccharide surface of Gram-negative bacteria, such as *E. coli* [87].

1.6.1 Making SIFs microbe-resistant

Roughly, antimicrobial effect of a material may emerge from three antimicrobial strategies: antifouling (anti-adhesive), antibacterial, and dual-action, as a combination of both [98]. Changes in surface properties can be achieved by physically or chemically modifying surface topography to adjust micro- or nanoroughness, or by altering surface chemistry, leading to changes in overall physicochemical properties [81] (**Figure 11**). These modifications either inhibit the adhesion of microorganisms on its surface (antifouling) or give bactericidal properties by affecting the microorganisms upon direct contact with the surface or the leaching biocide [93], [98].

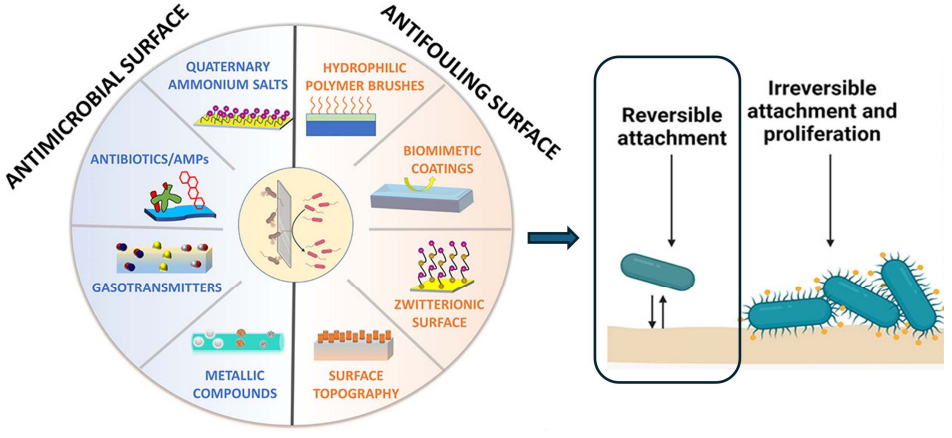

Figure 11. Different surface modification strategies for inhibiting bacterial adhesion and for decreasing bacterial viability. *Note: AMPs – antimicrobial particles.* Partial image reproduced from Chug and Brisbois 2022 [98], licensed under CC-BY-NC-ND 4.0.

An open-cellular foam is more susceptible to contamination by microorganisms due to its porous interconnected structure. In **Figure 12,** an exemplary SIF, a polysiloxane foam (left), and magnification of its surface with adhered bacteria (right) depict that the foam cells and interconnecting pores are relatively large to facilitate the mobility of microorganisms in the macroporous material.

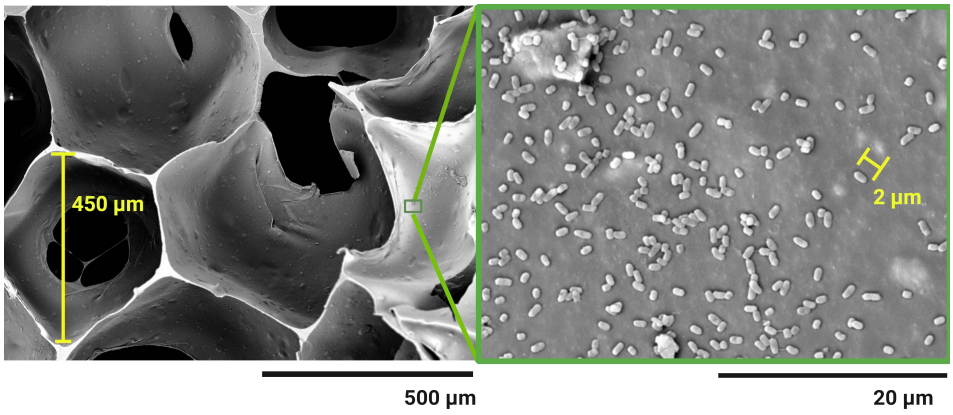

Figure 12. Cell dimensions of a silicone foam (on the left) and the *E. coli* adhered to its surface. The relatively large pores interconnecting the cells do not limit the movement of singular nor clustered bacteria (on the right).

Attributing antimicrobial properties to a foam depends on its function in a specific application and whether the antimicrobial properties are desired throughout the material or on the contact surface only.

1.6.1.1 Surface modifications

Chemical surface modification, sometimes preceded by plasma treatment, aims to suppress bacterial adhesion by either increasing the polymer hydrophilicity [9], [87], [92], [94], damaging bacterial membranes, or disrupting biofilm upon external stimuli [98], [99]. Altering surface properties of already crosslinked elastomers is suitable for non-porous surfaces, such as polysiloxane-based components of a medical device. Grafting hydrophilic moieties to the siloxane chain before crosslinking may be used to decrease hydrophobicity. In recent years, for example, the emerging thiol-ene ‘click’ reaction in silicone chemistry led to thiol functional siloxanes, which, upon reacting with C=C bonds, led to hydrophilic PEG-modified PDMS [100]. Changing polysiloxane surface chemistry from hydrophobic to hydrophilic is found to have a short-term effect due to the migration of siloxane chains to the surface, termed as a hydrophobic recovery [100]. Here, another trade-off in properties should be considered, as in some applications, it is particularly important to maintain the hydrophobic nature of the SIFs, especially in cushioning and insulation applications. Functionalizing its surface with hydrophilic groups extensively would revoke its water-deterring property to some extent.

1.6.1.2 Bulk modifications

Examples of bulk modifications include dip-coating or spraying the foam with an antibacterial solution, which, upon drying, would provide the foam either a modified surface or add a fungicidal or bactericidal effect. Dip-coating is less suitable for micro- and macrocellular materials due to the uptake of coating solutions, which increases its mass and production time. Also, because of the dynamic use of SIFs and their open-cellular structure, surface treatment may not provide sufficient antibacterial activity in the deeper layers of the foam. Further re-applications due to the material's wear are usually avoided, and the intrinsic antibacterial property of the ready-made material is preferred.

Another bulk modification, which is also discussed more in-depth in **Chapter 6**, is incorporating organic or inorganic additives into a cross-linkable polymer blend that changes the elastomer's surface properties so that bacterial adhesion is potentially less favored. Using fillers or specific additives is a simplistic technique to introduce topological roughness into the elastomer as a bulk. Some evidence suggests that lowering surface energy by increasing surface roughness decreases the initial adhesion of *E. coli* onto polymer (polystyrene) surfaces. Yuan *et al.* showed that *E. coli* adhesion was significantly lower on super-hydrophilic or superhydrophobic surfaces, and increased surface roughness decreases the solid area fraction and concomitantly bacterial adhesion [87]. Increasing the concentration of filler or additive particles in the expandable polymer mixture makes it possible to improve the likelihood of these particles contacting the surface, such as the polymer-air interface, directly affecting the surface properties and the adhesion of microorganisms. This can be achieved by carefully adjusting the particle sizes and their distribution in the polymer blend, considering the final d_{wall} of the foam. Since fillers comprise a considerable proportion of a traditional polysiloxane composition, a change in surface roughness is expected because of foam expansion and cell wall thinning. For example, it is found that submicron topographies limit bacterial adhesion in case of surface roughness or cavities being comparable to or slightly larger than that of the *E. coli* itself so that the effective area for attachment is decreased [81]. Such submicron roughness is complicated to obtain using conventional fillers applied in polysiloxane elastomer synthesis. Increasing the amount of antibacterial or other additives typically involves trade-offs and can influence the original properties of the material in various ways. Undesired filler-filler and polymer-filler interactions can lead to a degradation of the tensile properties of the elastomer. Significant changes in the polymer blend's viscosity ultimately impact its capacity to expand and, eventually, its ρ_{app}. This phenomenon is not exclusive to polysiloxane blends; alterations in the formulation necessitate reevaluating and adjusting the crosslinking dynamics and the kinetics of gas evolution.

1.6.2 Assessing bacterial adhesion in foams

The bacterial adhesion can be quantitatively described by adhesion number, which involves counting the cells on the surface with and without antimicrobial ingredients, relying on imaging equipment [7], [101]. Earlier research provides examples of gentle washing steps to detach adherent cells and comparing surfaces via SEM analysis for the preferential location of bacterial adhesion and the area fraction of bacterial adhesion qualitatively using contrasted images [7], [87]. Additionally, SEM imaging and direct counting methods were applied on inoculated glass substrates after allowing the gravitational detachment of adhered bacteria in a liquid [96]. However, evaluating the adhered number of bacteria inside cellular foam material is complex. In such cases, the bacterial population densities in the porous structure could be presented as average values. One option would be to compare adhesion to certain surfaces and structures via detachment profiles under systematic mechanical agitation (*i.e.*, washing) by taking into account the structural characteristics of the samples, such as density and volume [102], surface area, fraction of open volume, and surface porosity.

1.6.3 Antimicrobial additives and toxicity

Studies on using additives with known antibacterial activity, as well as antimicrobial surfaces in general, have significantly increased in recent years [84]. For example, platinum **nanoparticles** as a catalyst [103], and silver nanoparticles (AgNPs) [104] have been reported to give polysiloxane elastomers antibacterial activity; however, there are safety concerns due to their toxicity to mammalian cells [98]. **Inorganic fillers** such as zinc oxide (ZnO)[105] and copper oxide (CuO) are used for their antimicrobial properties in polysiloxane elastomers. However, the total environmental impact of these nanoparticles is not yet fully understood, and further research is necessary to ensure their safe application.

Armugam *et al.* reported that blending imidazolium polymer as a **biocidal** ingredient to Sylgard 184, a commercial polysiloxane elastomer formulation, effectively inhibits or eliminates the colonization of both Gram-positive and Gram-negative bacteria, as well as fungi [91]. Recent reviews summarize that a significant drawback in using the biocide release method is the reduced effectiveness of bactericidal molecules not being released in sufficient amounts or their eventual depletion from the material [98] and growing concern about the potential for promoting antimicrobial resistance [89].

The studies mentioned above were conducted on elastomer films, but the same antimicrobial effect is expected to occur similarly on foam cell walls. To achieve a uniform antimicrobial effect in porous open-cellular SIFs, higher concentrations of antimicrobial particles are needed to ensure even distribution in the expanded polymer. However, higher concentrations of antimicrobial particles may lead to poisoning or allergic reactions in some applications. Therefore, for small-scale use (e.g., in wound dressings [106]), where depletion is not an issue, it is recommended to use nature-derived, **organic additives**, while in cushioning or insulation materials, using organic additives is less desirable due to the potential reduction in fire retardancy from increased organic matter.

2 AIMS AND SCOPE OF THE STUDY

This doctoral dissertation is based on three peer-reviewed articles exploring the development of polysiloxane-based polymeric foams for human contact applications. The **primary aims of this dissertation are** as follows:

1. To investigate how the dehydrocondensation reaction contributes to the creation of elastomeric polysiloxane foams with densities below 100 $kg \cdot m^{-3}$, with a specific focus on using water-alcohol blends as blowing agents and improving the physicomechanical properties of these foams.
2. To investigate whether specific additives in polysiloxane foam formulation affect the adhesion and growth of Gram-negative bacteria. The incentive is to avoid enhancing bacterial growth in foams characteristically designed for human-contact applications while maintaining or improving the physicomechanical characteristics of these materials. Both antibacterially active additives and additives without known antibacterial effects, as well as polyurethane foams for reference, were used in this study.

In **Publication I**, we investigated the impact of monoalcohol molecular descriptors on the kinetics of hydrogen evolution and their applicability as blowing agents in catalytic dehydrocondensation reactions with hydride-functionalized polysiloxanes (PMHS). This study, which was conducted independently of the standard multicomponent foam synthesis process, aimed to elucidate the role of various monoalcohols in chemical blowing.

Publication II examines how foam structure, density, and tensile properties depend on assemblies that form crosslinks of varying lengths and rigidity. Chemically blown silicone foams were prepared and characterized, with systematic variations in blowing blends using water, dialcohols, glycerol, and methanol in a multi-reaction system involving dehydrocondensation and crosslinking reactions.

Publication III attempts to analyze bacterial adhesion on synthesized silicone composites and the potential antibacterial effects of fillers and additives used in silicone foam synthesis. An unconventional sample preparation method for bacterial cell imaging and simplified microbiological testing identified *E. coli* on the inner surface of porous foams and bacterial growth surrounding foam samples.

3 MATERIALS AND METHODS

3.1 Kinetic study of PMHS alcoholysis

To determine the performance of monoalcohols in yielding H_2 in a catalyzed dehydrocondensation with hydride-functionalized polysiloxane, the reaction was investigated separately from a multi-component polymer system. In the alcoholysis of PMHS, the hydride containing unit Si–H is substituted by the alkoxy nucleophile (-OR), yielding the corresponding alkoxysiloxane and H_2 [107]. A similar route under various conditions, catalysts, and concentrations has been applied by Safa *et al* [108] for simple and functional alcohols, and by Mukbaniani *et al* [109] for allyl alcohol, with a focus on polymer grafting.

3.1.1 Formulation of dehydrocondensation reaction

In this study, individual monoalcohols and hydride-functionalized polysiloxane were introduced into the reaction in a 10x molar excess to avoid a premature increase in viscosity due to the progressing alkoxylation and to facilitate the access of the low-molecular alcohol nucleophile to the Si–H electrophile, and the mobility of Pt-catalyst. The polymeric hydride-functional siloxane was chosen due to its high Si–H content (100 mol% of [-Si(CH_3)(H)O-]) and its good application practices in preparing LSR foams. In actual polymer composition, Karstedt's catalyst, due to its fast and reliable catalytic action, would be the first choice. Here, a more moderate Lamoreaux catalyst was chosen for catalytic dehydrocondensation (see **Reaction 1**). Based on the structural characteristics, five different monoalcohols and water were chosen to find the relationships between the specific properties of each component and their reaction kinetics. The components used in kinetic experiments are listed in **Table 1**.

Before the kinetic measurements, the Si–H content in PMHS was determined (see *^{1}H-NMR: Determining Si–H content in PMHS*). Alcohols were dehydrated, as suggested by Burfield and Smithers [110], using 20 wt%/vol of the 3 Å preactivated molecular sieves (by FUJIFILM Wako Pure Chemical Corporation) for a minimum of 5 days. The alcohols used in this study had a water content of less than 0.025% determined by Karl-Fischer coulometric titration (Metrohm Coulometer 831 KF).

Table 1. Reactants and solvents used in dehydrocondensation reaction between PMHS and monoalcohols.

Reactant	Acronym	Specifications	Function(ality)
poly(methylhydro-siloxane)	PMHS	n ≈ 30, 20–35 cSt, HMS-992, M_w=1900–2100 g·mol^{-1}	hydride-functional polymeric siloxane
methanol	MeOH	≥99.8%, ACS, [a]	hydroxy-functional
propan-2-ol	iPrOH	99.5%, anhydr., [a]	
2-methylbutan-2-ol	tAmOH	≥99%, GC, [e]	
butan-2-ol	secBuOH	99.5%, anhydr., [a]	
2-ethylhexan-1-ol	iOctOH	≥98.5%, GC, [b]	
water	H_2O	MilliQ+	hydroxy-functional
Pt $^{II, IV}$ in octanol	Lamoreaux' catalyst	2%–2.5% Pt, SIP6833.2, [c]	catalyst
toluene	toluene	HPLC plus, [a]	solvent, used for catalyst dilution

[a] *Sigma Aldrich,* [b] *ACROS Organics,* [c] *Gelest,* [d] *Reachim,* [e] *Supelco, Emplura®.*

For the reaction, 325 mg (5 mmol of Si–H) of poly(methylhydrosiloxane) (PMHS) and 10 µl of Pt catalyst (Pt $^{II/IV}$as octanal-octanol complex) solution in toluene were added to a 50 ml heat gun dried flask. Catalyst solution concentration was varied to conserve 15 ppm of Pt for all experiments. A magnetic stirrer bar was carefully inserted into the flask, and the system was connected to Norprene® tubing. The closed system was then purged with nitrogen to remove humidity, as the water vapor readily reacts with PMHS under these mild conditions. For repositioning the level of the water meniscus in the cylinder, hydrogen was added through the system into the cylinder. The reagents were conditioned at 27 °C (~300 K) in a polyethylene glycol bath at a constant mixing speed of 200 rpm. To begin the reaction, 10 equivalents (50 mmol) of mono alcohol were added through the septum by syringe in varying volumes, corresponding to a 1:10 molar ratio of Si–H functional groups of PMHS to -OH groups of water or alkanols.

The catalyzed reaction between Si–H (5 mmol) and R–OH takes place in 1:1 stoichiometry, therefore resulting in 1 mole of hydrogen (H_2) and 1 mole of alkoxysiloxane. The V_{H_2} produced will depend on the catalyst, reactivity of the hydride and alcohol, and their molecular parameters. The theoretical maximum volume of H_2 at 27 °C is 124.28 ≈ 125 mL, following the ideal gas law, $pV = nRT$, where p=1004 mbar, R=83.1446 mL·mbar·K^{-1}·mmol^{-1}, T=300.15 K, and n=5 mmol.

3.1.2 Setup for detecting hydrogen volume change

A simplistic setting consisting of a smartphone device and fixtures was used for the detection of dV_{H_2} during the reactions by using time-lapse video recording mode (**Figure 13**).

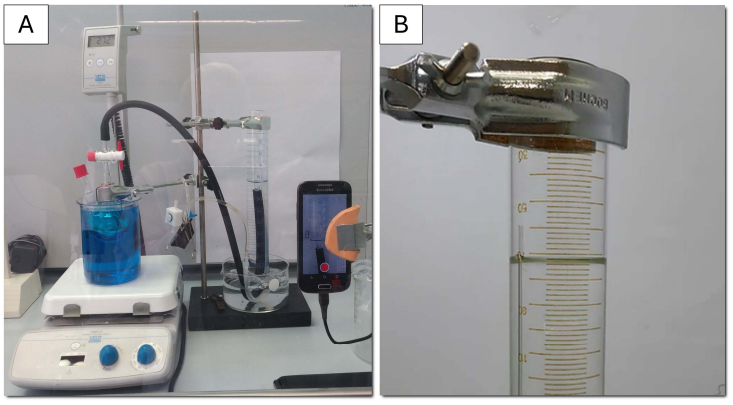

Figure 13. (A) Measurement setup for monitoring gas volume increase by water displacement principle. (B) Gaseous reaction product is directed into the 250 mL calibrated cylinder.

The recorded frames were analyzed using MATLAB (MathWorks) by running specifically written code for this purpose (by *T. Laasfeld*) to detect the change in meniscus coordinates in time. This data was converted to V_{H_2} (mL)/TIME (sec), with corrections due to occupied volume by glass pipette. As the hydrogen is prone to escape the system easily, including permeation through silicone rubber tubing, a background measurement was performed for possible leakage. Norprene tubing was selected as the most impermeable tubing for hydrogen flux. The standard error at 95% confidence intervals for the y-axis (V_{H_2}) was 0.04. A very steady linear leakage was accounted for in the calculations.

3.2 Fabrication of polymeric SIFs

3.2.1 Formulation of blowable polymer blends

The SIFs were fabricated using a specifically formulated curable elastomer-forming blend, divided into two volumetrically equal parts, both approximately equal in viscosity. First, the formula components were weighed and homogenized using a standalone mixer equipped with a PTFE-covered rotary blade. The PTFE-covered blade was chosen for its ease of cleaning after mixing. Both parts were mixed thoroughly for 5 minutes at an average speed of 400 rpm, which was the most comfortable speed for this process.

The ratio of components making up the polymeric scaffold was stoichiometrically maintained throughout the experiments. The reagents and non-reactive components are listed in the following **Table 2**, and the relevant (FT-IR/^{1}H-NMR) spectra are referred to in *Spectroscopic characterizations*.

Table 2. List of materials tested and applied in foam synthesis.

Material	Acronym	Chemical name	Function(ality)
Organo-siloxane polymer	OH-PDMS	dihydroxy dimethyl terminated polysiloxane, [c]	silanol-functional polymer
	Vi-PDMS	divinyl dimethyl terminated polysiloxane, [c]	vinyl-functional polymer
	PMHS	poly(methylhydrosiloxane), [b] HMS-992, 100 mol% hydride	hydride-functional polymer, n≈30,
catalyst	Karstedt's catalyst	platinum(0)-1,3-divinyl-1,1,3,3-tetramethyl-disiloxane complex,[c]	reaction catalysis
moderator	–	2,4,6,8-tetramethyl-2,4,6,8-tetravinylcyclotetrasiloxane,[e]	moderating catalyst activity
filler	FS	silicon dioxide, fumed silica, SIS6962.0, >97%, [b]	functional filler, hexa-methyldisilazane (HMDZ) treated
additive	mica	muscovite mica mineral, $[KAl_2(AlSi_3O_{10})(OH)_2]$,[h]	functional filler, 20–50 μm
water, alkanols	water	water, Milli Rho grade	hydroxy-functional
	MeOH	methanol, ≥99.8%, ACS, [e]	
	n/a	ethane-1,2-diol, 99%, [e]	dihydroxy-functional, crosslinker
	n/a	propane-1,2-diol, pur., [d]	
	n/a	propane-1,3-diol, 96%, [f]	
	glycerol	propane-1,2,3-triol, [g]	
	n/a	butane-1,4-diol, [i]	
	n/a	pentane-1,5-diol, puriss., GC, [d]	
	n/a	hexane-1,6-diol, pur., [d]	
	n/a	heptane-1,7-diol, pur., [d]	

[a] Solid hexane-1,6-diol dissolved in MilliQ water. Suppliers: [b] Gelest Inc, [c] Hubei Chem, [d] Fluka Honeywell, [e] Sigma Aldrich, [f] Ferak, [g] Lah-ner, [h] OMYA, Norway, [i] ACROS Organics; n/a – not applied.

3.2.2 Two-part blend injection molding

The premixtures were combined and processed using an in-house foam injection molding (FIM) device specifically designed for these experiments. This FIM device allowed precise control over dispensing, mixing (300 rpm), and pressure, ensuring reproducibility. Both FIM vessels (separating premixtures) were equipped with temperature control (23 ± 2 °C). In approximately 6 to 8 seconds, 300 mL two-part premixtures were simultaneously combined and dispensed into molds. Following a 3-minute expansion and cross-linking period at RT, the resulting foams were post-cured at 80 °C for a minimum of 30 minutes. Subsequently, the foam was allowed to cool to RT before further testing.

3.3 Determining bacterial growth in foams

3.3.1 Foam samples and additives

The SIFs used in inoculation experiments were fabricated as described in previous sections, with the addition of specific additives for physicomechanical property enhancement purposes. Polyurethane foams were characterized as is and were not fabricated by us. The foams' properties are listed below in **Table 3**, and the characteristics of used additives are in **Table 4**.

Table 3. Characteristics of the foam samples selected for inoculation with *E. coli* and the additives varied in the corresponding formulations of SIFs. All SIF formulations contain a fixed ratio of mica and fumed silica as base fillers. Within this work, $kg \cdot m^{-3}$ is used as a unit for the apparent density, ρ_{app}, of foams.

Sample group	ρ_{app} ($kg \cdot m^{-3}$)	open volume (%)	surface porosity (%)[b]	d_{cell} (μm)[b]	additive in polymer blend (wt%)	
SIF	88	91	87±2	500±100	none	–
SIF-AC	117	88	91±3	500±200	activated carbon	0.9
SIF-SHU	150	85	85±3	200±100	shungite	0.5
SIF-CHI	135	87	88±1	300±200	chitosan	0.5
SIF-MeC	110	89	95±1	500±100	methylcellulose	5.0
SIF-TAN	175	83	89±2	300±200	tannic acid	0.5
PUR	90	91	92±1	400±100[c]	–	–
PUR-EG/APP	100	90	92±2	500±200[c]	expandable graphite, ammonium polyphosphate[a]	n/a

[a] Additives in PUR-EG/APP are applied as synergistic fire retardant additives but are not necessarily considered antibacterial in the scope of this work; [b] cell diameters were measured, and porosity calculated based on SEM micrographs and ImageJ software Fiji; [c] pores in cell walls were excluded from the calculations.

The foam samples were cut into cubes, each weighing approximately 0.2–0.4 g., and sterilized in a vacuum oven (Memmert) for 60 minutes at 200 °C and 3 mbar and placed in an autoclaved flask prior to inoculation experiments (§ 3.3.2).

Both the synthesized SIFs and the analyzed PURs contained known additives, which are listed in the following table:

Table 4. Specifications of additives and their properties.

Additive	Specifications	Particles	Solubility	Reported as antibacterial
Activated carbon (AC)	Merck	<100 µm fraction	water-insoluble	NO
tannic acid (TA)	$C_{76}H_{52}O_{46}$, Alfa Aesar, 17022,	powder solid	water-soluble	YES **[111], [112]**
methyl-cellulose	Methocel K15MS, Dow	<212 µm (>95%)	water-soluble	NO
chitosan	75–85% deacetylated, Sigma Aldrich	crystals, medium M_w	water-insoluble /soluble in dilut. aqueous acid	YES/ NO **[113]**
ammonium polyphosphate (APP) [a]	Exolit AP 422, Clariant Ltd.	17 µm, <50 µm (>95%)	low, 0.5 w/w%	n/a
shungite	<50% (C) [b], Gyllenhaal OÜ, Russia	powder	water-insoluble /partially soluble, [b]	YES **[114]**
expandable graphite (EG)[a]	GHL PX 98 N, Georg H. Luh, GmbH	300 µm	water-insoluble	YES **[115]** /NO

[a] *Additives in PUR-EG/APP are applied as fire-retardant additives but are not necessarily considered antibacterial in the scope of this work;* [b] *carbon in different modifications/metal oxides and silicon oxide attributes to partial hydrophilicity* [116].

3.3.2 Inoculating polymer foams with *E. coli*

We used the dynamic shake flask test to evaluate the antibacterial effectiveness of the foams quantitatively, based on ISO 23641:2021 [102] – a standardized method for testing flexible cellular polymers. This method ensures good contact between bacteria and the sample by constant agitation of the foam samples within a bacterial suspension for 24 hours. The samples were submerged in a liquid medium containing growth media and a non-pathogenic strain of *Escherichia coli*, Nissle 1917 (EcN), which is typically used as a probiotic. **Figure 14** is a schematic illustration depicting the process for determining bacterial concentrations in the growth media and in the phosphate buffer saline (PBS) used for washing out planktonic and adhered bacteria from the foam specimens.

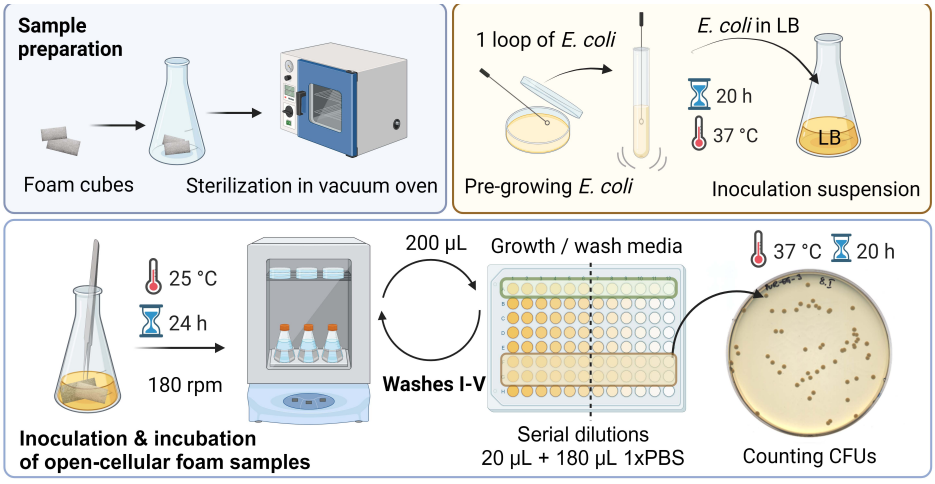

Figure 14. Schematics of the shake flask method to evaluate bacterial growth in the growth and in the wash medium. The main steps are described: sterilizing samples, preparation of inoculation suspension, inoculation of foams, growth medium collection and dilution, and plating and counting viable cells.

Different foam specimens were introduced to inoculation suspension consisting of 0.5 mL *E. coli* of bacterial inoculum and 30 mL of LB (Lysogeny Broth Lennox, Difco) medium, a hydrophilic aqueous nutrient broth containing tryptone, yeast extract, and NaCl (10/5/5) in deionized water. LB medium was used as a nutrient source for bacteria, and 0.1 M PBS, was used as a neutral washing medium. To avoid uneven inoculation of the sample due to the hydrophobic nature of SIFs, the cubes submerged in inoculation suspension were squeezed with sterilized tweezers to eliminate entrapped air until no visible air bubbles appeared. The foam cubes and *E. coli*/LB suspension flasks were shaken for 24 hours at 25 °C and 180 rpm. After the incubation period, a foam sample from each set was stored for further imaging by submerging it in a 3.7% formaldehyde solution (Panreac AppliChem) for cell fixation. The cell density in the growth media was evaluated by the absorbance of the bacterial suspension as turbidity as the OD600 (UV/VIS spectrophotometer Ultrospec 7000, Biochrom). The concentration of viable cells in the 24-hour growth media was approximately (0.5…1.0)x10^8 CFU/ml, determined by plating dilutions and counting colonies in triplicate.

The effect of foams and additives used on bacterial growth was evaluated by the change in bacterial count compared to a foamless inoculum and the inoculum starting concentration. For this, aliquots were first collected from the 24-hour growth medium surrounding the foam cubes. To evaluate the bacterial growth and adhesion in the open-cellular structure of the foams, a series of washes were followed to extract the bacteria from the cubes. This was done by transferring the sample into a sterile Erlenmeyer flask containing 30 ml of 0.1M PBS and subjected to five subsequent wash cycles of 10 minutes at 25 °C and 180 rpm. The bacterial cell density of the wash samples was assessed by OD600, and the

aliquots collected from the wash media were serially diluted 10-fold in each step using PBS. 100 µL of dilutions were plated onto LB agar plates and incubated overnight at 37 °C. The bacterial colonies were counted, and initial concentrations were calculated from the counted colony numbers, considering specific dilution factors.

Additionally, we investigated how reducing the amount of LB growth medium and removing agitation and aeration affect the growth of *E. coli*. To achieve this, we compared foam samples that did not benefit from these factors by immersing SIF and SIF-AC samples (sample set '**AIR'**) in the inoculation suspension and incubated them at 37 °C for 24 hours in a controlled humidity environment. These samples were analyzed using the subsequent washing as described previously for other foams.

3.4 Characterization

3.4.1 Determining physicomechanical properties of foams

3.4.1.1 Apparent density of foams

Apparent densities (hereafter defined as ρ_{app}, kg·m^{-3}) of molded foams were determined via glass bead pycnometry. To determine the density of the skinless foam, rectangular parallelepiped specimens were cut from a vertically sliced cross-section of the molded foam, and its weight and dimensions were used to calculate the ρ_{app} of the foam. The expanded measurement uncertainty was U(density, molded) = 3 kg·m^{-3} with a confidence level of 95% (k = 1.9), which also shows excellent reproducibility of the foams using the injection molding technique.

3.4.1.2 Cellular morphology of foams

The cellular structure of foams synthesized using different blowing blends was determined using SEM (TM-3000, Hitachi HighTechnologies Corporation, Tokyo, Japan). The foam samples were sputter-coated with a 10 nm thick gold layer (Leica EM ACE600 Sputter Coater, Wetzlar, Germany) and observed under 15 kV. The average d_{cell} and d_{wall} were determined from the cross-sectional areas of torn foam specimens by analyzing SEM micrographs in Fiji application in ImageJ 1.54f [117]. The results are expressed as the average of 100 measurements for each sample; respective data and standard deviation values of foam's cellular structure are presented in **Publication II** as part of the *Appendix*, in *Table A2*.

Foam samples investigated before and after inoculating with bacteria were sputter-coated with a 7.5 nm thick gold layer. Foam's structural information, including surface porosities, was acquired as described in the previous paragraph.

3.4.1.3 Water contact angle measurement

Static contact angles (θ_C) for DI water were measured by applying the sessile drop method to evaluate the foams' wettability for both the open-cell foam and the skin-like layer that forms upon molding. The measurements were performed at RT, mounting 5 ± 1 µL liquid droplets in three different areas of the sample; the mean values of WCA with a measurement accuracy of ±0.5° were determined using Surftens Universal Software (Surftens Version 4.6) [118]. Both polyurethane foam samples, PUR and PUR-EG/APP, and two SIF representative samples, SIF and SIF-AC, were analyzed. Results are summarised in Supplementary material of **Publication III** in **Table S1**.

3.4.1.4 Tensile properties

Elongation at break ($\boldsymbol{\varepsilon_b}$, %) and tensile strength ($\boldsymbol{\sigma_b}$, MPa) of the foam samples were measured at 300 mm·min^{-1} test speed using a motorized test stand (model AEL-A-1000 by Hefei Vetus Electronic Technology, 3–1000 N) following the procedures in the ISO 1798:2008 [102] and ASTM D 3574-17 [119] standards. The test specimens were die-cut from a flat sheet obtained from a vertical cross-section (foam rising direction) and were free of ragged edges. The foam specimens were secured using a screw-type jagged plate grip that exerted uniform pressure across the gripping surface. All measurements conducted at RT (22±2 °C) were performed in triplicate, and the expanded measurement uncertainty for each foam sample was calculated. From ρ_{app} and σ_b values, specific strength values of foams were calculated.

3.4.2 Determining physicomechanical properties of blends

3.4.2.1 Viscosity measurements of polymers and polymer blends

Viscosity directly affects the homogenization during the mixing process, equal distribution of components A and B from the IM machine, the flowability of the dispensed blend, and eventually, the density of the final foam. Predicting blend viscosity is reasonable when the viscosities of combined fluids do not differ by more than one magnitude. However, polymers with kinematic viscosities (the measure of the volume flow of a liquid) varying from 25 to 80000 cSt were blended here, and several particulates and blowing additives were introduced. To avoid severe fluctuations in premixture viscosities, we conducted control measurements using a commercial NDJ-5S VEVOR digital rotary viscometer measuring the dynamic viscosity of polymers and blends (1–6000000 mPa·s). In addition, viscosity measurements are also important for quality reasons. Due to the allowed fluctuations in viscosities of industrial chemicals, specifically high M_w polymers, the actual values are needed to maintain the viscosity for a controlled LIM process, thereby increasing the number of variables.

3.4.3 Spectroscopic characterizations

3.4.3.1 ^{1}H-NMR: Determining Si–H content in PMHS

To determine the actual Si–H content in PMHS (HMS-992) used in kinetic experiments, a ^{1}H-NMR characterization was performed on a Bruker Ascend 700 MHz spectrometer, using chloroform-*d* as solvent and dioxane as an internal standard. The obtained chemical shifts were as follows: δSi–H=4.71 ppm (1.09, d, 1.2 Hz), δSi–CH_3=0.19 ppm (3.36, s).

The –H% calculated from ^{1}H-NMR measurements was 101.09% (15.55 mmol·g^{-1}) which stays within the uncertainty of the measurement. According to the reagent data provided by the supplier, the -H concentration is approximately 15.38 mmol·g^{-1}; for PMHS as a low M_w, such fluctuations in actual content are allowed. The characterization data were identical to those previously reported in the literature [108]. The respective ^{1}H-NMR spectrum is found in the Supporting information of **Publication I**.

3.4.3.2 FT-IR: Determining Si–H content in cured SIFs

The infrared spectra were collected using FT-IR (Bruker, Billerica, MA, USA, Platinum-ATR, diamond crystal to characterize the foam structure, specifically the extent of Si–H conversion. The cured SIF samples analyzed were 100% water-blown, 10 mol% glycerol, methanol, and butane-1,4-diol blown foams. In addition, the Si–H peaks for PMHS polymer and an uncured polymer blend (containing water as the blowing agent) are shown. The FT-IR analysis proved that hydrosilylation did occur, resulting in a highly crosslinked network. The spectra are available in the Supplementary information of the related study, **Publication II**.

3.4.3.3 Elemental mapping of polymer composite surface of SIFs

The SEM-EDX technique was applied to acquire the surface composition of foam materials with SEM (Hitachi TM3000) equipped with an EDX detector and special hardware and software (SwiftED3000 by Oxford Instruments). Elemental compositions were studied by retrieving data from 20 points, and the results were averaged. Elemental data for SIF-SHU, SIF-CHI, and SIF-TAN are presented in *Figure 5* in **Publication III.**

3.4.3.4 Imaging the adhered bacteria via SEM

Before applying SEM, it was essential to fix the bacterial cells inside the foam cells, as well as on the surface of the foam sample, and to extract the liquid medium from the porous test cubes. Additional preparative procedures include cutting and sputter-coating, which are summarized in **Figure 15**.

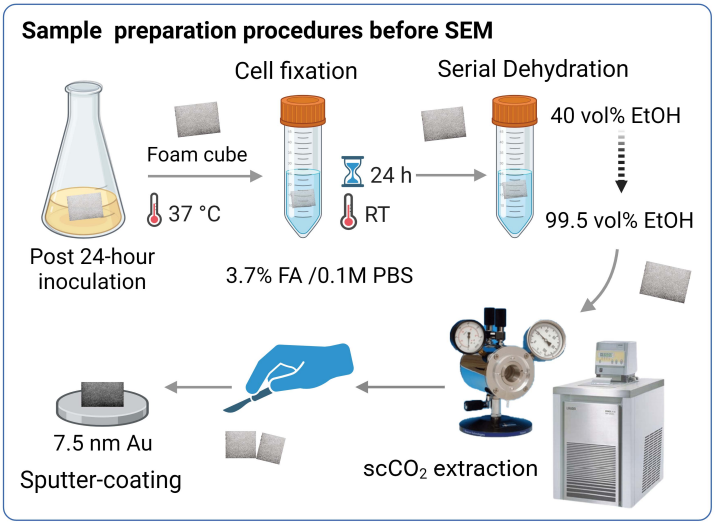

Figure 15. Process scheme for preparing inoculated foam samples for SEM imaging.

After the inoculation period (24 hours), a test cube from each inoculation set was removed and placed in a 3.7% formaldehyde/PBS solution for another 24 hours. The cubes were then stored at 4 °C. Subsequently, the aqueous solution used for cell fixation was gradually exchanged with ethanol (99.5%) by a step-wise process of serial dehydration. The foam samples were sequentially immersed in ethanol-water solutions with increasing ethanol content (from 40% to 90% ethanol in water, in 10% increments) for 2 hours in every solution, followed by another 2 hours in a 96% ethanol/water solution. Additionally, the samples were left overnight in 99.5% ethanol and another 99.5 % for storage. The ethanol was then extracted from the foam porous structure along with the CO_2 under super-critical conditions. We used a manual critical point dryer (E3100, Quorum Technologies) and a thermostat (Proline RP 1845, LAUDA) maintaining 15 °C. This technique adopted from Priks *et al.* [35] proved efficient, as no integrally damaged bacterial cells were later observed in the sample pores by electron microscope. The samples were first freeze-dried and carefully cut with a stainless steel blade with a slow incision so as not to damage the bacterial formations in the pores. The cut specimens were coated with a 7.5 nm layer of gold via physical vapor deposition (Leica EM ACE600 Sputter Coater, Wetzlar, Germany) for further imaging under SEM (Hitachi TM3000) using 15 kV as observation mode.

4 FOAM FORMATION

In this chapter, the findings presented in **Publication I** are discussed, focusing on the role of the dehydrocondensation reaction, which is an integral process in the chemical blowing of SIFs. A particular emphasis is placed on the use of low molecular weight (M_w) alcohols as a potential hydrogen source. The study detailed in **Publication I** explores how logical molecular descriptors for monoalcohols influence hydride conversion, reaction kinetics, and their performance as blowing agents in catalytic dehydrocondensation reactions with hydride-functionalized polysiloxanes. Conducted independently of the conventional multi-component foam synthesis process, this research aims to clarify the contributions of various monoalcohols in chemical blowing.

4.1 Enhancing the foam structure via additional Si–H conversions

Compared to various independent polymer blowing techniques, the evolution of gas from chemical reactions taking place on the polymer backbone is more controllable and supports the formation of a homogeneous cellular structure [120], [121]. During foam synthesis, it is crucial to carefully time the evolution of gas from a chemical reaction while simultaneously facilitating crosslinking, particularly when most of the Si–H in PMHS is being consumed. This approach allows for more efficient capturing of gas, leading to a decrease in foam density (ρ_{app}). Since crosslinking and gas evolution arising from dehydrocondensation occur simultaneously, any changes in reaction conditions or reactant properties can significantly impact the final outcome. These considerations serve as the foundational principles for the material's density and mechanical properties, thereby influencing its performance in various applications.

Currently, we are missing consistent and systematic information on the reaction kinetics of the dehydrocondensation reaction, which would endorse the selection of reactants for SIF blowing. Understanding the kinetics is essential to designing the desired cellular structure of the foam – the cell density, d_{cell}, d_{wall}, and shape of the struts connecting the cells. In order to improve our understanding of dehydrocondensation reaction we examined the kinetics of H_2 evolution from reaction between PMHS and monoalcohols. Hydrogen released from this reaction is the gas that creates a porous structure.

4.1.1 Non-crosslinking dehydrocondensation of PMHS with monoalcohols: State of the art

In addition to OH-PDMS, introducing low M_w hydroxyl group containing molecules is, in fact, often used as an additional means for generating gas. In this context, alcohol and PMHS are reacted to generate H_2 inherently (see **Reaction** 1).

The dehydrocondensation reaction, also known as dehydrogenative coupling or alcoholysis in this context, is a catalytic process in which the hydride in the Si–H bond is substituted by the alkoxy nucleophile -OR, resulting in the formation of the corresponding alkoxy siloxane and the liberation of H_2 [107].

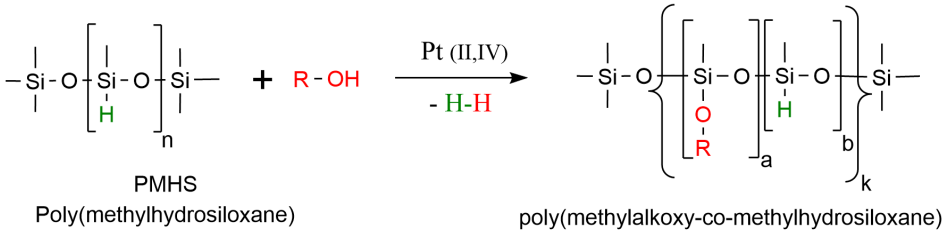

Reaction 1. Dehydrocondensation reaction between Si–H functionality of polymeric PMHS and alkanol (i.e. R=alkyl). Dihydrogen is released as a sole by-product.

Such reactions can be conducted at RT, therefore being more economical than using alcohols as volatile organic compounds (VOCs) at heightened temperatures. Harinath *et al.* have stated that "catalytic dehydrogenative coupling of alcohols with hydrosilanes represents the most attractive and atom-economical route to obtain silyl ethers as this process produces hydrogen gas as the sole by-product" [122]. We can look at PMHS as a polymeric example of a hydrosilane with a multitude of distinct silane groups attached to the siloxane backbone.

The Lamoreaux catalyst, a $Pt^{II,IV}$ in octanol complex, facilitates the reaction between the Si–H bond and the hydroxyl group to form an alkoxysiloxane. This mechanism involves several steps. Firstly, the catalyst activates the Si–H bond in PMHS, making it more reactive. Subsequently, the alcohol's hydroxyl group acts as a nucleophile and attacks the activated silicon atom. The hydrogen from the Si–H bond is transferred to the hydroxyl group, forming hydrogen gas and a new Si–O bond. This results in a new siloxane linkage (Si–O–R) and the release of H_2.

The primary focus of previous studies examining the alcoholysis of hydride-functional siloxanes has been on macromolecular grafting and the analysis of the resulting alkoxysiloxanes [83], [84], [85]. These studies have paid considerably less attention to the molecular properties that may influence the reaction and conversion depth. Owing to the quantitative nature of the reaction between Si–H and R–OH, the discussions in these studies have centered on the catalyst's type and its concentration, reaction conditions, and, in some instances, the reactant molar ratios. The reaction temperature and catalyst concentrations often vary to optimize the yield of alkoxysiloxane.

4.1.2 Catalysts applied in PMHS alcoholysis

Studies from recent decades reflect the increasing use of platinum-group metal catalysts in research and industry [58]. Besides initiating hydrosilylation, these catalysts are also applied in dehydrocondensation reactions with alcohols. In

2005, Chauhan *et al.* demonstrated the effectiveness of palladium-nanocluster catalyst in alcoholysis of PMHS homopolymer (n=32–33) at RT with various (primary, secondary, tertiary, organic, and functional) alcohols, including ethanol, 2-butanol, and tert-butanol (listed in the order of decreasing activity) [123]. Safa *et al.* (2009) conclude that Pt catalysts are suitable for initiating dehydrocondensation between PMHS and alcohols, and the corresponding catalytic mechanism is applicable in reactions with primary, secondary, and functional alcohols [108]. Among Pt-species, Karstedt's catalyst is shown to be more efficient than Speier's, activating dehydrocondensation reaction under mild conditions ($[Pt^0]/[Si–H]=15\times10^{-5}$, 20 °C, air) and yielding near-maximum products in a few hours [108].

4.1.3 Comparative analysis of alcohol reactivities towards PMHS

In a previous study, Juraskova *et al.* [124] compared the alcoholysis of hydride functional crosslinkers and variations of PMHS. The study showed that at least 500 ppm (mPt/mHydrosilane x 10^6=500 ppm) of Pt (Karstedt's catalyst) is required for the ethanolysis of telechelic H-PDMS-H to achieve a Si–H conversion above 90 mol%. The authors found that in reactions involving various pendant PMHS-*co*-PDMS with different levels of H-functionalization (7%–9%, 15%–18%, and 45%–55%), increasing Si–H mol% in the polymer chain led to decreased overall conversion and earlier plateauing, without reaching maximum yields under the provided conditions. The study concluded that higher Pt concentrations are necessary for full conversion over the same period. The earlier plateauing of the reaction is attributed to increased steric hindrance resulting from grafting, which leads to the formation of alkoxy groups and associated increases in viscosity. Additionally, the authors investigated the reaction of telechelic H-PDMS-H with various alcohols (see **Figure 16**) and found that the resulting reaction curves effectively demonstrate the steric hindrance of bulkier alcohols (*t*-BuOH, IPA (=*iPrOH in this dissertation*) and the poor miscibility of methanol (MeOH). Although highly H-functionalized PMHS was not used in the study, the reaction with telechelic chains provides valuable insights into the applicability of both PMHS and monoalcohols in such reactions.

The current research focuses on using reactions for molecular grafting in alkoxysiloxanes, which are important industrial crosslinkers [124]. The PMHS homopolymer is less commonly utilized, likely due to low product yields or impractical mechanical properties. While the use of water and alcohols in SIF blowing has been addressed in patents [125], [126], variations in polymer blends, catalyst concentrations, and synthesis conditions make it difficult to compare their effectiveness as chemical blowing agents. There is still uncertainty regarding the specific performance of alcohols, particularly how the rates of catalyzed dehydrocondensation reactions vary with Si–H conversion and which monoalcohols are most effective for H_2 generation. Additional studies on the alcoholysis of polymeric hydride, specifically PMHS, would help clarify the role of monoalcohols in SIF synthesis.

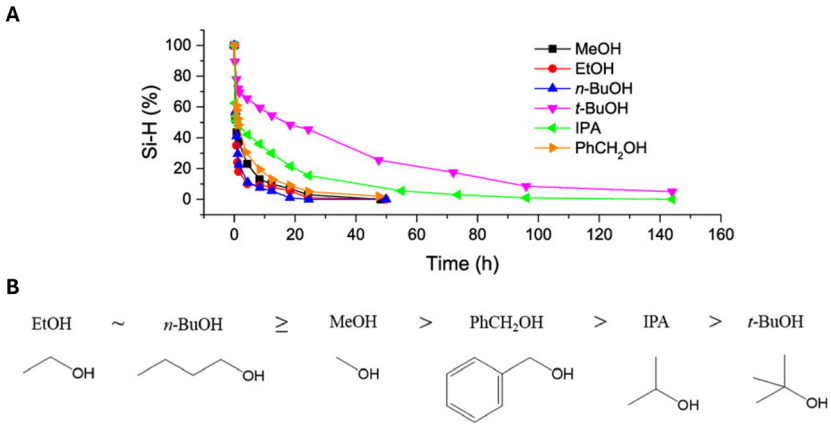

Figure 16. Alcoholysis of telechelic hydride-functional crosslinker (H-D_8-H). Catalytic Si–H conversion by various alcohols (A) and alcohol reactivity order (B). "D" represents -$(CH_3)_2SiO$-, *i.e.* dimethylsiloxane unit, IPA=isopropyl alcohol (2-propanol). Adapted with permission from Jurásková *et al.* [124]. ©2020 American Chemical Society.

For effective bubble nucleation and H_2 evolution, the efficiency of the dehydrocondensation reaction must match the concurrent crosslinking early in the reaction. Ideally, a higher volume of H_2 should be produced in the initial minutes of foaming for optimal expansion. The reaction between Si–H and R–OH likely varies early on due to different alcohol structures and reactivities. A more detailed comparison of conversion rates for different alcohols during the first minutes of the reaction would give greater insight into identifying suitable blowing agents. Our focus has been on the evolution kinetics of H_2 rather than total yields. The next chapter details kinetic measurements and discusses the findings.

4.2 Studying the kinetics of PMHS alcoholysis

4.2.1 Discussion on dehydrocondensation reaction kinetics

A platinum-catalyzed dehydrocondensation reaction between PMHS and a selection of monoalcohols was studied in isolation under mild conditions. The Si–H conversion with monoalcohols was intentionally observed separately from the typical foam synthesis involving multiple entities, as the objective was to understand the role of distinct monoalcohols. The study aimed to understand how different logical descriptors for alcohols describe the reaction's kinetic parameters and the formation of hydrogen at various stages of the reaction.

Although the discussion focuses on monoalcohols and their reactivity, the same reaction was conducted by applying water as a hydride source. Water is not only a desirable blowing agent, but it also acts as a potential crosslinker, or more precisely, as a propagator of additional crosslinks. This is due to the sequential dehydrocondensation reactions that occur, starting with the formation of silanol (from Si–H to Si–OH and the evolution of dihydrogen). This is followed by

crosslink formation between Si–OH and another Si–H in the vicinity. Relatively rapid crosslinking between PMHS chains causes progressing solidification of the reaction mixture, thus restricting the mobility of reactants and hindering further conversion. Due to these circumstances, the expected conversion depth, hence hydrogen volume, was not reached. The respective Si–O–Si crosslinks formed between PMHS chains in dehydrocondensation reactions are extremely short, and the expanded foam would exhibit higher brittleness, especially for high crosslink densities.

However, since monoalcohols do not form crosslinks between siloxane chains, these monofunctional molecules can be implemented as cell size and porosity adjusters by progressively increasing the viscosity of the reaction blend due to the polymer grafting while simultaneously benefiting from generated hydrogen. To study the contribution of alcohols to the blowing process, we considered a range of simplest monoalcohols covering diverse structural features. Starting with alcohols with the lowest M_w (methanol), increasing towards more complex (propan-2-ol, 2-methylbutan-2-ol, butan-2-ol, 2-ethylhexan-1-ol), varying in length and branching of the hydrocarbon chain. For brevity, the acronyms listed in **Table 1** and **Table 5** are used for further discussions.

4.2.2 Molecular descriptors

Molecular descriptors are experimentally measured or theoretically calculated representations of the physicochemical properties of molecules. These quantitative descriptors, derived from a molecule's structure, can be used to predict the behavior of chemicals under various conditions, including their activities [127]. Based on the collected data in **Table 5** we could hypothesize about the individual performance of these alcohols and the kinetic performance of the catalytic dehydrocondensation reaction. First, an explanation of these properties is necessary.

Table 5. Properties and molecular descriptors of the alcohols considered in analysis: Taft–Dubois steric constant (E_s) [128], relative permittivity (ε_r) [129], [130], log of the octanol-water partition coefficient (logP), and calculated and experimental values of acid's dissociation constant pK_a in dimethyl sulfoxide (DMSO) and water. [Pub I]

Alcohol	**-R, alkyl chain**	***M_w,*** *g/mol*	***E_s*** [128]	***ε_r*** [129]	***logP*** *exp* [131] */pred*	***pK_a*** *in DMSO, exp / pred*	*in water, exp / pred*
MeOH	$-CH_3$	32.04	0.00	33.0	–0.77/–0.81	29.0/29.2	15.5[b]/16.2
iPrOH	$-CH(CH_3)_2$	60.09	–0.48	18.3	0.05[g]/–0.16	30.3/29.0	16.5[c]/16.8
secBuOH	$CH_3(-CH)C_2H_5$	74.12	–1.00	16.56	0.61 / 0.47	n/a /28.9	17.6 /16.9
tAmOH	$-C(CH_3)_2CH_2CH_3$	88.15	–2.28	5.78	0.89 / 0.93	n/a /29.4	n/a /17.6
iOctOH	$-CH_2CH(C_2H_5)(CH_2)_3CH_3$	130.23	~ –1	7.70	2.84 / 2.95	n/a /27.7	n/a /16.7

Note: Specifications of values obtained and corresponding references are presented in the authors' original article ***Publication I.***

4.2.2.1 Alcohol performance based on molecular descriptor data

The **molecular weight** ($\mathbf{M_w}$) of a molecule significantly impacts reaction kinetics by influencing the mobility of molecules and the energy landscape of chemical reactions. In general, molecules with lower molecular weights diffuse faster, leading to quicker reaction rates. Therefore, it would be logical to conclude that the increasing M_w of the alkoxylated PMHS will affect the reaction rate as the conversion progresses. Longer alkyl chain (C_n), branching, and higher M_w of alcohol, in general, all contribute to increased lipophilicity due to increased methyl content and lower polarity, favoring miscibility in hydrophobic polysiloxane and leading to a more uniform reaction. In comparing mono-functional alcohols, the MeOH is the least, and iOctOH is the most miscible in PMHS. Although the diffusivity of alcohols is expected to be lower at higher M_w, this effect may become negligible as the nonpolar interactions are favored and support the interaction of reactants and catalysts. These fundamental differences arising from alcohols' M_w may cause significant changes in the conversion rates during the progressing alkoxylation, namely when the steric hindrance of Si–H on PMHS increases and the Si–H/R–OH ratio decreases.

Hence, the values of the **octanol-water partition coefficient, logP**, are especially informative in predicting the tendency of the miscibility of these alcohols in a hydrophobic polymer blend. Generally, similar logP values favor better miscibility of the reactants. Introducing relatively hydrophilic alcohols into hydrophobic PMHS results in a bi-phase reaction environment, which can hinder the mobility of the catalyst and reactants, thus affecting the reaction rate. The lipophilic PMHS chains (logP ~2.7) could predict the most preferable hydrophobic interactions with iOctOH (logP ~2.8), followed by less miscible tAmOH, secBuOH, iPrOH, and MeOH as the least hydrophobic alcohol. The progressive grafting of siloxane units with -OR (where R=alkyl) substituting -H suggests a change in alkoxysiloxane logP value due to the added relatively polar pendant groups, however, accompanying alkyl groups also contribute to the hydrophobicity.

The **dielectric constant**, denoted as $\boldsymbol{\varepsilon_r}$ and also known as relative permittivity, is a critical factor in chemical reactions, influencing primarily the reactant solubility and the rate of reactions. As an indicator of **solvent polarity**, ε_r describes the (i.e. alcohols) **solvation effectiveness** and the Gibbs free energy, which are vital for the spontaneity and progression of reactions. Moreover, a high ε_r can reduce the activation energy needed, thereby accelerating reaction rates. Generally, lower M_w alcohols have higher ε_r values, indicating their higher polarity as solvents. However, changes in molecular structure, such as branching on tAmOH, decrease the ε_r (5.78), suggesting stronger nonpolar interactions with PMHS than for iOctOH with higher ε_r (7.70). Although beneficial for reaction rate acceleration, the more polar molecules have weaker interactions in nonpolar PMHS. Hence, the lowest ε_r (5.78) for tAmOH suggests the weakest rate acceleration, proposedly noticed during the initial phase.

A key factor in catalysis, especially in reactions involving proton transfer, is the alcohol as an acid's (in the context of this study) ability to donate a proton in

aq. solution [133] which is described by the **dissociation constant pK_a**. The pK_a value is directly related to the structure of the given compound and indicates how readily the alcohol molecule will participate in the reaction, consequently influencing the rate and outcome of the process. In our alcohol selection, the tAmOH holds the highest (predicted) pK_a value – both in water and DMSO – indicating that tAmOH, the weakest acid, would be least favored to proceed towards completion than other alcohols. The strongest acid based on pK_a in DMSO would be iOctOH (27.7), followed by secBuOH and iPrOH with similar values (28.9, 29.0).

Taft's steric parameter (E_s) is used to describe the steric effects of substituents on the reactivity of a molecule. A higher E_s (value more negative) indicates higher steric hindrance, which can slow down or halt reactions, especially those that require close proximity to reactants, such as nucleophilic substitutions. On the other hand, a lower E_s (near 0 value) suggests less steric hindrance and potentially faster reaction rates. Based on the theoretical E_s data, the steric hindrance is highest for tAmOH, a tertiary alcohol. The E_s of iOctOH is lower than that of tAmOH due to the ethyl substitution location at the second carbon, making the OH group more accessible (E_s estimated ~ –1.0); secBuOH bears a similar E_s value (–1.0).

Combining these assumptions, the molecular descriptors mentioned above describe the reaction rates in a somewhat predictable manner if handled individually. As the progressing reaction involves changes in M_w, viscosities, and reactant diffusion, the role of one individual descriptor may become less decisive over another. In the next section, the results of catalyzed alcoholysis are discussed.

4.2.3 Hydrogen volume profiles

4.2.3.1 Evolution profiles for 12-hour conversion

It is known that the gas evolution kinetics will depend on the overall kinetic performance of the reaction, dependent on reaction conditions, catalyst, and the reactivity of alcohol towards the polymeric hydride. With fixed ratios of $[Pt^0]$/[Si–H] (i.e. 15 ppm Pt/5 mmol Si–H) and [Si–H]/[R–OH] (1:10 molar ratio of Si–H : R–OH), the only variables in these reactions are monoalcohols and their physicochemical properties.

During the catalytic alcoholysis reaction, the gaseous hydrogen is given off quantitatively in 1:1 stoichiometry. The conversion of Si–H groups can, thus, be calculated from the evolved H_2 by applying (2)–(4):

$$[Si-H]_t = \frac{n_{t_0}(-H) - n_t(H_2)}{V_s}, \tag{2}$$

$$n_t(H_2) = \frac{pV_t(H_2)}{RT}, \tag{3}$$

$$[Si-H]\% = 100\% - 100\% \frac{[Si-H]_t}{[Si-H]_{t_0}}, \tag{4}$$

where **[Si–H]** is the concentration of Si–H groups in the reaction mixture at a given time ***t*,** or as a **%** of unconverted Si–H groups remaining initial concentration, ***n*** is the number of moles for -H in PMHS and reaction product H_2, and $\mathbf{V_s}$ is the volume of the reaction mixture, V_t is the volume of H_2 at given time *t*. In this quantitative catalyzed reaction under provided conditions (50 mmol of R–OH, 5 mmol Si–H, 15 ppm Pt, 27 °C, H_2 atmosphere), the theoretical V_{max} of H_2 is ≈ **125 mL**, corresponding to a 100% conversion of Si–H (see *Formulation of dehydrocondensation reaction* in the *MATERIALS AND METHODS* section).

In 12 hours, complete conversion was not achieved for any of the studied alcohols (**Figure 17**).

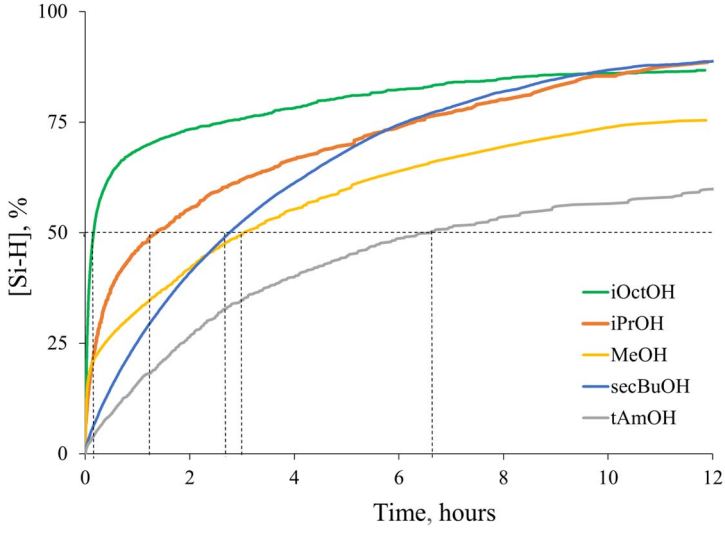

Figure 17. Decrease of hydride group concentration in PMHS ([Si–H], %) upon reaction with different alcohols. Horizontal line intersections correspond to the specific half-lives ($\tau_{1/2}$). [Pub I] © 2022 Wiley Periodicals LLC.

Different alcohols displayed varying behavior in the alkoxylation reaction, leading to different reaction rates, half-lives ($\tau_{1/2}$), and conversions. Under the specified conditions, the overall conversion of Si–H in 12 hours (and for 24 hours), in decreasing order, is (**Figure 18**):

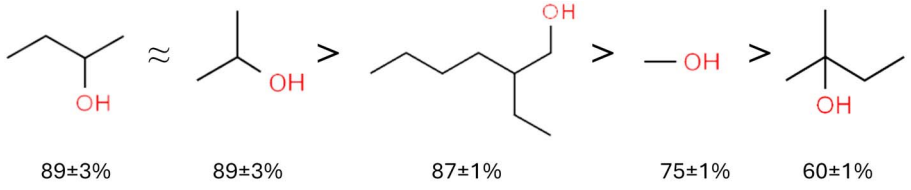

Figure 18. Overall conversion performance of alcohols in 12 and 24 hours based on gas evolution kinetics.

The similar performances of secBuOH and iPrOH, or the performance of other alcohols in comparison, cannot be simply explained using a single logical descriptor despite their performance being the closest to theoretical values of pK_a in DMSO (**Table 5**).

Likewise, the alkoxylation process cannot be accurately described by a single rate constant from start to finish. This is because one of the reactants, PMHS, undergoes gradual changes during each reaction step. Consequently, once the initial -OR is grafted onto the polymer backbone, the original state of PMHS is no longer maintained. Under gradual alkoxylation, the monomer fragments of PMHS increase in size, and the amount of unreacted Si–H decreases. An exemplary kinetic curve in **Figure 19** for iOctOH depicts how, after a good head-start, the conversion reaction curve starts to plateau the soonest (past half-time) without ever reaching full conversion. Further miscibility and access to consecutive Si–H groups may become complicated as the bulkiness increases; thus, a significant % of the [Si–H] remains unreacted.

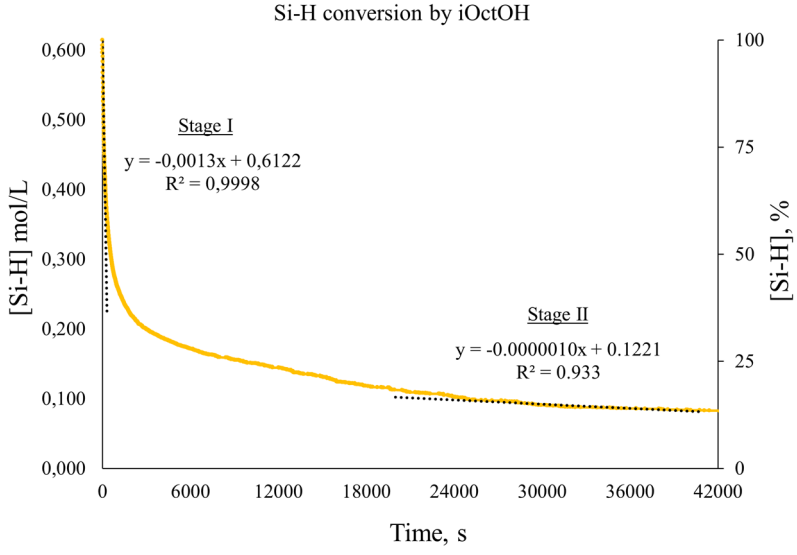

Figure 19. First 12 hours of PMHS alcoholysis with iOctOH: Decrease in [Si–H] ($mol \cdot L^{-1}$) with distinguished reaction stages and rate constants from slopes of linear correlations. **[Pub I]** © 2022 Wiley Periodicals LLC.

We observed a distinctive change in reactivities after the initial stages (from 30 min and forward), especially for MeOH and iOctOH being initially the highest performers. After nearly 25% conversion of Si–H with MeOH, the reaction slows down and remains incomplete at 12 hours. The second performer during the initial stage was iOctOH; however, after a significant > 50% conversion in ~ 15 minutes, the reaction kinetics changed. In contrast, the slow and steady performance of secBuOH in Si–H conversion eventually resulted in one of the highest conversions (89%) like for iPrOH (89%), whereas the performance of tAmOH

met our expectations of both slow rate and low depth of conversion due to the high steric hindrance of this tertiary alcohol.

While it would be ideal to have a specific rate constant for each step of the reaction, determining these values is highly complex and often leads to inconclusive results. However, it is possible to pinpoint certain stages of the reaction where the rate constants remain relatively stable. Fortunately, one such stage is the initial phase (stage I) of the reaction, when the PMHS undergoes minimal modification. For practical applications, it is naturally also the most important stage of the reactions. Understanding the final stage (stage II), just before reaching the conversion plateau, is important as it allows for the selection of desired process durations and hydrogen evolution rates. Therefore, for blowing enhancement purposes, it is important to consider the individual stages of the reactions rather than the entire reaction.

4.2.3.2 Reaction order of the initial stage

The first part of the reaction, where the kinetic curves correspond to linear regions (where the coefficient of determination is high, $R^2>0.991$), was regarded as the initial stage ("stage I" in **Figure 19**). The individual stage I graphs depicting the conversion of [Si–H] (mol·L^{-1}) by alcohol plotted against time (s) are presented in *Figure 4* of **Publication I**, and the rate constants from stage I (k_I) and stage II (k_{II}) in *Table 3* in **Publication I**. The Pt-catalyzed alcoholysis of PMHS in stage I appears to be of zeroth order with respect to PMHS, thus being independent of the reactant concentration. Given that no side reactions take place, the reaction rate $\boldsymbol{v}$ for the catalyzed dehydrocondensation, thus, for the formation of H_2 over time (t) in this stage, can be described with the rate law:

$$v = -\frac{d[Si-H]}{dt} = \frac{d[H_2]}{dt} = k. \quad (5)$$

Recalling that the initial molar ratio of Si–H to R–OH in this reaction is a constant ten-fold excess of alcohol, the reaction order can be regarded as a pseudo-zero order, during which the reaction rate remains constant only in a stage where the alcohol in excess is not yet significantly consumed. Hence, a major factor in conversion is the reactant diffusivity under the reaction conditions provided. As the process is agitated by constant stirring, the likelihood of reactive functionalities and catalysts coming into proximity and binding to the catalyst increases, leading to reaction rates approaching their theoretical values.

The performance of alcohols based on the **rate constants** (or reaction rate, as $\boldsymbol{v} = k_I$, (5)) for the initial stage (k_I), in decreasing order, is as follows (**Figure 20**):

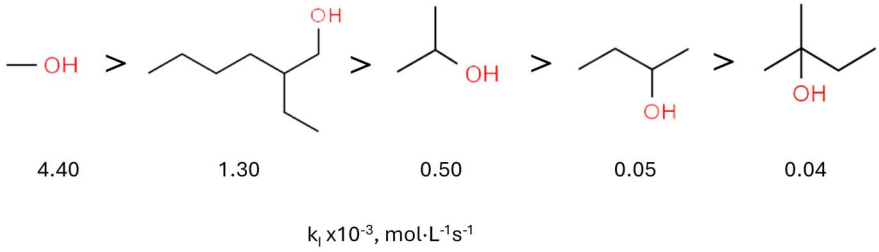

Figure 20. Order of alcohol reactivity in catalyzed dehydrocondensation reaction with PMHS according to the reaction rates for the initial stage (Stage I).

The k_I values vary largely and seemingly correlate with the performance of bulkier alcohols with the exception of iOctOH; however, we found that the performance in stage I is in accordance with the predicted pK_a values in water. Over the full course of the reaction, a similar tendency of primary alcohols to overperform secondary simple alcohols was observed by Safa *et al.* [108].

The duration of stage I varies for each alcohol in the catalyzed reaction. Considering the necessity for a fast cure and, therefore, maximized gas evolution in a relatively short time (< 5 min), the respective **half-times τ½** (represented in *Table 1* in **Publication I**) should be considered in addition to the k_I. Here, τ½ is a critical indicator of the actual performance due to the duration of conversion where $v = k_I$ varies among alcohols. Based on the τ½, the performance in converting half of the Si–H groups into H_2, in decreasing order, is (**Figure 21**):

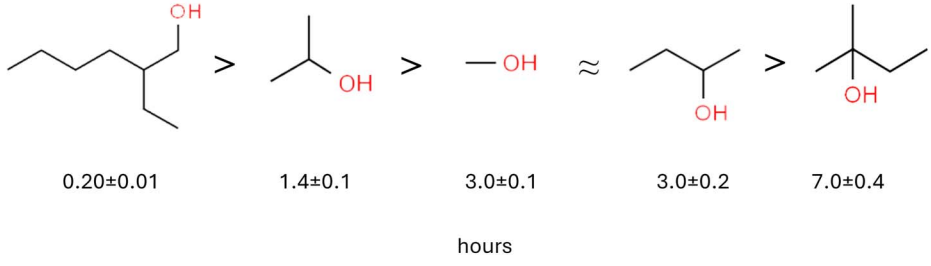

Figure 21. Performance of monoalcohols in hydrogen generation based on **τ½**.

Comparing the orders in reaction rates (**Figure 20**) and τ½ (**Figure 21**), it is evident that under the provided conditions, iOctOH outperforms other alcohols significantly, being the workhorse for PMHS alcoholysis in terms of gas generation. The following section compares and discusses the reaction profiles for the first five minutes to better understand the reasons behind the performance orders.

4.2.3.3 Hydrogen evolution profile of first 5 minutes of reaction

It was previously shown that in stage I ($v = k_1$), the primary alcohols, MeOH and iOctOH, outperform secondary and tertiary alcohols (see **Figure 20**). Focusing on the **first five minutes**, a similar order is seen with the exception of iOctOH outperforming MeOH and other alcohols, as shown in **Figure 22** and **Figure 23**.

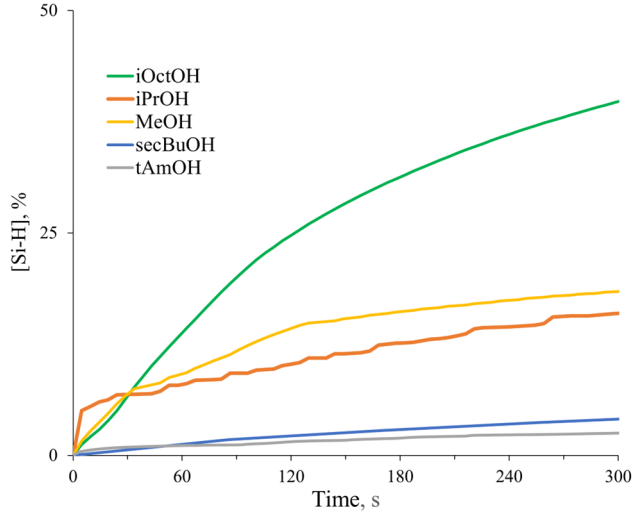

Figure 22. Hydrogen evolution during the first 5 minutes, expressed as Si–H conversion (%) from the initial concentration.

Based on the reaction profiles in **Figure 22** the order of Si–H conversion performance is:

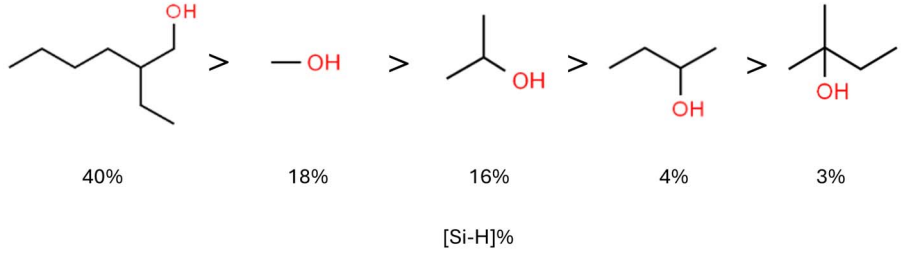

Figure 23. Si–H conversion performance (%) in the first 5 minutes in decreasing order.

The reactivity and performance of iOctOH are obviously beneficial for a steady H_2 evolution during polymer matrix solidification. We can see that the reactivity of MeOH and iPrOH significantly contributes to the rapid production of gas. However, the conversion slows down by 30 seconds, which could become a concern due to the unreacted alcohol remaining in the mixture.

4.2.3.4 Consideration of solvent effects

Due to the variations in alcohol molar volume, the fixed (1:10) ratio of reactive Si–H and R–OH groups constituted different reaction volumes. The catalyst concentration in the reaction was maintained at 15 ppm of Pt by precise volumetric insertion of 10 µL Pt/toluene solution per reaction. It is known that PMHS is soluble in toluene [108]. No solvents were used for the reactants nor as the reaction medium. As integral to the Lamoreaux catalyst, $Pt^{II,IV}$ is complexed by octanol as a carrier medium. Based on its miscibility, arising from similar logP values with iOctOH or PMHS, it is unclear whether the catalyst carrier medium favors the reaction or this effect is negligible.

4.2.4 Factors determining alcohol performance

Methanol (MeOH), the simplest primary alcohol, was initially expected to be the most reactive due to its accessible structure. Surprisingly, it exhibited lower activity than iOctOH, which can be attributed to its significantly lower solubility in polysiloxanes. Previous hypotheses suggested that the solubility of alcohols affects their reactivity with PMHS. It is generally believed that the more polar the molecule, the less effective the alcohol would be as a solvent for nonpolar PMHS molecules. However, our experimental results revealed that this relationship is more complex.

The most nonpolar alcohol in the experiments, iOctOH, exhibited high conversion rates. In contrast, tAmOH, despite its relatively higher polarity, exhibited the lowest performance in the first five minutes (**Figure 23**). Since experimental pK_a values for all alcohols were unavailable, we utilized predicted values from COSMO-RS computations as references (**Table 5).** The pK_a values decrease in the following order:

- **pK_a in water**: tAmOH > secBuOH > iPrOH > iOctOH > MeOH
- **pK_a in DMSO**: tAmOH > MeOH > iPrOH > secBuOH > iOctOH

The predicted pK_a values in water seem to describe the reaction only in the initial stages (first 5, 15, and 30 min). Only the conversion for iOctOH is significantly higher than for MeOH or iPrOH. This difference can be explained by the relatively higher miscibility between the less polar iOctOH and PMHS compared to the other more polar alcohols. The predicted pK_a in DMSO for MeOH was similar to that of tAmOH, supporting the 24-hour conversion order for this reaction. The rest of the alcohols showed noticeably higher and similar conversions with respect to each other (iPrOH 88.9%, secBuOH 89.5%, iOctOH 87.0%).

In conclusion, the values of pK_a in DMSO seem to support the overall conversion depth as well as the extraordinary performance of iOctOH in the catalyzed dehydrocondensation reaction, while the pK_a values in water help interpret the conversion for the initial 30 min.

Several other factors, such as variations in alcohol hydrophobicity relative to PMHS, may influence the alkoxylation reaction. For our set of alcohols, the logP values increase with increasing molar mass (see Table 2), with MeOH being the most hydrophilic and iOctOH the most hydrophobic. As PHMS chains are highly hydrophobic (logP ~2.730), logP values could predict preferable hydrophobic interactions with iOctOH (logP ~2.855). The logP values correlate well with the conversion for iOctOH only since iOctOH has the highest and steepest conversion rate during the first 30 min, which is surprising considering its relatively large ethyl substituent and steric hindrance. The logP data should support good miscibility for tAmOH, but the measured results do not agree. The catalyst selected was a Pt-octanal/octanol complex, the hydrophobic alkyl chains of which serve as a suitable transfer medium incorporating Pt between hydrophobic PMHS chains and may assist the reaction with iOctOH, increasing the reaction probability compared to other alcohols with higher polarity, thus lowering miscibility with PMHS.

None of the previous parameters alone can adequately interpret the results of kinetic measurements or describe the thermodynamics of the reaction. Therefore, we should examine how they collectively influence the process. As the polymer chains undergo gradual alkoxylation during the reaction, the monomer fragments of PMHS become bulkier, which hinders the accessibility of unreacted Si–H bonds. We observe a decrease in the reaction rate for iOctOH, which is the least polar and most hydrophobic. After an initial rapid reaction phase, its reaction curve starts to plateau the soonest and does not reach complete conversion. The increasing bulkiness of the polymer complicates further miscibility and access to consecutive Si–H groups, resulting in some Si–H bonds remaining unreacted.

4.2.5 Summarizing the results

Our initial assumption was that molecular weight (M_w) is the most influential molecular parameter (*0D* descriptor) affecting overall kinetic performance, primarily due to the increasing bulk from progressive alkoxylation. Additionally, we believed that the reaction rate and depth would be determined by the steric hindrance of the alkyl substituents in R–OH, which affects the accessibility of the reactive site. However, we did not observe clear correlations as the alcohol M_w increased. Based on the selected molecular descriptors, we proposed a collective effect on the behavior of the PMHS-alcohol reaction blend, which includes the following points:

- MeOH, the most hydrophilic alcohol, has no steric hindrance against nucleophilic attack but has the lowest miscibility in polysiloxanes. Conversely, iOctOH has a long alkyl tail and a branched structure, making it significantly more hydrophobic than the other investigated alcohols, thereby enhancing its miscibility with PMHS before and during the catalytic reaction.
- Lower polarity and higher logP values offer advantages in the catalyzed dehydrocondensation reaction with PMHS. Despite having the most positive

steric hindrance value (E_s=0) and an accessible -OH group, MeOH's limited miscibility in PMHS outweighs these advantages. Steric hindrance appears to play a more significant role in the case of secondary (e.g., secBuOH) and tertiary (e.g., tAmOH) alcohols, while iPrOH values seem to correlate with the molecular properties and fall in between the two.

- pK_a data supports the order of reactivities in the initial reaction stage, although isooctanol performed unexpectedly, showing higher reactivity than anticipated.

While molecular weight and steric hindrance are important factors in the PMHS-alcohol reaction blend, limited miscibility of MeOH and unexpectedly high reactivity of iOctOH highlight the complexity of their interactions.

4.3 Conclusions on dehydrocondensation reaction in foam formation

We investigated the kinetics of catalytic alcoholysis of polymeric hydride in isolation, without additional solvents, to assess its applicability in polymer blends. The most promising monoalcohols for reaction rates and conversion depths with PMHS were MeOH, iOctOH, and iPrOH. In the first 5 and 30 minutes, iOctOH demonstrated more than 2-fold Si–H conversion ability compared to the other alcohols. This suggests that, despite the lower E_s for MeOH and iPrOH, the miscibility of iOctOH in PMHS facilitates access to the reaction center and potentially to the octanol medium of the Lamoreaux catalyst. MeOH, iPrOH, and iOctOH can serve as effective non-crosslinking blowing agents, improving foam expansion while slowing the increase in viscosity during the reaction. The performance of these monoalcohols indicates their suitability for RTV foam synthesis, particularly in injection molding applications. Monoalcohols with lower conversion rates during stage I ($v = k_I$) can be advantageous in systems with higher viscosities and where slower crosslinking rates are required. MeOH was further employed in foam synthesis, even though the alcoholysis with iOctOH also showed excellent performance in the kinetics tests. Despite the high performance of iOctOH in this 1:1 stoichiometric reaction, differences in molar volume necessitate viscosity adjustments in the polymer mixture to prevent undesirable changes in the final foam structure.

The Si–H conversion rate, and therefore the volume of H_2 produced in a specified time, is strongly dependent on the catalytic processes and can be altered by temperature, catalyst nature, and concentration. Although these variables were fixed in this study, further experimenting is supported to reveal any deviations in reactivity order using other catalysts, such as Karstedt's.

5 THE BULK PROPERTIES OF FOAMS

In this chapter, I discuss the findings presented in **Publication II**, which investigates how foam structure, density, and tensile properties are influenced by assemblies forming crosslinks of varying lengths and rigidity. The study involved the preparation and characterization of chemically blown silicone foams, with systematic variations in blowing blends incorporating water, dialcohols, glycerol, and methanol. These experiments were conducted within a multi-reaction system that included both dehydrocondensation and crosslinking reactions.

5.1 Observations on the effects of water-based blowing blends

During SIF synthesis, adjusting blowing to crosslinking is not only beneficial for obtaining low densities but also serves as a means to tune the strength, elasticity, and deformability of the foams. By manipulating cell size, shape, distribution, and the foam's open- or closed-cellular structure, the potential applications of SIFs are greatly expanded. In systems where the crosslinking progresses too slowly, the emerging gas bubbles tend to coalesce and leave the blend too early due to insufficient viscosity increase. Also, when the crosslinking rate is too high, the polymer blend solidifies before a desired cellular structure is formed, generally leading to smaller d_{cell} values, often in an elliptical shape due to the gas shaping the cells in the rising direction. In extreme cases, the solidifying foam can rupture due to the escaping and expanding gas. To avoid such extremities, one approach is to either adjust the reactions for the blowing, the crosslinking, or both.

Fortunately, simultaneous crosslinking and gas generation can originate from the same reaction – catalytic dehydrocondensation – between PMHS and at least dihydroxy-functional alcohol. As discussed in previous sections, reacting PMHS with monoalcohols results in an alkoxy-grafted siloxane backbone and simultaneous H_2 evolution without the formation of crosslinks. However, additional crosslinking during expansion would support the viscosity increase in the polymer blend, which in turn aids the foam formation by retaining the gas phase for a prolonged time. As blowing additives, water and at least dihydroxy-functional alkanols can be applied to expand and solidify SIFs simultaneously. For an additional crosslinking possibility, a trifunctional alcohol – glycerol – can be applied as part of the blowing formula.

On the basis of established SIF blowing with water, we were further interested in combining different mono-, di-, and trihydroxy-functional alcohols with water in a catalyzed reaction with PMHS. These combinations as blowing blends could be beneficial in fine-tuning the physicomechanical properties of SIFs in the low-density range (considered ρ_{app}<250 kg·m^{-3} for elastomeric polymer foams). By utilizing the chemistry of siloxane chains, particularly the Si–H functional groups, the reaction sites where gas bubbles nucleate are more uniformly

distributed. The catalytic conversion of Si–H involves competitive processes between Vi-PDMS, OH-PDMS, and hydroxy-functional compounds, each performing at different rates. Therefore, the general composition and stoichiometry (denoted as ***r*** in **(1)**, a ratio of two different reactive functionalities) were maintained, and additional PMHS was used for the reaction by blowing blends.

Adjusting the molar ratio of compounds in the blowing blend in a fixed polymer blend formulation leads to changes in the cellular structure of resulting foams due to the different performances of the low M_w alkanols. These variations in foam structure directly impact the mechanical properties of the prepared foams.

As the dihydroxy-functional blowing compounds themselves act as crosslinkers between PMHS chains, varying alkanol-water blends result in different crosslink lengths. Such alteration affects the deformability of the expanding blend by expanding gas, the polymer scaffold's elastic properties, and finally, the physicomechanical properties of the resulting foams.

Applying water as a single blowing agent in our formulation leads to structurally consistent low-density foams. In addition to hydrogen formation from condensation reaction, a rapid crosslinking of the polymer blend occurs, leading to a relatively fast cure. Although short curing time is beneficial, the mechanical properties of these foams are impacted by the relatively short and rigid Si–O–Si crosslinks. Rapid crosslinking also increases the blend viscosity and may become problematic for filling the molds, leading to structural inhomogeneities. Such foams are low in density but need optimization in mechanical properties. However, **partially replacing water with mono-, di- or trifunctional alcohols** alters the progressing crosslinking, blend viscosity, and resulting foams' structural and mechanical properties. By using a hydride-functional polysiloxane along with low-molecular hydroxy-functional compounds as a hydrogen source, it is possible to easily and catalytically control the blowing of SIFs and to alter their physicomechanical properties. This can be done without the need for other physical or chemical blowing agents, which can often lead to the production of undesired by-products or require complex process controls. Optimization of blowing (and crosslinking) via hydroxyl blends in an established polymer formulation is one of many possibilities for creating SIFs and will be the main topic of further discussion.

5.2 Methanol-water blowing blends

Water, as the only blowing agent, is especially effective for fabricating soft, low-density open-cellular foams. To tune the foam's internal cell structure, one option is to slow down the otherwise rapid crosslinking but not gas evolution. Thereby the viscosity increase is presumably slower and promotes the formation of larger cells. Based on kinetic experiments discussed in the previous chapter, it was shown that MeOH and iOctOH were the most reactive in producing hydrogen from dehydrocondensation reaction with PMHS during the initial stage. Due to the significantly higher blowing agent volume upon using iOctOH, we opted for

MeOH as part of the blowing blend, although the iOctOH has far better polysiloxane miscibility. *Note.* MeOH is more volatile, and in case of an incomplete reaction, its residues evaporate quickly from the formed structure, leaving no odor in the foam, contrary to iOctOH.

For reference, water-only blown foams were synthesized with an average ρ_{app}=105 kg·m^{-3} by increasingly substituting water with MeOH. The increasing MeOH-to-water ratio (*i.e.*, MeOH/water) brought substantial changes in the SIF structure (see **Figure 24**) with an evident increase in both the average cell diameter (d_{cell}) and the cell wall thickness (d_{wall}) (Figure 25 (A)).

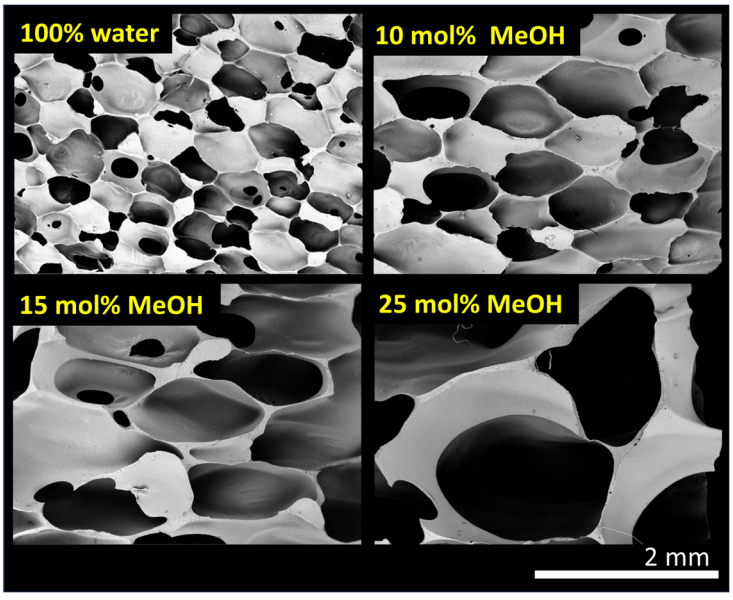

Figure 24. Effect of increasing the MeOH mol% in MeOH-water blowing blends on the morphology of chemically blown SIFs. Adapted from the author's original work. [Pub II]

A slight elongation of cells in the direction of foam rise becomes more evident for higher MeOH/water ratios. This, however, can be explained by theoretically fewer crosslinks and more alkoxy-grafted units formed due to the substitution of water with monoalcohol. In **Figure 25** (B), the interconnecting walls of two adjacent elongated cells are shown. It was observed in SEM micrographs that 25 mol% MeOH/water-blown foams featured microporosity in the polymer scaffold, which was not found in water-blown foams.

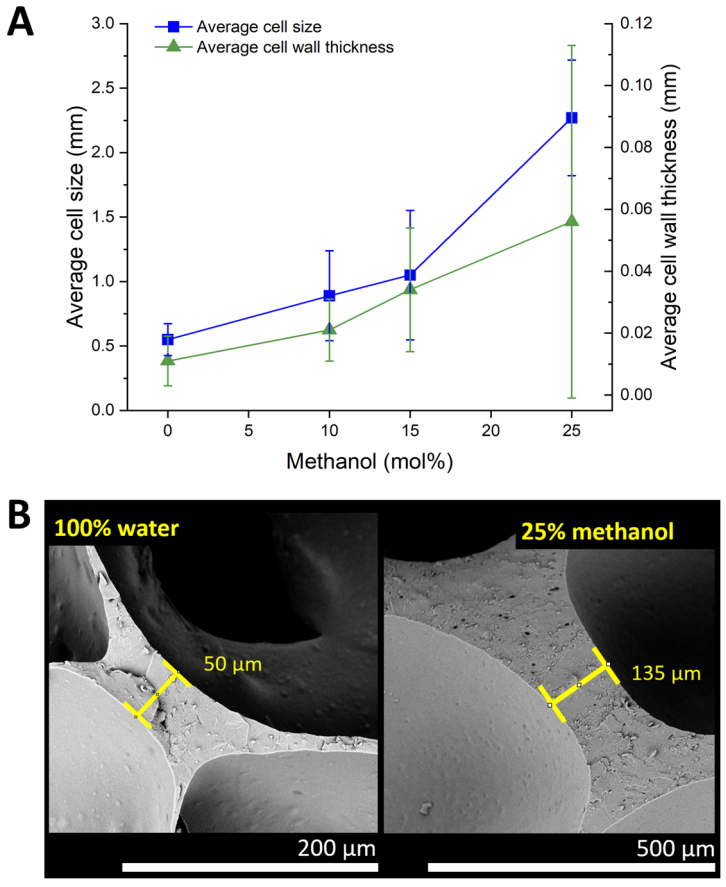

Figure 25. Average cell size (d_{cell}) and average cell wall thickness (d_{wall}) both increase when partially substituting water with MeOH in the blowing blend (A). Note the different magnification scales of SEM micrographs (B) for 100% water-blown and 25 mol% MeOH/water-blown foams. Adapted from the author's original work. [Pub II]

The ρ_{app} increased moderately with increasing MeOH content from 0 (=100 mol% water) to 25 mol% MeOH/water blowing blend and significantly for 50 mol% MeOH content (**Figure 26** (A)). Using ≥50 mol% MeOH blends in SIF synthesis resulted in apparent densities higher than 125 kg·m^{-3}. We observed a steep loss in tensile strength occurring at 10 mol% of MeOH; increasing its ratio in the blowing blend further keeps tensile strength values constantly low (**Figure 26** (B)).

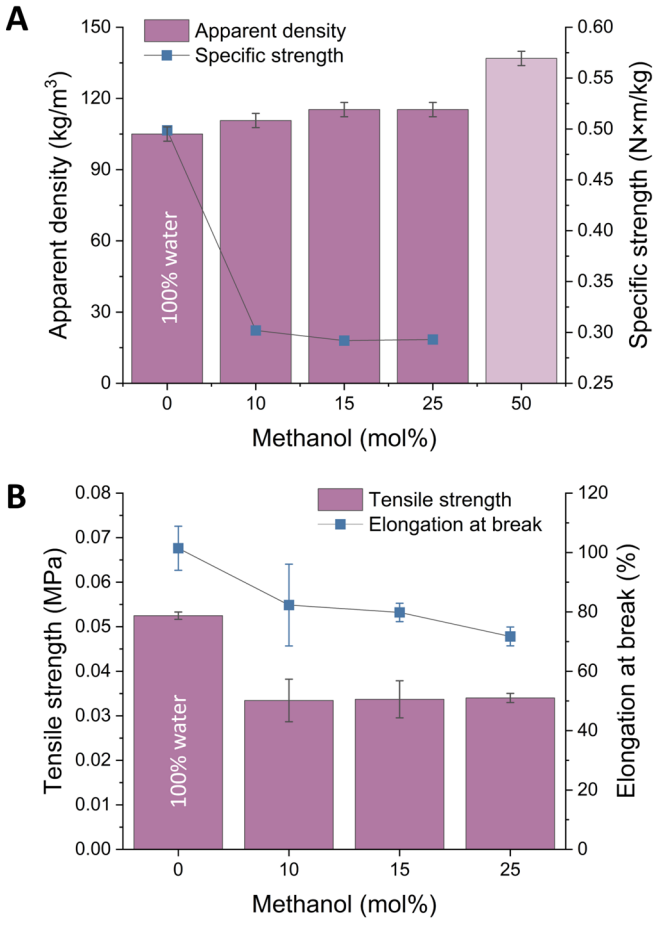

Figure 26. Increasing MeOH ratio in water causes (B) a decrease in tensile strength (σ_b), elongation at break (ε_b), and (A) specific strength (*Note:* 50 mol% not eligible).[Pub II]

Due to the relatively inhomogeneous cellular structure with larger d_{cell} and defects, the foams blown by 50 mol% MeOH and above were not applicable for tensile testing. The ε_b decreases with increasing d_{cell}, d_{wall}, and ρ_{app}. The occurrence of inhomogeneities in the structure is reflected in tensile strength values, which significantly lowers the foams' specific strength (**Figure 26** (A)).

MeOH, as a monoalcohol, was introduced to the blowing blend to enhance the physicomechanical properties by altering the cellular structure of the foams. The purpose was to decrease crosslinking during blowing while maintaining the amount of evolving gas. The resulting changes in the foam structure demonstrate the applicability of these blends as structure modifiers without compromising gas generation. Such cellular materials can be implemented in cushioning applications, where the density increase arising from the d_{wall} and d_{cell} increase is not an issue. Considering the lower theoretical crosslinking degree arising from the molar ratio variations, the low ε_b values suggest that the strength of the elastomer needs further improvement. One option to modify the material's physicomechanical properties is to partially replace the short crosslinks resulting from

secondary condensation due to using water with longer ones. Different di- and tri-functional alcohols can be beneficial for this purpose.

5.3 Diol-water combinations as blowing blends

5.3.1 Effect of alkyl chain length of diols on foams

We observed changes in the physical and mechanical properties of the foams by substituting 10 mol% of the water-only blowing blend with different diols based on alkyl chain length (C_n=2…7). For comparison to telechelic diols, we included a variation of the C_n=3 molecule with a pendant hydroxyl group, propane-1,2-diol. Introducing diols into the blowing blend alters the cellular structure of the foams more coarsely for longer alkyl chain lengths, as suggested by the cross-sectional morphology in **Figure 27**.

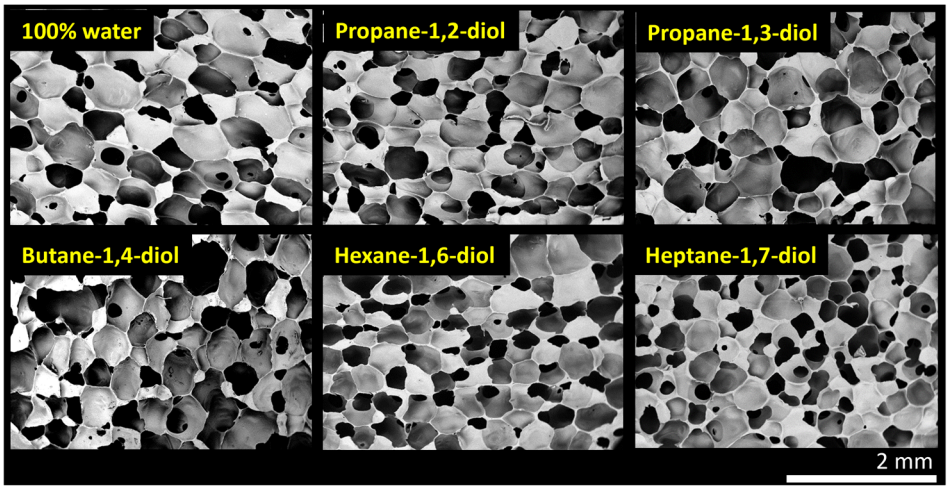

Figure 27. The cross-sectional morphology of foams blown with the water-only (100%) and the 10 mol% diol/water blends. [Pub II]

Without considering pendant diol-water blown foam, the correlation between ρ_{app} and d_{wall} values for 10 mol% telechelic diol/water-blown foams is evident (see **Figure 28** and **Figure 30** (A)). However, these averaged data must be interpreted with caution due to large standard deviations. For further exploration of variations in cell sizes, a lognormal distribution could provide more insight, as in **Figure 29** (B).

Based on the cross-sectional morphology, the average d_{cell} and d_{wall} both decrease linearly from C_2 to C_4 as the ρ_{app} decreases. Moving on, from C_4 to C_7, d_{wall} and ρ_{app} show a non-linear correlation by increasing in an odd-even pattern. It's worth noting that the foams with the lowest ρ_{app} among the observed 10 mol% diol/water-blown foams (C_4, butane-1,4-diol) also had the lowest d_{wall}. On the other hand, for the foam with the highest density, a 10 mol% heptane-1,7-diol blown foam, one of the highest d_{wall} values was observed (**Figure 28**).

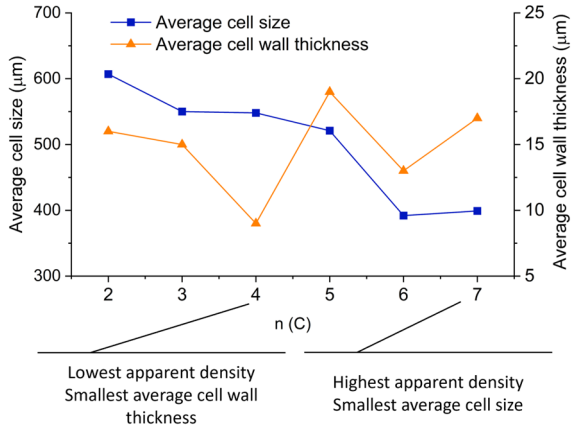

Figure 28. Structural parameters of macrocellular foams – averages of d_{cell} and d_{wall} – blown with telechelic diol-water blends. **[Pub II]**

Such foam cell thinning (*i.e.*, polymer film drainage) during blowing occurs in an uncured blend as a result of increasing gas pressure partly due to continuous bubble nucleation and coalescence until a certain degree of cross-linkage is achieved and the cellular structure sets. The parallel crosslinking via hydrosilylation reaction is expected to increase polymer blend viscosity independently from the cross-linking occurring via dehydrocondensation, thereby progressively hindering bubble coalescence as the blowing process continues. For the 10 mol% blends, the ratio of resulting crosslinks [≡Si–O–Si≡]/[≡Si–O–C_n–O–Si≡] is theoretically set, with variations in the C_n of the diol and the respective blowing blend volumes.

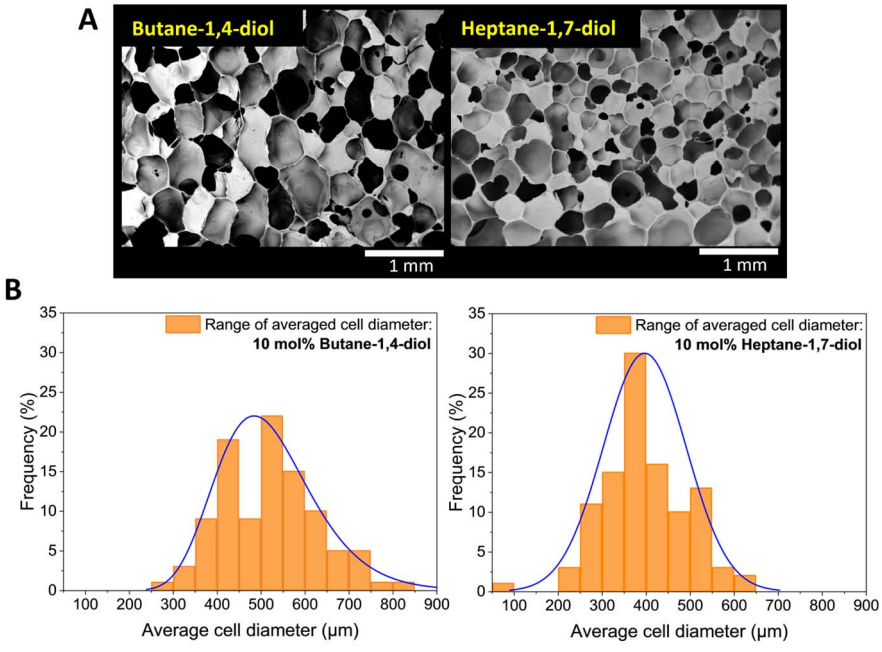

Figure 29. Foam morphologies for (A) 10 mol% butane-1,4-diol/water and 10 mol% heptane-1,7-diol/water-blown foams, and (B) respective lognormal distributions of d_{cell}.

Considering the use of such materials, the tensile strength σ_b [MPa] significantly contributes to the resilience and cushioning ability of elastomeric foams. At different apparent densities, the materials under strength comparison would already have different vantage points. For a more fair comparison, we used specific strength measures to express the mechanical properties of these foams. The relationship between ρ_{app} and σ_b is expressed as a specific strength [N·m·kg^{-1}], also known as a strength-to-weight ratio (force per unit area at failure). This measure is beneficial when we were to obtain foams with similar densities (of different materials/blowing components or under different conditions). This means that a low-density foam with high σ_b values also has high specific strength values.

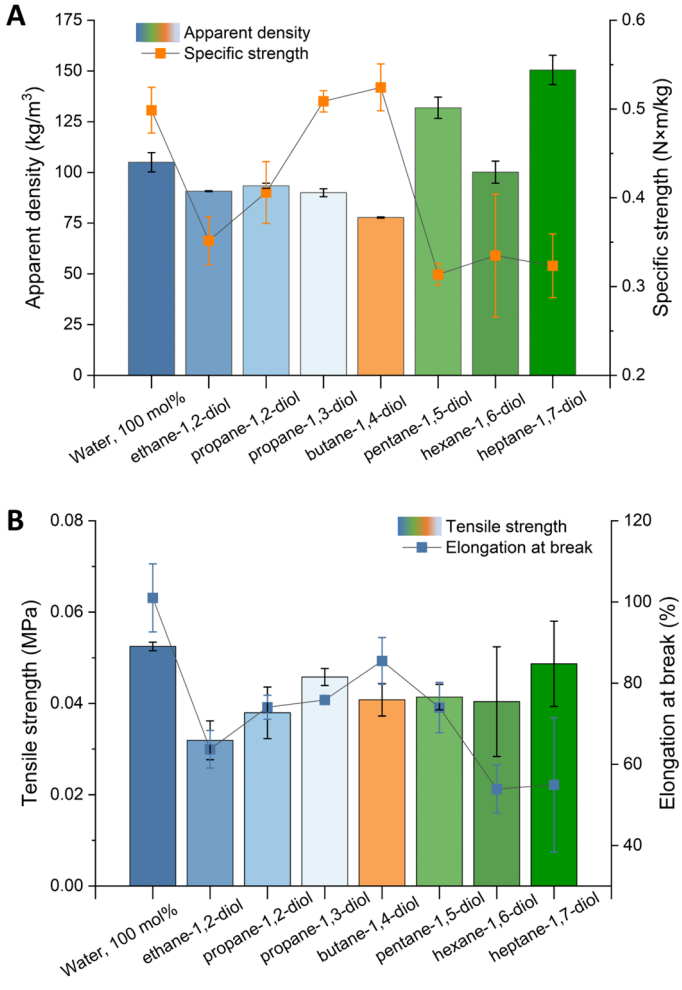

Figure 30. Apparent density (ρ_{app}) and tensile properties for foams blown with 10 mol% diol solutions in water compared to a 100 mol% water-only blown foam. (B) The respective changes in elongation at break (ε_b) and tensile strength (σ_b) and (A) specific strength dependent on the ρ_{app} are depicted in the increasing order of C_n, with the exceptions of 100 mol% water and 10 mol% of propane-1,2-diol in water blend. Adopted from the author's original work. [Pub II]

Experimental results indicate that a water-only blown foam has the highest σ_b at a relatively low ρ_{app} of 105±3 kg·m^{-3}. Additionally, this foam had the highest ε_b value, exceeding both the lowest and highest density foams. These results can be linked to the average d_{cell} of 0.6±0.2 mm and d_{wall} of 0.011±0.008 mm. The higher average d_{wall}, compared to butane-1,4-diol, and similar average d_{cell} values may contribute to the higher ρ_{app} and superior performance in tensile tests. Foams produced with 10 mol% blends of ethane-1,2-diol, propane-1,3-diol, and butane-1,4-diol/water resulted in the lowest density foams (91, 90, and 74 kg·m^{-3}, respectively). Among these, the latter two perform relatively well in tensile tests, with higher specific strength values than the others. The foam with the lowest density value (74 kg·m^{-3}) and its relatively good tensile strength (≈0.04 MPa) prompted an investigation into whether it is possible to further adjust the foam's physicomechanical properties by increasing the diol ratio in the diol-water blowing blend.

When water was partially substituted with a diol (10 mol%), the ρ_{app} and σ_b gradually decreased from C_2 to C_4. From C_4 and above, the odd-even effect for alkane chains seems to describe the correlation between the diol chain length and the alternating values of the ρ_{app} and d_{wall}. Compared to the 100% water-blown foam, replacing 10 mol% with butane-1,4-diol resulted in the lowest density among all the diols, whereas the specific strength values remained comparable to that of the water-only blown foam. Further increasing the diol content caused the ρ_{app} and σ_b to increase. The dominant effect on the ρ_{app} increase is the increase in d_{wall} near and above 50 mol% butane-1,4-diol solutions. The mean values of cellular dimensions, specifically d_{cell} and d_{wall}, exhibit significant error margins. Despite this, observable patterns emerge, including a diminution in d_{cell} with an increment in C_n, alongside variations in d_{wall}.

5.3.2 Variations in diol-to-water ratio

Butane-1,4-diol combinations with water offered more interest since the mechanical properties of the resulting low-density foams are attractive. Blends of 0, 10, 20, 35, and 50 mol% of **butane-1,4-diol**/water and of a 100 mol% diol were tested and compared to 100 mol% water-blown foams, as before (**Figure 31**).

Clearly, the partial substitution of water with butane-1,4-diol decreases the foam's ρ_{app} by up to 35 mol%. Increasing the diol/water ratio further, the structure densifies from the account of d_{cell} and d_{wall}, which both change drastically. An undesired density-increasing effect occurs above 50 mol% diol content. The densification effect could arise from two fundamental changes. First, due to the relatively higher M_w of butane-1,4-diol and its added volume, increasing its ratio also alters the blend viscosity, which in turn would favor the bubble coalescence [3]. However, this aspect is considered negligible due to its relative contribution to the formula and the measured viscosities (described in section *Viscosity measurements of polymers and polymer* blends). Herein, the effect of solubility and miscibility of diol-water blends with varying ratios was not evaluated but could propose some effect on the reaction rates. Secondly, changes in crosslinking rates,

lengths, ratios, and distribution are usually considered critical factors that determine the behavior of expanding polymer blends. These changes originate from decreasing the number of slower secondary condensation instances occurring in reactions with water after converting Si–H to Si–OH. It is obvious that the changes in foams' density influence specific strength values. The foams' ε_b clearly decreases along with increasing the diol ratio.

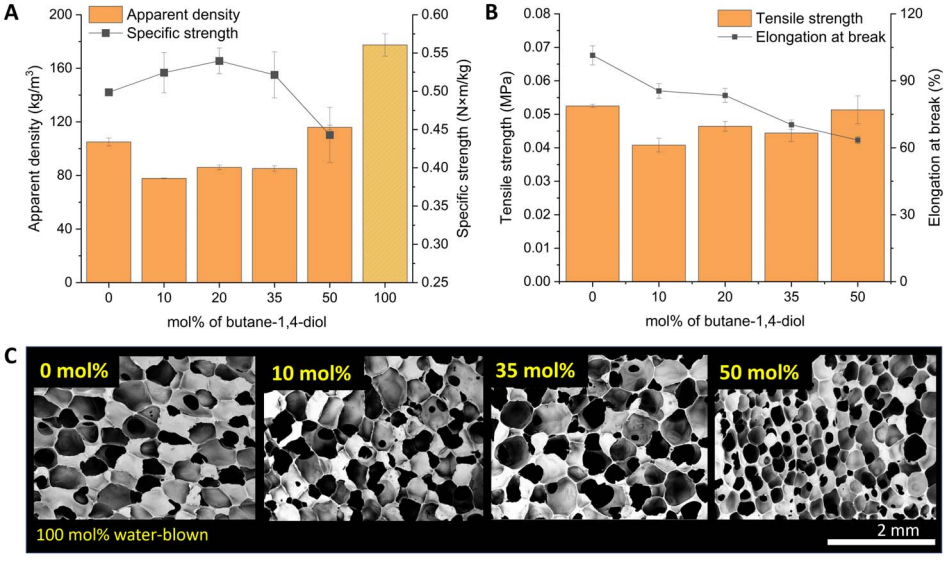

Figure 31. Variations in butane-1,4-diol ratio in water-based blowing blends and the characteristics of resulting foams – (A) apparent density (ρ_{app}) and specific strength, (B) tensile strength (σ_b) and elongation at break, and (C) cellular morphology. Adapted from the author's original work. [Pub II]

5.3.3 Effect of hydroxyl-group position on blowing

For 10 mol% diol/water experiments, we included two propanediols, 1,2- and 1,3-hydroxy-substituted. Another well-known propanol glycerol (propane-1,2,3-triol), which is widely used in industrial applications (**Figure 32** (C)). The respective higher ratio of -OH groups per mass/volume compared to monoalcohols is a major contributor to hydrogen volume, as well as to the overall cross-linkage. We were particularly interested in how these three propanols affect the final structure and mechanical properties of SIFs.

The foams produced by blowing and simultaneously crosslinking with a 10 mol% glycerol/water blend have an apparent density of ρ_{app}=76 kg·m^{-3}, which is approximately 30% lower than that of water-only blown and 17±2 % lower than that of other propanediol-blown foams (**Figure 32** (B)). This lower density is expected, given that each glycerol molecule contains three -OH groups that potentially react with the Si–H bond. As each crosslink is formed, the viscosity of the reaction mixture increases, preventing the escape of evolving hydrogen.

Furthermore, Nakagawa *et al.* reported that vicinal -OH groups in triols exhibit significant retardation in chain dynamics compared to monoalcohols attached to polymer chains [135]. For instance, propane-1,2-diol, which has -OH groups at vicinal positions, experiences more steric hindrance compared to propane-1,3-diol, which features a linear chain with terminal groups. As a result, the reactivity of propane-1,2-diol may be hindered during dehydrocondensation reactions at the first available reactive site [134]. In **glycerol**, the steric hindrance at carbons C_1 and C_3 is lower than at carbon C_2. Consequently, the -OH group attached to C_2 is more likely to engage in polymer chain entanglement and interact with the PMHS chain and catalyst, leading to additional bonds and an increase in rigidity. This, in turn, affects the foam's elasticity, resulting in lower ε_b and σ_b compared to 1,3-diol. Despite the lowest ε_b, the σ_b of the foam is comparable with that of propane-1,2-diol (**Figure 32** (A)) and is reflected in a relatively high specific strength.

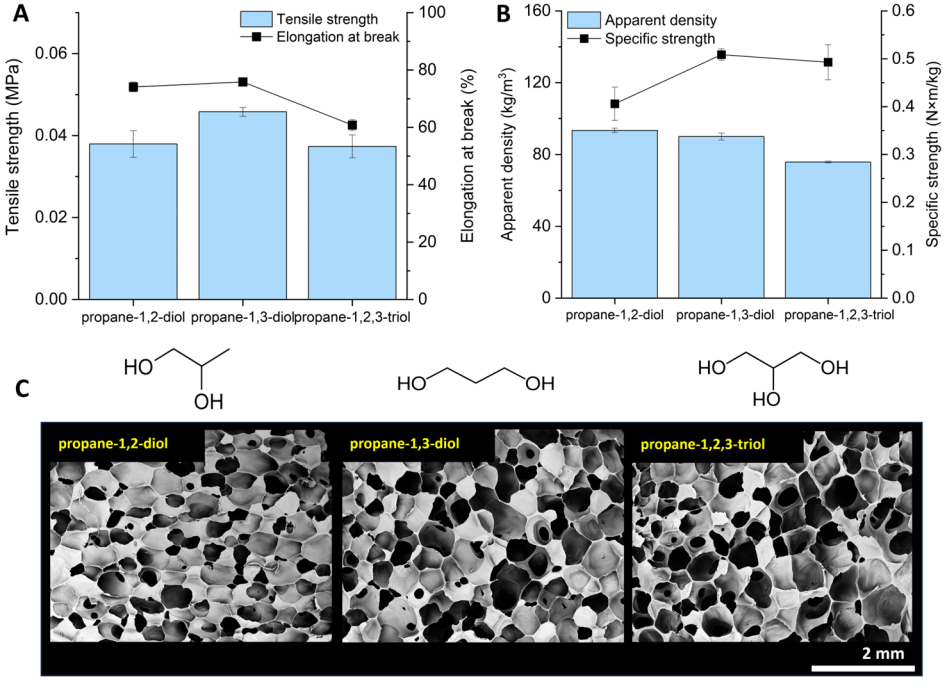

Figure 32. The effect of 10 mol% propanol/water blends on SIFs (A) tensile strength (σ_b) and elongation at break (ε_b), (B) apparent density (ρ_{app}) and specific strength, and (C) foam morphologies. Adapted from the author's original work. [Pub II]

However, diols enable the production of foams with higher ε_b values than triols. Additionally, dispensing and molding are more efficient due to the reasonable viscosity of the mixture during curing and expansion. This feature is particularly important for molding in the FIM process, where it is essential to fill small

cavities. It is worth noting that using higher ratios of triols may lead to decreased ε_b values due to the greater number of relatively short and closely positioned crosslinks.

5.4 Conclusions on the effects of blowing blend formulations

Chemical blowing in the form of inherent gas-generating reactions yields consistent, controllable, and repeatable results regarding the apparent density (ρ_{app}), structural parameters, and mechanical properties. Finding a balanced formula in this multireaction system for a desired application is an ongoing process; however, our results show that the synthesis of moldable low-density elastomeric SIFs with desired properties is achievable. While water-blown foams are low in density, their relatively weaker strength profiles (tensile strength, specific strength) tend to diminish their value in applications with repetitive deformation. By partially substituting water with alcohol, the general viscosity increases with fewer crosslinks forming, resulting in larger cells and thicker walls. In addition, introducing diols into the blowing blend naturally lengthens the crosslinks and, therefore, increases foam susceptibility to deformation. This may be a desired feature, although the mechanical properties of the resulting foams need further adjustment.

6 INTERACTION OF BACTERIA WITH FOAMS

The following chapter discusses the effect of different hydrophilic and hydrophobic additives on the surface properties of synthesized SIFs and the bacterial adhesion and growth in both SIFs and polyurethane (PUR) foams. The effect of different additives and foam types on bacterial growth in the surrounding growth medium is discussed.

6.1 The effect of fillers on surface properties

As SIF formulations are not entirely PDMS-based, everything that is added to the composition may affect the elastomer's surface properties, such as morphology (overall structure; texture, arrangement of surface features), topography (roughness, waviness, irregularities), surface functionality, and hydrophobicity (water contact angle, θ) [101], [136], [137]. Previous research demonstrates that these properties influence bacterial adhesion and growth by providing anchorage [101]. In addition, some additives may even promote the growth of bacteria.

In the framework of this dissertation, SIFs were synthesized based on the formulation and reactions described in Chapter **3.2**. All these foams include two default fillers: hydrophobized fumed silica (FS) and muscovite mica. Both were applied as an enforcement additive for the polymer matrix but categorized here as a filler due to their large overall content. Various foams studied herein were prepared using different additives, such as activated carbon, shungite, chitosan, methylcellulose, and tannic acid. Not all the additives are considered antibacterial but serve as either a nucleation site or emulsifier or are used for enforcement purposes like previously mentioned fillers. For example, tannic acid [111], [112], [138], shungite [114], and chitosan [139] particles have shown antibacterial activity, but neither methylcellulose nor activated carbon has been proposed specifically for this purpose. As an exception, grafting PDMS surface with alkylated methylcellulose has been used to mimic the non-adhesive property of glycocalyx, a cell cover of bacteria [139].

6.1.1 Cell size, open volume, and apparent density of foams

The **SIFs** used herein to study bacterial growth and adhesion are low-density (ρ_{app} =88–175 kg·m^{-3}) macrocellular structures with average d_{cell} in the range of 200–500 µm. The open volume ranged from 83% to 91%, with higher-density foams having the least open volume. As the cell dimensions were sufficiently large for the bacteria and bacterial aggregates to flow through the porous foam, this is not considered a limiting factor in the bacterial growth context. In **Figure 33**, the structural differences of the synthesized SIFs are distinctive from PUR foams used in inoculation tests as a comparative material.

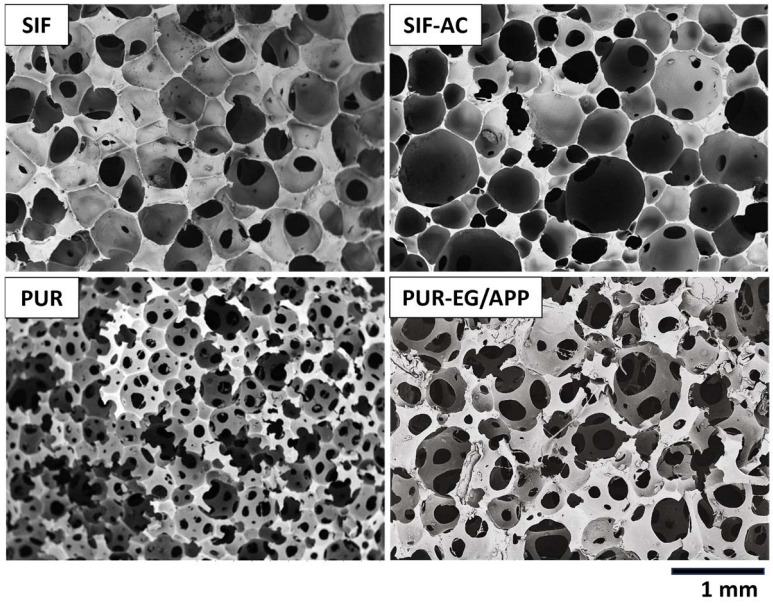

Figure 33. Cross-sectional porous structures of SIFs (pristine and with AC additive) and PUR foams (a regular and a fire-retardant foam). Adapted from the author's original work. [Pub III]

Although both have macrocellular structures, the occurrence of interconnecting pores in cell walls is higher for both PUR foams. *Note:* The list of test foams is presented in **Publication III** in *Table 1*, accompanied by the organic additive structures in *Figure 12*.

6.1.2 Water contact angles of SIF and PUR

It is generally considered that the changes in surface roughness would alter the surface hydrophobicity. Although the surface roughness is locally uneven and the additive concentrations vary, the main filler content (FS and mica), which forms a significant bulk of the SIF composition, is consistent for all foam specimens. To understand whether the surface hydrophobicity of porous structures would have changed and significantly affected bacterial adhesion, the WCA values (θ_C) were measured. Initially, the WCA was determined from horizontally cut foam surfaces. The interconnecting pores were generally sufficiently large for the liquid medium and the microorganisms to enter (see **Figure 12**). When evaluating static WCA, it was obvious that due to the porous nature of the foam it is difficult to get reasonable results as the water droplet would immerse almost immediately into its pores. This phenomenon cannot be considered an effect of high hydrophilicity, but rather, the size of the foam cells and the foam cell walls revealed on cut sides do not provide an even (or stable) surface for measurement. Such capillary effect was confirmed through a series of attempts via droplet application. Due to the rapid droplet immersion, the contact angle of a macro-

cellular foam is more challenging to measure than the properties of the skin material. However, during the molding of the foam, a skin-like layer of polymer is formed in contact with a smooth mold surface for both SIF and PUR foam. Despite a certain degree of microporosity in the polymer skin layer, the droplet stability allowed WCA to be determined. We measured the WCAs on both the smooth surface and on the cut sides of the foam for better accuracy; the averaged results are depicted in **Figure 34**. The WCA values for both open-porous foams and skin-like monolithic surfaces indicate that the SIF and PUR porous surfaces are hydrophobic (θ_C>90°).

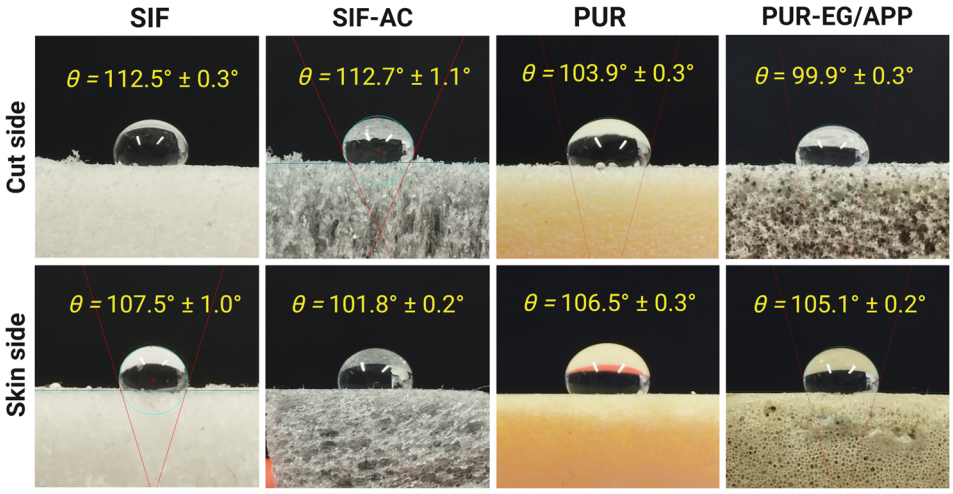

Figure 34. Static water contact angles (θ_C) on cut and skin-covered surfaces of SIF, SIF-AC, PUR-EG/APP, and PUR.

The water contact angle of SIF, referred to as a pristine polysiloxane foam, is θ_C =107.5° ± 1.0°, which is in accordance with WCA from earlier research (θ_C =107.1°, [90]). The observation that the WCA value is higher for open-cellular SIF surface (SIF, SIF-AC) is assumably due to the entrapped air residing in cells, which form air pockets under the water droplet [87]. The difference in WCAs of SIFs and PURs is not significant, although PUR foams are relatively more hydrophilic; also being in accordance with the previous literature [140]. Compared to SIF, the decrease in WCA of SIF-AC measured on the skin is θ_C <10%, which could be caused by the evenly distributed hydrophilic AC particles. However, it is important to note that the WCAs of foams do not depict the influence on local bacterial adhesion but rather a confirmation of the hydrophobicity of the samples and eliminate possible significant differences in surface wettability between PUR foams and SIFs. The opposing WCA values for PUR foam skin and cut side compared to SIFs could arise from the differences in pore dimensions inducing possible capillary effects from the air bubbles formed under water droplets, which minimize contact area, or both.

6.1.3 Surface microstructure

The general idea of possibly antibacterial (or at least anti-adhesive) effects arising from using fillers or antibacterial additives is less straightforward. On the one hand, particles on the elastomer surface would enhance the antibacterial effect in direct contact with bacterial cell walls. On the other, changes in topography, such as roughness, are found to influence bacterial adhesion, partially due to resulting changes in surface hydrophobicity but also due to the favored adhesion point for nutrients from broth or single bacterial cells.

It has been proposed that an antifouling effect would derive from nano- or micropatterned surface due to the altered total surface area and surface wetness, thereby affecting bacterial cell signaling, cell membrane expression, and the function of bacterial flagella [98].

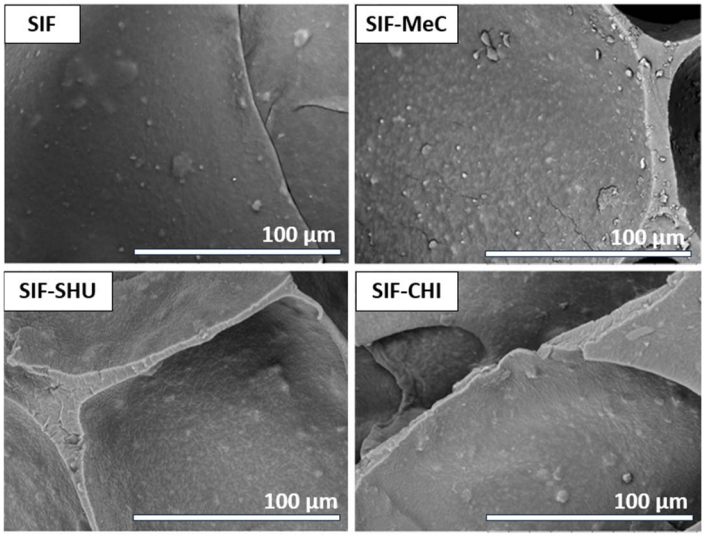

Figure 35. Foam cell wall surfaces of SIFs containing different additives (AC – activated carbon, MeC – methylcellulose, SHU – shungite, CHI – chitosan, TAN – tannic acid (TA). Changes in surface roughness are affected by the particle concentration; their protrusion from the polysiloxane is inhomogeneous. Adapted from the author's original work. [Pub III]

Each of the analyzed foam materials (**Table 3**) possesses satisfying mechanical and structural properties, which is why the effect of additives on the surface properties of these composites is particularly of interest. Despite the different concentrations, sizes, and shapes of particles used in the blends (**Table 4**), their effect on the surface morphology, hence the bacterial adhesion, can still be evaluated. The SEM micrographs reveal that the surface roughnesses, due to the use of fillers and additives, are visibly different for the synthesized foams (**Figure 35**).

Combined with EDX analysis, the defined regions in **Figure 36** could be identified as projections of filler particles. A majority of these solid filler particles

are covered by the polysiloxane layer and do not surface, either partially or entirely. The low surface tension causes the polysiloxane to spread and cover most of the particles despite the expansion of the material accompanied by cell wall thinning [62].

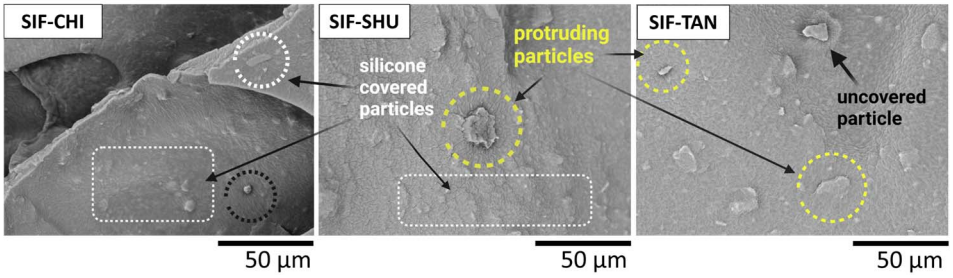

Figure 36. Surface profiles of SIF cell wall surfaces. Additive and filler particles seemingly protrude from the polysiloxane elastomer, although mostly covered by a thin polysiloxane layer.

From SEM-EDX compositional imaging, we detected carbon-dense areas in SIF-SHU foams proposed as shungite particles (**Figure 37**).

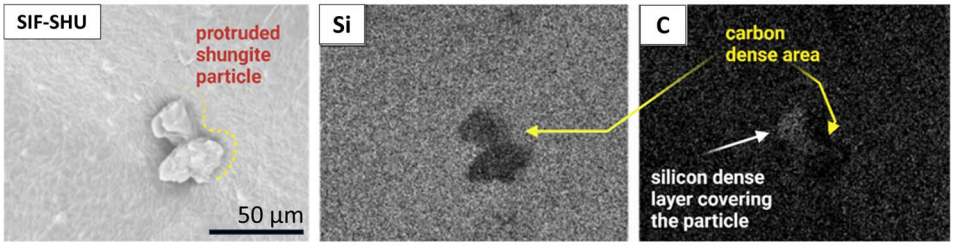

Figure 37. SEM analysis combined with EDX analysis with marked protruding regions identified as carbon-dense areas in SIF-SHU foam, considered shungite particles (~50 µm). A comparison of carbon (C) and silicon (Si) elemental distribution is a possible indication of a polysiloxane layer covering the particle. [Pub III]

In SEM-EDX, the elemental composition of foams is detected from approximately 1 micrometer (~0.5–3 µm) in-depth, and low elemental mass particles are difficult to distinguish. Therefore, based on SEM-EDX analysis, we can confirm that the protruding particles are partially covered with a polysiloxane elastomer layer. Consequently, the dominant filler/additive-induced antibacterial or anti-adhesive effect would arise from physicochemical or morphological changes in the surface. The potential effectiveness of using these particles as antibacterial additives in polysiloxane composites is not revealed. Although the expectations of using them as a surfacing additive are not met, there are several ways to modify the particle content, size, and distribution.

6.2 *E. coli* growth and adhesion in open-cellular foams

6.2.1 Bacterial growth in foams: Effect of additives in SIFs

Observation with SEM reveals that the extent of bacterial colonization on the polymer surfaces differs for different foam compositions (**Figure 38**). These differences, however, are not homogenous all over the foam but well describe the preferred population formations in specific foams.

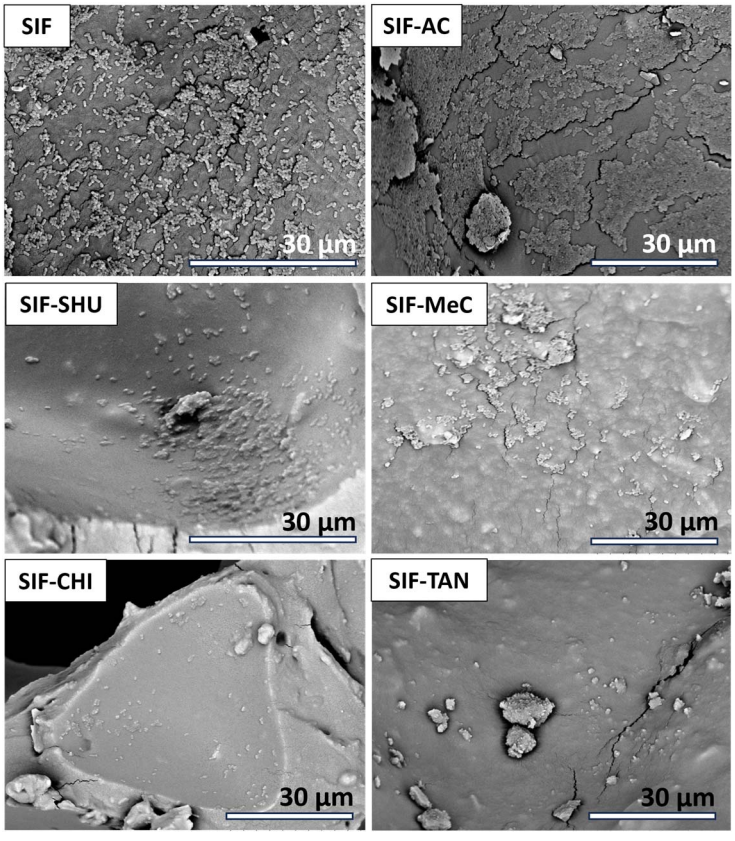

Figure 38. SEM micrographs of *E. coli* formations on SIF surfaces after 24-hour incubation in a growth medium under dynamic conditions. [Pub III]

6.2.1.1 Activated carbon

The adhered bacterial population of *E. coli* is considerably more extensive when the SIF contains AC (**Figure 39** (SIF-AC)). It was generally observed that the bacterial clusters and aggregates were a more frequent phenomenon, distinctively different from standard SIF surfaces. Activated carbon is hydrophilic and has high adsorption capacity, binding molecules from liquids by van der Waals forces [141]. Their hydrophilic nature could, therefore, affect surface properties, such as WCA.

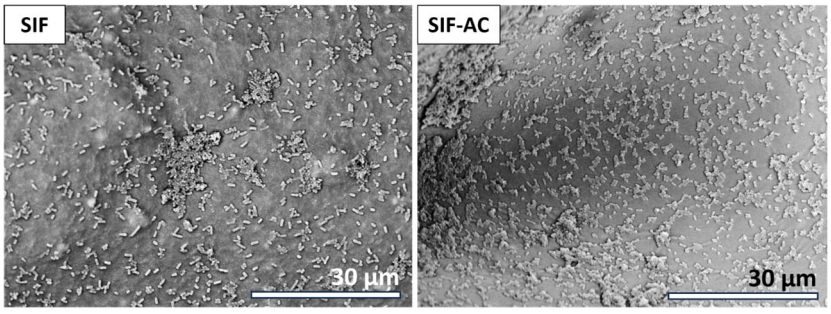

Figure 39. Distribution of *E. coli* on SIF (left) and SIF-AC (right) surfaces. Partially adapted from the author's original work. [Pub III]

In the previous section, we could see that the WCA measured on the polymer skin of SIF-AC (θ_C =101.8° ± 0.2°) is lower than for SIF (θ_C=107.5° ± 1.0°), indicating its higher surface hydrophilicity. Generally, the adsorption of inorganic or organic molecules, including nutrients from LB medium on AC, creates favorable conditions for population increase. To add, the formation of pili between adhered bacteria is evidence of suitable conditions and is considered an indication of the (Gram-negative) bacteria's readiness to share genetic information for multiplication purposes (*Figure 6*, in **Publication III**).

6.2.1.2 Methylcellulose

Including methylcellulose in the polysiloxane matrix (SIF-MeC) had a statistically insignificant effect on bacterial growth in the surrounding medium compared to pristine SIF. Methylcellulose is considered an emulsifier/blend thickening and strengthening additive, not intentionally for antibacterial purposes. However, its 0.5 wt% inclusion to the polymer matrix has visually increased the surface roughness (**Figure 38**), which can locally contribute to the adhesion of growth medium constituents.

6.2.1.3 Shungite

The results indicated that the average c[CFU] in the media surrounding shungite-containing foams was lower compared to the media for pristine SIF foam cubes, and slightly higher than for the foamless reference growth medium, although the difference may not be significant. As shungite is reported to have antibacterial properties in an aqueous medium, a more substantial effect might be expected on c[CFU] in the growth medium [114] as well as on the polymer surface (**Figure 38**).

6.2.1.4 Chitosan

Previous research by Qin *et al.* showed that water-insoluble chitosan ($M_w = 48 \cdot 10^{-3}$–$130 \cdot 10^{-3}$ g·mol^{-1}, 85.6–86.2% deacetylation) inhibits the growth of *E. coli*. Based on chitosan's solubility only in acidic media, its antibacterial

activity has been reported to diminish at pH 6.5 [142]. The antibacterial properties of chitosan are attributed to its polycationic structure, and its effectiveness is due to the acidic nature of the water acting as a medium [113], [143]. The pH of aqueous inoculum medium LB varies between 7.0–8.0; therefore, the antibacterial efficacy deriving from its polycationic structure and dissolution is questionable. Still, chitosan particles partially protrude from the surface and become exposed at the cut edges of the foam potentially minimizing colonization.

The absence of covalent bonding between hydrophobic polysiloxane elastomer and hydrophilic additive particles supports such protrusion. In this case, hydrophilic particles not bound to the polymer could surface with higher probability due to the weaker polymer-particle interactions and will be less covered by the polymer layer. This would enhance the exposure of particles to the LB medium containing microorganisms and improve antibacterial efficacy.

6.2.1.5 Tannic acid

During the 24-hour inoculation of SIF-TAN foams, the inoculum medium discolored from light-yellowish to brownish color, clearly indicating TA leakage from the cubes. As TA is a highly soluble molecular substance, its vibrational diffusion from a hydrophobic cross-linked polymer network and dissolution into an aqueous medium is possible [144]. This leakage is further facilitated by cutting the sample and exposing it to the solution since the additive particles are less covered by the polymer layer on the crossectional area. Of all the additive-doped foams evaluated, the SIF-TAN foam exhibited the strongest antibacterial properties, achieving a 0.5 log reduction in c[CFU] compared to the untreated SIF sample.

Using (hydrophilic) TA and chitosan in polymer foam formulation causes a distinguishable effect in inhibiting bacterial growth, meaning significantly lower c[CFU] values in the medium. Both additives are considered antibacterial, and their application in polysiloxane elastomers is described in various research.

6.2.2 Bacterial adhesion: Detachment from the foam structure

The hydrophobic and direct physical interactions encourage the adhesion of bacteria on polysiloxane surfaces. During bacterial division in growth medium the growing number of bacteria also promotes the cohesive planktonic formations. Different bacterial formations and population densities are visible on SEM micrographs, but whether these bacteria adhered to the surface during inoculation or were planktonic before immersing the foam samples in fixation solution is unclear without further investigation.

Extracting the bacteria from the foam was done in five sequential 10-minute washes using pH-neutral PBS solution as the washing medium, from which the determined c[CFU] shows the leaked bacterial concentration (**Figure 40**). Such agitated leakage describes the following situations: average bacterial concentration inside the foam, the relative strength of bacterial adhesion, and the effect

of the cellular structure of the foam. In addition, we can compare whether the bacterial population is larger in or around the foam cubes with the results discussed in Chapter **6.3**.

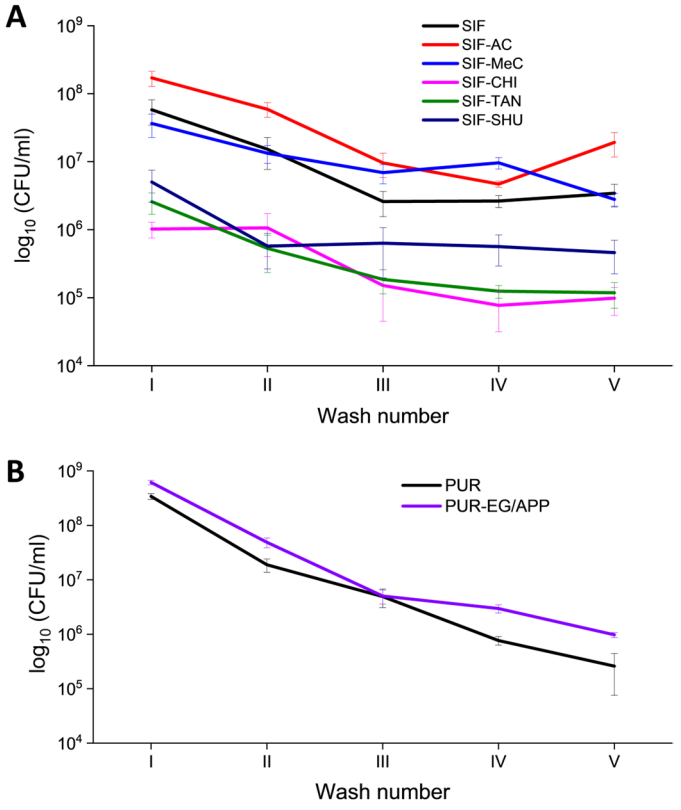

Figure 40. Extraction of bacteria from cubes via 5 subsequent wash cycles: concentrations of *E. coli* in the sequential washout media (CFU/ml of PBS). (A) Extraction profiles of polysiloxane-based foams are separated from (B) polyurethane foams due to the difference in cellular structure – the latter have significantly larger voids, which creates an advantage for a fast medium change. [Pub III]

During the agitation, planktonic cells are assumed to be washed out first, followed by the adhered cells by gradually detaching from cell walls. Due to the larger pores between cells of polyurethane foams, more bacteria are flushed into the washing medium during the first washes (**Figure 40**). As discussed in previous sections, the bacterial adhesion on PUR foam surfaces is minimal compared to SIF surfaces. Such rapid extraction correlates with the relatively higher hydrophilicity of the polyurethane foam surfaces. On the other hand, extracting bacteria from SIFs shows plateauing, indicating the slow detachment of bacteria, assumably from the foam walls. This phenomenon is supported by the relatively higher hydrophobicity of polysiloxanes and the concomitant higher bacterial population on their surfaces. The differences between SIFs are minor, although

the c[CFU] of SIF-AC from the fifth wash ('Wash V') increases. The c[CFU] around SIF-AC (**Figure 43**) and the adhered bacterial population seen on SEM micrographs (a growth medium for 24 hours under dynamic conditions) are the highest among other foams tested. Such distinct differences between the washout curves can be attributed to the eventual release of the bacterial biofilm layer shown in **Figure 38** (SIF-AC), thus increasing c[CFU] in PBS.

6.2.3 Bacterial adhesion: Restraints in inoculation conditions

Given enough time, the bacterial concentrations can increase several orders of magnitude in viable cell count, and bacterial adhesion to surfaces is stronger when the protective biofilm has formed. Dipping and squeezing the foam in inoculation suspension followed by immediate washout cycles show the release profiles of foam (0 hours) bacteria compared to the foams inoculated for 24 hours in the same conditions (**Figure 41**).

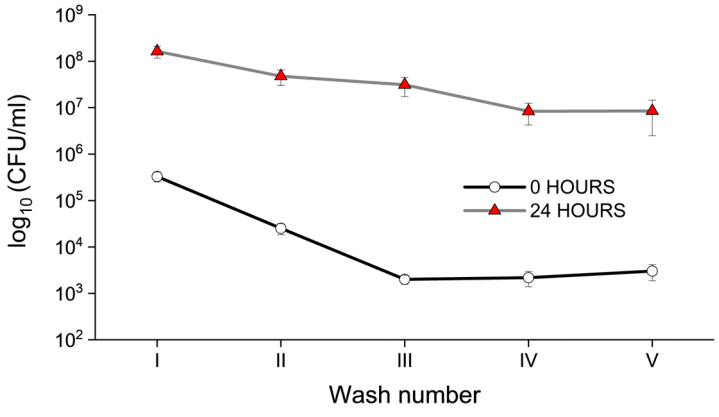

Figure 41. Release of bacteria from pristine SIF foams at different durations of inoculation: foam inoculated for 24 h and foams washed immediately after the inoculation step (no antibacterial additives). [Pub III]

Despite the differences in c[CFU]s, the extraction of bacteria from foams describes their step-by-step slow detachment from foams inoculated for 24 hours. the immediate washout extracts more bacteria initially, but from the plateauing curve of dipped foam, we can assume the hydrophobic interactions have caused the bacteria to adhere.

In previous discussions, there has always been an excess of nutrients for *E. coli* to thrive. However, in real applications, these conditions are not always met, and the available nutrients and agitation are often short-term or incidental. The question is: will the bacteria thrive and adhere to the foam surface if nutrients are scarce and there is no simulated aeration or agitation? Determining the bacterial growth in limited conditions showed that the LB nutrients filling the cube pores were sufficient for bacterial growth even without agitation (**Figure 42**).

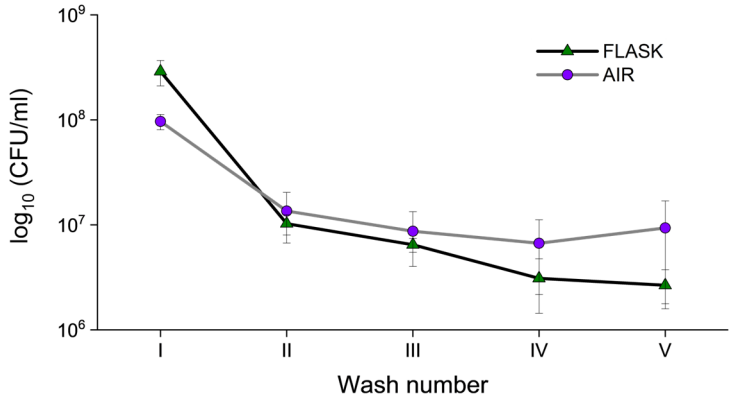

Figure 42. Differences in viable bacterial cell concentrations in pristine SIFs after 24-hour inoculation arise from different growing conditions. Experiments conducted in controlled humidity and temperature (**AIR**) had no excess broth, additional aeration, or shaking, contrary to the previously applied flask method (**FLASK**). [Pub III]

The washout curves reflect stronger bacterial adhesion in these cubes than in SIFs inoculated and agitated in the flask. This phenomenon is supported by the favored settlement of microorganisms and nutrients from the *E. coli*/LB broth suspension onto the polysiloxane surface. Considering that the outer faces of the cubes conditioned in humid air are not agitated in excess of broth, the surface area for adhesion is smaller compared to cubes that are shaken in a flask and continuously in contact with *E. coli*/LB broth.

6.3 *E. coli* growth in the surrounding medium

6.3.1 Effect of polymers and additives

In previous sections, the bacterial adhesion on the polymeric foam cell surfaces was explored, showing different bacterial formations and trending population densities. By now, it is evident that the foams tested, and polysiloxanes in general, favor bacterial adhesion. Considering the solubility of certain additives in water and the vacant free volume between polymer chains, we were interested in whether the additives in foams affect the overall viable bacterial concentration. We assessed the *E. coli* growth in the surrounding medium by measuring the bacterial concentration c[CFU] (colony forming units, or viable cell count) before and after a 24-hour inoculation period. The viable cells were counted from plated serial dilutions originating from the growth media. A foam-less inoculated medium and an inoculated medium with pristine SIF (no additive) were analyzed for reference. The c[CFU]s in the growth media are depicted relative to the initial c[CFU] in the medium, approximately 10^6 CFUs (**Figure 43**).

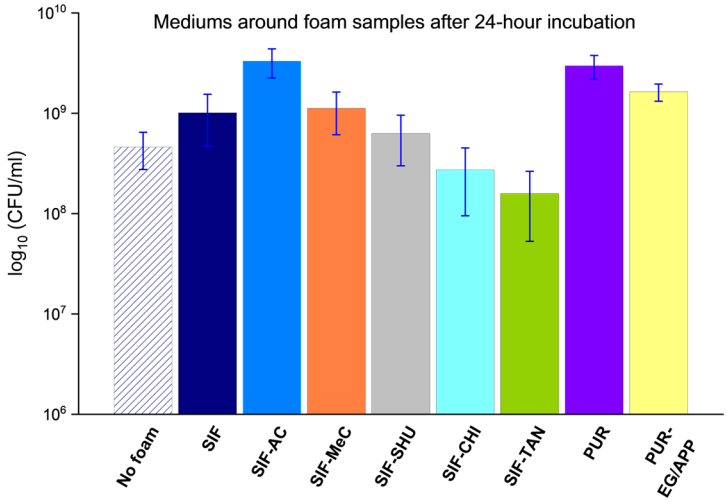

Figure 43. The viable cell counts (*E. coli*) in 24-inoculation suspensions surrounding polymeric foam samples and in a foamless reference sample. Note: CHI – chitosan, TAN – tannic acid, AC – activated carbon, MeC – methyl-cellulose, SHU – shungite, EG/APP – exp. graphite/ammonium polyphosphate. [Pub III]

Since the growth medium with foam cubes was vigorously agitated, the c[CFU] in the 24-hour growth medium is expected to indicate whether the foam components possess any antibacterial or bacteriostatic effect. This occurs when the additives in the polymer scaffold are accessible for dissolution in an aqueous medium via vibrational and solvent diffusion and upon mechanical stress. Whether adhesion is promoted or inhibited impacts the concentration of bacteria in the surrounding medium (inside and around the foam) as well as on the polymer surface. Bacteria that adhere to the surface can multiply and then become planktonic when they detach during the final growth phase. [101]

Firstly, when compared to a foamless growth medium ("No foam"), the increase in c[CFU] around the pristine foam sample (SIF) indicates enhanced bacterial growth due to the presence of the open-cellular foam cube (**Figure 43**). This comparison makes it difficult to determine whether such population growth occurred on the sample surface, inside pores, or both, or whether the bacterial microcolonies have formed as planktonic in the medium due to cohesion. Typically, such growth occurs when the initially stationary cells divide, and daughter cells spread, leading to the exponential growth phase. A one-way ANOVA was performed to compare the effect of polymer foams on c[CFU] in the 24-hour growth medium. At the p=0.05 level, the population means are significantly different (F=4.53897). Tukey's test for multiple comparisons found that the mean value of c[CFU] was significantly different between SIF-TAN and SIF-AC, and SIF-AC and SIF-CHI (p=0.05). However, there was no statistically significant difference between SIF and foamless medium, or between SIF and PUR.

6.3.2 Effect of structural differences in SIFs and PUR foams

Polyurethane foams act similarly to AC-doped SIFs by allowing increased bacterial growth in the medium. The WCA values show that polysiloxane and polyurethane-based foams were both moderately hydrophobic. The expandable graphite and polyphosphate in PUR-EG/APP foams cause slightly lower concentrations of *E. coli* in the growth medium compared to regular PUR. However, the difference of more than five times in c[CFU] between SIFs and PURs could also derive from structural differences of the foams. Near similar apparent foam densities, SEM micrographs reveal higher porosity of the PURs, which, on one hand, suggests that the bacteria have less surface area to adhere to and, therefore, to multiply, and on the other hand, the vigorous movement of the medium during shaking could hinder the adhesion of bacteria or simply eases the mobility of both planktonic and detached, previously adhered bacteria. Observing the surfaces, both PURs had a smooth and continuous surface with no visual microroughness compared to pristine SIF and SIF-AC. The bacterial adhesion on PUR occurs on the "bridge-like" polymer strands in **Figure 44** (B, and F), previously emerged during the foam formation.

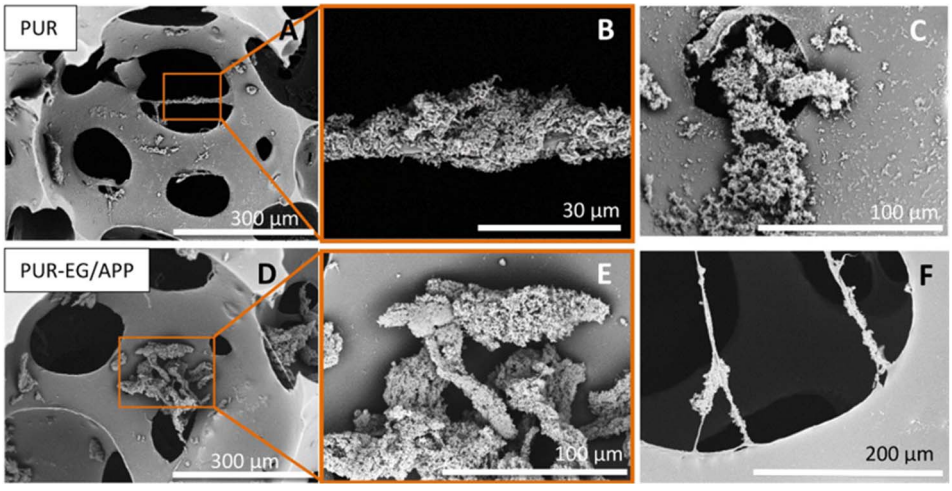

Figure 44. Polyurethane foams PUR (A–C) and PUR-EG/APP (D–F) have a distinguished hollow structure. Most bacteria have adhered to the thread-like formations across the pore interconnections, as seen on A, B, and F. For PURs in general, multiple large bacterial formations of *E. coli* are found which were not prevalent in SIFs. Adapted from the author's original work. [Pub III]

As the inoculation/growth medium flows through the channels, the planktonic bacteria adhere to these sites, leading to the assembly of larger colonies. For PUR-EG/APP foams, we noticed that most bacteria remaining in the structure formed large colonies in densely populated random locations rather than being sparse on the elastomer surface, as seen for SIFs. For PURs, *E. coli* has adhered to material bridges on the pore interconnections, forming a multilayered colony indicative of a biofilm.

6.4 Conclusions on SIF inoculation with *E. coli*

Studying SIFs reveals that the incorporated additive particles change the surface microstructure, being characteristic of the additive content and physical parameters. It was evident that these particles are only partially protruded. Hence, the majority were covered with a polysiloxane elastomer layer. Because there is no direct contact between the bacteria and protruding particles, the antibacterial activity arises indirectly from the elastomer's surface characteristics and from the dissolution effect due to the polysiloxane elastomer's permeability to water vapor and the physical dimensions of the relatively thin cell walls.

The dissolution of TA from the matrix is proposed as the main factor for antibacterial effect, decreasing c[CFU] in the surrounding medium and also inside the foam significantly. This effect would be especially beneficial when the material is exposed to wet or simply moist conditions, which enhance the antibacterial effect arising from physical dissolution. In general, by applying water-soluble additives, we could see an antibacterial effect in both the surrounding medium and on the surface.

We also observed that using AC in foam composition entices the Gram-negative *E. coli* bacterium on the polysiloxane surface. The AC concentrations used in our experiments are relatively low. Considering that in the polymer composite industry, different types of carbon-based additives are extensively applied in polymeric foam formulations in higher concentrations, it is likely to increase the bacterial spread in these materials.

7 CONCLUSIONS AND FUTURE PERSPECTIVES

7.1 Conclusions on structure-property effects in SIFs

This dissertation seeks to elucidate the connections between the blowing process and the resultant structure and properties of polysiloxane composite foams, commonly referred to as silicone foams (SIFs), particularly in light of their current and future uses. Overall, the synthesis of moldable elastomeric SIFs with considerably good mechanical properties at low densities was discussed in this dissertation, targeting technically upscalable compositions. As antibacterial performance is often expected, their interaction with microorganisms is investigated reflecting on their use in human contact applications.

Kinetic performance of monoalcohols

The aim of this study was to provide a better understanding of applying both water and its blends of other hydroxy-functional simple molecules as blowing agents involved in a dehydrocondensation reaction with **polymeric hydride-functional polysiloxane.**

The kinetic performance of different primary, secondary, and tertiary alcohols was compared under mild catalytic conditions. The evolution of H_2 from the reaction with **poly(methylhydrosiloxane) (PMHS)** was evaluated in terms of reaction rate, from which it was evident that the performance of alcohols differs from what has been proposed, and different sets of molecular descriptor combinations and reaction conditions are needed to describe the progressing reaction. Despite its simple structure and low steric hindrance, methanol (MeOH) is a highly polar molecule whose reactivity is limited due to the hydrophobic nature of PMHS. In contrast, 2-ethylhexanol (iOctOH) benefits from its high miscibility with PMHS and the accessibility of its hydroxyl group (OH), which enhances its performance. Among the alcohols studied, structural bulkiness is the most significant factor hindering reactivity in terms of overall performace, even when some alcohols exhibit relatively low polarity and high miscibility with PMHS. Furthermore, the pK_a values calculated using COSMO-RS in water correlate well with the initial reactivity of the alcohols during the conversion process. However, to fully understand the reactivity of the alcohols in the catalyzed dehydrocondensation with hydrophobic PMHS, pK_a data must be considered alongside factors such as hydrophobicity and steric hindrance.

Enhancing foam structure

Water and mono-, di- and trifunctional alcohols were applied as blowing blends that simultaneously partake in dehydrocondensation and crosslinking processes. Their effectivity was discussed **based on the structure-property relationships of** the resulting **foams**. Both improvements and degradations in physical and mechanical properties show that by balancing the alkanol/water molar ratio, it is possible to achieve low-density foams without severely compromising their

mechanical integrity. The study showed that water as the main blowing agent promotes the formation of low-density silicone foams due to the rapid setting of the cellular structure during crosslinking and expansion of the polymer matrix. However, the partial replacement of water with dialcohols with varying alkyl lengths improved the foam's mechanical and physical properties, attributed to the altered dehydrocondensation kinetics and the less rigid crosslinks formed in the elastomer network.

Bacterial interactions with polymeric foams

In this study, a Gram-negative *E. coli* was used as a model bacterium to screen the bacterial adhesion and evaluate the effect of surface properties of polymer foams on bacterial adhesion and growth. The antimicrobial characteristics of elastic foams vary depending on the foam material and the availability of the additives. Polysiloxane foams chosen for inoculation tests varied in apparent density and mechanical properties and were macrocellular in nature. These foam formulations with a fixed content of different organic and inorganic additives were designed based on their cure kinetics and mechanical properties. Arising from differences in additive particle shape, size, and surface properties, their use in foam formulations integral to crosslinked polysiloxane scaffold favored their use as functional additives.

The study concluded that the antibacterial activity primarily arises from the polysiloxane elastomer's surface characteristics and the dissolution of the antibacterial agent, particularly in moist conditions. Despite the additive particles remaining covered by the polymer layer, the antibacterial effect of tannic acid was significant due to its dissolution from the polymer matrix, which, however, may lead to its depletion and antibacterial effect. Additionally, using activated carbon attracts Gram-negative *E. coli* to the surface, raising concerns about potential bacterial proliferation when higher concentrations of carbon-based additives are used in polymer composites, which is common practice for rubber material manufacturing. Although the antimicrobial effect of numerous additives in silicones is shown by other works, the antifouling approach is generally considered more feasible than the active leaching of the antimicrobial reservoir, which will deplete over time. However, considering the application of such foams mainly as cushioning in dry or humid environments, then such leakage, to some extent, is favored and could be an additional attribute for antifouling surfaces.

7.2 Limitations and avenues for further research

Structural and mechanical properties

The current research explores how variations in cellular structures, namely cell diameter, cell wall thickness of synthesized water-alkanol blown silicone foams contribute to the overall deformability of these structures. Moreover, nano- and microcellular architectures are being developed, partly due to the increased

insulation and mechanical performance arising from the homogeneous structures of high cell densities. By understanding the relationship between cellular architecture and mechanical properties, materials with tailored stiffness properties optimize them for various applications in fields such as biomedical engineering, materials science, and structural engineering.

Polymeric foams and microorganisms

Considering the current and potential applications of elastomeric silicone foams as cushioning materials, it's clear that enhancing their non-existent antimicrobial properties is necessary. The choice of antimicrobial strategy will depend on the material's application and needs further development based on the mechanisms involved. The antifouling or antimicrobial properties can derive from the synergistic effect of surface properties and leakage of antimicrobial agents, which gives access to numerous possible combinations. For polysiloxanes, preventing the adhesion of microorganisms is the first and basic maneuver to avoid further biofilm formation. To enhance the selection of foams and their properties, the formulations for bulk SIFs can be altered so that the surface properties do not favor the hydrophilic-hydrophilic interactions between polysiloxane and bacteria. Introducing surface roughness in bulk by increasing filler content would be one perspective, and synergistic improvement in mechanical properties would help to minimize the accompanying degradation of elastomer's mechanical properties.

To enhance understanding of bacterial interactions with additive-polymer composites and foams, the following research directions can be considered:

- Balancing SIF formulations to facilitate effective ratio of antimicrobial additives
- investigating a variety of bacteria, taking into account differences in properties, shapes, and surface charges since these factors significantly influence adhesion
- examining and tuning the porous nature of SIFs and their ability to utilize capillary action for fluid absorption.

Such studies are essential for improving the use of SIFs in the medical field, going beyond their traditional use as cushioning materials. Another possible strategy is in **encouraging the hierarchical growth of an open cell structure along with maintained biocompatibility**, allowing SIFs to be used as a scaffolds for biomedical applications where microcellular architectures can be considered.

Sustainability in formulations

The sustainability of this work depends on using readily available low-molecular reagents, often derived from industrial byproducts. However, heavy reliance on Pt-catalytic processes could potentially restrict future production volumes, as platinum is considered a scarce material. While Karstedt's catalyst is effective, it

is not sustainable for elastomers destined for landfills. Therefore, it is recommended to explore other catalysts to avoid the high cost of platinum. The research on sustainable catalysts is increasingly crucial for future developments. In summary, polysiloxane foams are an important group of elastomeric foams that significantly impact the automotive, aviation, medical, and polymer. The ability to modify the properties of the polymeric scaffold and the resulting cellular structure allows for customization for specific applications, ranging from cushioning to wound treatments, without limiting the possibilities. While there are environmental concerns to consider, ongoing research and innovation promise a future where polysiloxanes can continue to offer their numerous benefits in a more sustainable manner. Understanding polysiloxanes and their potential enables us to make use of their benefits while mitigating their drawbacks, thereby advancing the field of material science.

SUMMARY IN ESTONIAN

Vormitava silikoonvahu struktuur-omadussõltuvuste kirjeldamine

Elastomeersed vahud on tänapäeval laialdaselt levinud materjalid, mis lisaks istmepehmendusmaterjalidele leiavad rakendust nii transpordi-, ehitus- kui ka meditsiinitööstuses. Siloksaanpolümeeridel põhinevatel elastomeersetel vahtudel (silikoonvahtudel) on võrreldes ulatuslikult kasutusel olevate polüuretaanvahude ees olulisi eeliseid, milledest olulisemad on eelkõige ohutus inimorganismile ja keskkonnale. Kuigi polüsiloksaanide lähteainete süntees on saanud kuluka protsessi maine, on nendest elastomeeride ja elastomeersete vahtude tootmine oluliselt väiksema keskkonnamõjuga.

Silikoonvahtude jätkusuutlikkus konkreetsetes rakendustes sõltub suuresti materjali karkassi moodustava komposiidi koostisest, avatud poorsusega vahu struktuurist ning saavutatud tihedusest, mis omakorda mõjutavad suuresti ka materjali mehaanilisi omadusi. Et saavutada järjest madalama tihedusega elastseid silikoonvahte mis omaksid ka seni kasutusel olevate vahtudega vähemalt samaväärseid tugevusomadusi, on oluline ajastada kahte paralleelset protsessi – gaasieraldumist ning ristsidemete teket polümeerahelate vahel. Olenemata gaasitekkereaktsiooni valikust, panustavad mõlemad protsessid reaktsioonisegu viskoossuse kasvu ning vahu lõppstruktuuri kujunemisesse. Vahu karkassi moodustava elastomeeri moodustumisel osaleb lisaks ristseostuvatele polümeerahelatele, katalüsaatorile ning moderaatorile ka mitmeid erineva funktsiooniga täidiseid. Seetõttu on iga varasemalt uuritud eksperimentaalsed süsteemid ja reaktsioonitingimused erinevad. Et uurida erinevate gaasitekitavate segude efektiivsust ja ulatust silikoonvahu paisutamisel, peab sellise polümeerse segu paisutamine toimuma kontrollitud tingimustes ja väljatöötatud elastomeerse segu baasil.

Antud doktoritöös on uuritud läbivalt kahte peamist teemat – katalüütilisel dehüdrokondensatsioonireaktsioonil tekkiva vesiniku eraldumise kineetikat ning gaasitekkeks kasutatavate segude mõju vahu füüsikalis-mehaanilistele omadustele. Kolmanda teemana on uuritud sünteesitud silikoonvahtude interaktsiooni Gram-negatiivse kolibakteriga, simuleerides sellega taoliste vahtude rakendusi ja neist tulenevaid tingimusi. Kuna mahult on elastsete polümeervahtude põhiliseks kasutusalaks istmepehmendused ja madratsid, siis on vajalik ära hoida mikroorganismide levik nii nende pinnal kui ka sisemuses, seda eelkõige nakkuse leviku vältimiseks ja materjali füüsikalis-esteetiliste omaduste halvenemist ajas. Kasutatud lähtematerjalide valik põhineb väljatöötatud elastomeeri moodustaval koostisel, millest Si–H funktsionaliseeritud polüsiloksaanil (polü(metüülhüdrosiloksaanil)) on kandev roll ristsidujana kuid mis on võimeline reageerima hüdroksüülrühma kandva molekuliga. Sellisest reakstioonist eralduv vesinik tekib hajutatult üle polümeerse segu, tagades ühtlasema nukleatsiooni ja avatud poorususega vahustruktuuri. Küll aga mõjutab gaasieraldumise kineetikat selleks valitud hüdroksüül-segu koostis.

Tulemused näitavad, et vesi ainsa gaasitekke reagendina tagab kiire ja ühtlase vahustruktuuri madalate tiheduste juures läbi kahe järjestikuse ja võrdlemisi kiire reaktsiooni. Võrdlemisi pehme ja peene struktuuriga vahu tugevusomaduste edasiarendamiseks võeti kasutusele madalmolekulaarsed alkoholid ning varieeriti vee-alkoholi molaarsuhet, seejuures tagades reaktsiooniks vajaliku hulga siloksaanhüdriidi. Monoalkoholid ei moodusta polümeerahelate vahel ristsidemeid ning neid on võimalik kasutada ristsidemete osakaalu vähendamiseks ilma eralduva gaasi kogust vähendamata. Sellest tulenevad muutused reaktsioonisegu viskoossuses ja karkassi elastsuses muudavad ka tekkiva vahu struktuuri. Seega on võimalik monoalkohole ja nende segusid veega kasutada just struktuuri ja ka tiheduse modifitseerimisel. Seevastu on dialkoholide ja glütserooli potentsiaal põhjendamatult alahinnatud silikoonvahtude sünteesis, kuna lisaks ristsidujana ja gaasitekkeallikana on tegemist ka võrdlemisi soodsate reagentidega, mida kaasates on võimalik mõjutada tekkiva vahu struktuuri madalate tiheduste juures. Vee ja konkreetse dialkoholi molaarsuhte varieerimine näitas, et vee domineeriv osakaal on vajalik optimaalse tiheduse saavutamiseks, ning dialkoholi sisaldus vee-alkoholi segus omakorda annab tulemuseks suurema eritugevusega vahud.

Silikoonelastomeerid on oma olemuselt hüdrofoobsed ning mikroorganismide kinnitumine pinnale ja soodsate tingimuste puhul nende edasine vohamine ajendab leidma lahendusi, mis vähendaksid nende esmast kontakti ja püsivat kinnitumist. Pooride pinna ja selle koostise uurimisel selgus, et silikoon kui väga madala pindpinevusega polümeer katab suuremas osas täidiseosakesi, mistõttu nende kokkupuude mikroorganismidega on piiratud. Vesilahustuvad lisandid, nagu näiteks tanniinhape, on võimelised ahelatevahelise vaba ruumala tõttu välja lahustuma, vähendades seega elusbakterite populatsiooni kasvulahuses. Kuna täidiste ja lisandite osakaal elastomeeri moodustavas segus on piiratud, eelkõige segu viskoossust ja tahenenud elastomeeri mehaaniliste omaduste tõttu, on paisutamisel õhenenud poori vaheseinast eenduvad erinevate mõõtmete ja kujuga osakesed ebaühtlaselt hajutatud ning ei suurenda oluliselt pinnakarendust. Antimikroobse efektiivsuse tagamiseks vajalikku nanoskaalas kareduse saavutamine on seeläbi keeruline, seega oleks vajalik uurida alternatiivseid lähenemisi silikoonil põhineva komposiitmaterjali pinnaomaduste muutmiseks või tõhustada mikroobivastaste ainete eraldumist materjalist.

Kokkuvõttes võib öelda, et vesi, alkoholid ja nende segud on elastomeersete silikoonvahtude sünteesis praktilised ning efektiivsed gaasitekitajad, pidades seejuures silmas ka tööstuslikul skaalal tootmist. Lisaks madalatele tihedustele ja avatud poorsusele omavad nende abil kergitatud vahud ka märkimisväärselt häid mehaanilisi omadusi.

REFERENCES

[1] N. Dinmore, "Train fires: Understanding the risks and controlling them," *Global Railway Review*, no. 1 2021, May 10, 2021. [Online]. Available: https://www.globalrailwayreview.com/article/122673/train-fires-risks-controlling/

[2] S. Hamdani, C. Longuet, D. Perrin, J.-M. Lopez-cuesta, and F. Ganachaud, "Flame retardancy of silicone-based materials," *Polymer Degradation and Stability*, vol. 94, no. 4, pp. 465–495, Apr. 2009, doi: 10.1016/j.polymdegradstab.2008.11.019.

[3] T. Métivier and P. Cassagnau, "Foaming behavior of silicone/fluorosilicone blends," *Polymer*, vol. 146, pp. 21–30, Jun. 2018, doi: https://doi-org.ezproxy.utlib.ut.ee/10.1016/j.polymer.2018.05.028.

[4] H. Braunwarth and F. H. H. Brill, "Antimicrobial efficacy of modern wound dressings: Oligodynamic bactericidal versus hydrophobic adsorption effect," *Wound Medicine*, vol. 5, pp. 16–20, Jun. 2014, doi: 10.1016/j.wndm.2014.04.003.

[5] P. Chadwick, F. Taherinejad, K. Hamberg, and M. Waring, "Clinical and scientific data on a silver-containing soft-silicone foam dressing: an overview," *J Wound Care*, vol. 18, no. 11, pp. 483–490, Nov. 2009, doi: 10.12968/jowc.2009.18.11.45001.

[6] M. Townend, C. Haylock, and J. F. Wolfaardt, "Macrocellular silicone foam for mechanically retaining orbital prostheses," *The Journal of Prosthetic Dentistry*, vol. 57, no. 5, pp. 611–616, May 1987, doi: 10.1016/0022-3913(87)90346-5.

[7] A. Abram *et al.*, "Bacterial Adhesion on Prosthetic and Orthotic Material Surfaces," *Coatings*, vol. 11, no. 12, p. 1469, Nov. 2021, doi: 10.3390/coatings11121469.

[8] F. De Buyl and H. Gastaldi, "Insights into the Use of Biocides in Silicones Sealants: Test Methods and Durability Aspects," in *Durability of Building and Construction Sealants and Adhesives*, ASTM International100 Barr Harbor Drive, PO Box C700, West Conshohocken, PA 19428–2959, 2004, pp. 228–251. doi: 10.1520/STP12566S.

[9] M. Nowacka, A. Rygała, D. Kręgiel, and A. Kowalewska, "New Antiadhesive Hydrophobic Polysiloxanes," *Molecules*, vol. 26, no. 4, p. 814, Feb. 2021, doi: 10.3390/molecules26040814.

[10] B. E. Obi, "Polymeric Foams Structure-Property-Performance," in *Polymeric Foams Structure-Property-Performance*, Elsevier, 2018. doi: 10.1016/B978-1-4557-7755-6.00006-9.

[11] "ISO 3386-1:1986, Polymeric materials, cellular flexible – Determination of stress-strain characteristic in compression – Part 1 : Low-density materials," ISO, Jun. 1986. [Online]. Available: https://www.iso.org/standard/8683.html

[12] F. M. De Souza, Y. Desai, and R. K. Gupta, "Introduction to Polymeric Foams," in *ACS Symposium Series*, vol. 1439, R. K. Gupta, Ed., Washington, DC: American Chemical Society, 2023, pp. 1–23. doi: 10.1021/bk-2023-1439.ch001.

[13] A. Ito, T. Semba, and M. Ohshima, "Effect of crosslinking points on bubble nucleation in the microcellular foaming of thermosets," *Polymer*, vol. 216, p. 123414, Feb. 2021, doi: 10.1016/j.polymer.2021.123414.

[14] S. Wang *et al.*, "Surface coated rigid polyurethane foam with durable flame retardancy and improved mechanical property," *Chem. Eng. J.*, vol. 385, p. 123755, Apr. 2020, doi: 10.1016/j.cej.2019.123755.

[15] D. K. Chattopadhyay and D. C. Webster, "Thermal stability and flame retardancy of polyurethanes," *Progress in Polymer Science*, vol. 34, no. 10, pp. 1068–1133, Oct. 2009, doi: 10.1016/j.progpolymsci.2009.06.002.

[16] R. Nowell, “EN 45545 in transition – a GB perspective,” RSSB, 2016. Accessed: May 25, 2018. [Online]. Available: http://www.ikolej.pl/fileadmin/4.EN_45545_in_transition%E2%80%A6_a_GB_perspective_-_Richard_Nowell.pdf
[17] “UL 94 – Standard for Tests for Flammability of Plastic Materials for Parts in Devices and Appliances.” [Online]. Available: https://www.ulttc.com/en/solutions/test-methods/combustion-fire/flammability/flammability-ul-94-v.html
[18] *EN 45545-2:2020+A1:2023, Railway applications – Fire protection on railway vehicles – Part 2: Requirements for fire behavior of materials and components*.
[19] “Cushioning.” Accessed: Jan. 12, 2024. [Online]. Available: https://rogerscorp.com/Applications/Cushioning
[20] F. Dankert and C. Hänisch, “Siloxane Coordination Revisited: Si−O Bond Character, Reactivity and Magnificent Molecular Shapes,” *Eur. J. Inorg. Chem.*, vol. 2021, no. 29, pp. 2907–2927, Aug. 2021, doi: 10.1002/ejic.202100275.
[21] E. Yilgör and I. Yilgör, “Silicone containing copolymers: Synthesis, properties and applications,” *Progress in Polymer Science*, vol. 39, no. 6, pp. 1165–1195, Jun. 2014, doi: 10.1016/j.progpolymsci.2013.11.003.
[22] D. Son *et al.*, “An integrated self-healable electronic skin system fabricated via dynamic reconstruction of a nanostructured conducting network,” *Nature Nanotech*, vol. 13, no. 11, pp. 1057–1065, Nov. 2018, doi: 10.1038/s41565-018-0244-6.
[23] P. Hu, J. Madsen, and A. L. Skov, “One reaction to make highly stretchable or extremely soft silicone elastomers from easily available materials,” *Nat Commun*, vol. 13, no. 1, p. 370, Jan. 2022, doi: 10.1038/s41467-022-28015-2.
[24] M. A. Brook, “Functional silicone oils and elastomers: new routes lead to new properties,” *Chem. Commun.*, p. 10.1039.D3CC03531J, 2023, doi: 10.1039/D3CC03531J.
[25] M. Andriot, J. V. DeGroot, and R. Meeks, “Silicones in Industrial Applications,” 2007, pp. 61–161. Accessed: Nov. 09, 2023. [Online]. Available: https://www.researchgate.net/publication/321293316_Chapter_2_-_Silicones_in_Industrial_Applications_pp_61-161
[26] M. J. Owen and P. R. Dvornic, “General Introduction to Silicone Surfaces,” in *Silicone Surface Science*, vol. 4, M. J. Owen and P. R. Dvornic, Eds., in Advances in Silicon Science, vol. 4. , Dordrecht: Springer Netherlands, 2012, pp. 1–21. doi: 10.1007/978-94-007-3876-8_1.
[27] P. Bian, Y. Wang, and T. J. McCarthy, “Rediscovering Silicones: The Anomalous Water Permeability of ‘Hydrophobic’ PDMS Suggests Nanostructure and Applications in Water Purification and Anti-Icing,” *Macromol. Rapid Commun.*, vol. 42, no. 5, p. 2000682, Mar. 2021, doi: 10.1002/marc.202000682.
[28] H. Weber, I. De Grave, E. Röhrl, and V. Altstädt, “Foamed Plastics,” in *Ullmann’s Encyclopedia of Industrial Chemistry*, Wiley-VCH Verlag GmbH & Co. KGaA, Ed., Weinheim, Germany: Wiley-VCH Verlag GmbH & Co. KGaA, 2016, pp. 1–54. doi: 10.1002/14356007.a11_435.pub2.
[29] *Polymeric Foams Structure-Property-Performance*. Elsevier, 2018. doi: 10.1016/B978-1-4557-7755-6.00006-9.
[30] “BISCO® Products – MF1® Bun Silicones.” Accessed: May 17, 2019. [Online]. Available: https://www.rogerscorp.com/ems/bisco/products/4/25/MF1-Bun-Silicones.aspx
[31] “Silicone Sponge Extrusions,” Silicone Engineering Ltd, Product Specifications. [Online]. Available: https://silicone.co.uk/products/silicone-sponge-extrusions/

[32] “Silicone Sponge and Silicone Foam Sheet Material Data Sheets,” Stockwell Elastomerics, Inc. [Online]. Available: https://www.stockwell.com/silicone-sponge-foam-data-sheets/
[33] H. Moretto, M. Schulze, and G. Wagner, “Silicones,” in *Ullmann’s Encyclopedia of Industrial Chemistry*, 1st ed., Wiley-VCH, Ed., Wiley, 2000. doi: 10.1002/14356007.a24_057.
[34] T. Métivier and P. Cassagnau, “New trends in cellular silicone: Innovations and applications,” *Journal of Cellular Plastics*, vol. 55, no. 2, pp. 151–200, Mar. 2019, doi: 10.1177/0021955X18806845.
[35] “Silicone Chemistry Overview|Dow Corning,” 2003.
[36] C. L. Lee, R. G. Niemi, and K. M. Kelly, “New Silicone RTV Foam,” *Journal of Cellular Plastics*, vol. 13, no. 1, pp. 62–67, Jan. 1977, doi: 10.1177/0021955X7701300108.
[37] C. L. Lee and G. M. Ronk, “Flame Resistant Open-Cell Silicone Foam,” *Journal of Cellular Plastics*, vol. 18, no. 3, pp. 178–182, May 1982, doi: 10.1177/0021955X8201800304.
[38] T. Takeoka, “About Silicone Foam (Foamed Silicone),” *Three Bond Technical News*, no. 35, Sep. 21, 1991. Accessed: Mar. 23, 2018. [Online]. Available: http://www.threebond.com/technical/technicalnews/pdf/tech35.pdf
[39] Y. Pang, Y. Cao, W. Zheng, and C. B. Park, “A comprehensive review of cell structure variation and general rules for polymer microcellular foams,” *Chem. Eng. J.*, vol. 430, p. 132662, Feb. 2022, doi: 10.1016/j.cej.2021.132662.
[40] E. Rostami-Tapeh-Esmaeil and D. Rodrigue, “Morphological, Mechanical and Thermal Properties of Rubber Foams: A Review Based on Recent Investigations,” *Materials*, vol. 16, no. 5, p. 1934, Feb. 2023, doi: 10.3390/ma16051934.
[41] D. Zhu, S. Handschuh-Wang, and X. Zhou, “Recent progress in fabrication and application of polydimethylsiloxane sponges,” *J. Mater. Chem. A*, vol. 5, no. 32, pp. 16467–16497, 2017, doi: 10.1039/C7TA04577H.
[42] S. J. Yeo, M. J. Oh, and P. J. Yoo, “Structurally Controlled Cellular Architectures for High-Performance Ultra-Lightweight Materials,” *Adv. Mater.*, vol. 31, no. 34, p. 1803670, Aug. 2019, doi: 10.1002/adma.201803670.
[43] Grogan Group, *Rogers MF-1 seat foam for the rail industry*, (Feb. 10, 2011). Accessed: Jan. 15, 2024. [Online Video]. Available: https://www.youtube.com/watch?v=XrVixVW5CCk
[44] Y.-Y. Wu *et al.*, “Large-scale and facile fabrication of phenyl-containing silicone foam materials with lightweight, wide-temperature flexibility and tunable pore structure for exceptional thermal insulation,” *Chemical Engineering Journal*, vol. 492, p. 152183, Jul. 2024, doi: 10.1016/j.cej.2024.152183.
[45] “BS 6853:1999, Code of practice for fire precautions in the design and construction of passenger carrying trains,” British Standards Institution.
[46] M. Nowacka, A. Kowalewska, A. Rygala, D. Kregiel, and W. Kaczorowski, “Hybrid Bio-Based Silicone Coatings with Anti-adhesive Properties,” *Materials*, vol. 16, no. 4, p. 1381, Feb. 2023, doi: 10.3390/ma16041381.
[47] T. Liu, Y. Lei, F. Zhang, S. Guo, and S. Luo, “Microcellular Crosslinked Silicone Rubber Foams: Influence of Nucleation Agent (Polyhedral Oligomeric Silsesquioxane) on the Rheological, Vulcanizing, Cell Morphological Properties,” *Polymer-Plastics Technology and Engineering*, vol. 57, no. 16, pp. 1623–1633, Nov. 2018, doi: 10.1080/03602559.2017.1410845.

[48] L. N. Lewis, J. Stein, Y. Gao, R. E. Colborn, and G. Hutchins, “Platinum Catalysts Used in the Silicones Industry,” *Platinum Metals Rev.*, vol. 41, no. 2, pp. 66–75, 1997.

[49] T. Hofmann, R.-U. Giesen, and H.-P. Heim, “High Consistency Silicone Rubber Foams,” *Polymers*, vol. 16, no. 9, p. 1181, Apr. 2024, doi: 10.3390/polym16091181.

[50] M. Sauceau, J. Fages, A. Common, C. Nikitine, and E. Rodier, “New challenges in polymer foaming: A review of extrusion processes assisted by supercritical carbon dioxide,” *Progress in Polymer Science*, vol. 36, no. 6, pp. 749–766, Jun. 2011, doi: 10.1016/j.progpolymsci.2010.12.004.

[51] J. E. Mark and B. Erman, *Rubberlike elasticity: a molecular primer*, 2nd ed. Cambridge ; New York: Cambridge University Press, 2007.

[52] A. G. Bejenariu, J. Ö. Poulsen, A. L. Skov, and L. Henriksen, “A Comparative Study on the Influence of the Platinum Catalyst in Poly(dimethylsiloxane) Based Networks Synthesis,” *Annual Transactions – The Nordic Rheology Society*, vol. 17, no. 2009, pp. 269–276, 2009, [Online]. Available: https://pdfs.semanticscholar.org/b228/3371f08c0e50d10110052ddd31534791e210.pdf

[53] M. A. Brook, “New Control Over Silicone Synthesis using SiH Chemistry: The Piers-Rubinsztajn Reaction,” *Chem. Eur. J.*, vol. 24, no. 34, pp. 8458–8469, Jun. 2018, doi: 10.1002/chem.201800123.

[54] A. C. C. Esteves *et al.*, “Influence of cross-linker concentration on the cross-linking of PDMS and the network structures formed,” *Polymer*, vol. 50, no. 16, pp. 3955–3966, Jul. 2009, doi: 10.1016/j.polymer.2009.06.022.

[55] P. Mazurek, S. Vudayagiri, and A. L. Skov, “How to tailor flexible silicone elastomers with mechanical integrity: a tutorial review,” *Chem. Soc. Rev.*, vol. 48, no. 6, pp. 1448–1464, 2019, doi: 10.1039/C8CS00963E.

[56] A. M. Stricher, R. G. Rinaldi, C. Barrès, F. Ganachaud, and L. Chazeau, “How I met your elastomers: from network topology to mechanical behaviours of conventional silicone materials,” *RSC Adv.*, vol. 5, no. 66, pp. 53713–53725, 2015, doi: 10.1039/C5RA06965C.

[57] “Reactive Silicones,” Reactive Silicones by Gelest. [Online]. Available: https://technical.gelest.com/brochures/reactive-silicones/hydride-functional-polymers/

[58] T. K. Meister, K. Riener, P. Gigler, J. Stohrer, W. A. Herrmann, and F. E. Kühn, “Platinum Catalysis Revisited – Unraveling Principles of Catalytic Olefin Hydrosilylation,” *ACS Catal.*, vol. 6, no. 2, pp. 1274–1284, Feb. 2016, doi: 10.1021/acscatal.5b02624.

[59] H. F. Lamoreaux, “Organosilicon process using a chloroplatinic acid reaction product as the catalyst,” US3220972A, Nov. 30, 1965 Accessed: Jul. 12, 2021. [Online]. Available: https://patents.google.com/patent/US3220972A/en?oq=US3220972A

[60] D. Chung and T. G. Kim, “Study on the effect of platinum catalyst for the synthesis of polydimethylsiloxane grafted with polyoxyethylene,” *Journal of Industrial and Engineering Chemistry*, vol. 13, no. 4, pp. 571–577, 2007, [Online]. Available: https://api.semanticscholar.org/CorpusID:55855054

[61] D. Troegel and J. Stohrer, “Recent advances and actual challenges in late transition metal catalyzed hydrosilylation of olefins from an industrial point of view,” *Coordination Chemistry Reviews*, vol. 255, no. 13–14, pp. 1440–1459, Jul. 2011, doi: 10.1016/j.ccr.2010.12.025.

[62] L. N. Lewis and C. A. Sumpter, “Cyclodextrin modification of the hydrosilylation reaction,” *Journal of Molecular Catalysis A: Chemical*, vol. 104, no. 3, pp. 293–297, jaanuar 1996, doi: 10.1016/1381-1169(95)00147-6.

[63] R. Yu. Lukin, A. M. Kuchkaev, A. V. Sukhov, G. E. Bekmukhamedov, and D. G. Yakhvarov, “Platinum-Catalyzed Hydrosilylation in Polymer Chemistry,” *Polymers*, vol. 12, no. 10, p. 2174, Sep. 2020, doi: 10.3390/polym12102174.

[64] B. MARCINIEC, Ed., “CHAPTER 4 – The Effect of Substituents at Silicon on the Reactivity of the Si–H Bond in Hydrosilylation,” in *Comprehensive Handbook on Hydrosilylation*, Amsterdam: Pergamon, 1992, pp. 160–177. doi: 10.1016/B978-0-08-040272-7.50009-0.

[65] R. Rothon, *Fillers for Polymer Applications*. in Polymers and Polymeric Composites: A Reference Series. Cham: Springer International Publishing, 2017. doi: 10.1007/978-3-319-28117-9_9.

[66] L. Huang *et al.*, “Understanding the Reinforcement Effect of Fumed Silica on Silicone Rubber: Bound Rubber and Its Entanglement Network,” *Macromolecules*, vol. 56, no. 1, pp. 323–334, 2023, doi: 10.1021/acs.macromol.2c01969.

[67] V. Allen, L. Chen, M. Englert, A. Moussaoui, and W. Pisula, “Control of Mullins stress softening in silicone elastomer composites by rational design of fumed silica fillers,” *Composites Science and Technology*, vol. 214, p. 108955, Sep. 2021, doi: 10.1016/j.compscitech.2021.108955.

[68] D. R. Paul and J. E. Mark, “Fillers for polysiloxane (‘silicone’) elastomers,” *Progress in Polymer Science*, vol. 35, no. 7, pp. 893–901, Jul. 2010, doi: 10.1016/j.progpolymsci.2010.03.004.

[69] M. H. N. Famili, H. Janani, and M. S. Enayati, “Foaming of a polymer-nanoparticle system: Effect of the particle properties,” *J. Appl. Polym. Sci.*, vol. 119, no. 5, pp. 2847–2856, Mar. 2011, doi: 10.1002/app.32969.

[70] M. A. Osman, A. Atallah, M. Müller, and U. W. Suter, “Reinforcement of poly(dimethylsiloxane) networks by mica flakes,” *Polymer*, vol. 42, no. 15, pp. 6545–6556, Jul. 2001, doi: 10.1016/S0032-3861(01)00128-8.

[71] Z. Jia, S. Chen, and J. Zhang, “Preparation and properties of polydimethylsiloxane-mica composites,” *J of Applied Polymer Sci*, vol. 127, no. 4, pp. 3017–3025, Feb. 2013, doi: 10.1002/app.37654.

[72] Y. Xu, D. Zhao, X. Fang, G. Jiang, Y. Shen, and T. Wang, “‘Mica/ SILICATE GLASS FRIT -armored skeleton’ in PDMS composite foam for improving fire-proofing performance,” *J of Applied Polymer Sci*, vol. 140, no. 23, p. e53938, Jun. 2023, doi: 10.1002/app.53938.

[73] L. Lindgren, D. Hansson, and S. Eibpoosh, “Foamed silicone in wound care,” US10744225B2, 2016

[74] T. Zhang, S. Yao, L. Wang, W. Zhen, and L. Zhao, “Key factors for regulation of cell morphology in supercritical CO2 direct rapid depressurization foaming silicone rubber process,” *The Journal of Supercritical Fluids*, vol. 202, p. 106036, Nov. 2023, doi: 10.1016/j.supflu.2023.106036.

[75] B.-F. Guo *et al.*, “Restricted assembly of ultralow loading of graphene oxide for lightweight, mechanically flexible and flame retardant polydimethylsiloxane foam composites,” *Composites Part B*, vol. 247, p. 110290, Dec. 2022, doi: 10.1016/j.compositesb.2022.110290.

[76] R. Riesco *et al.*, “Water-in-PDMS Emulsion Templating of Highly Interconnected Porous Architectures for 3D Cell Culture,” *ACS Appl. Mater. Interfaces*, vol. 11, no. 32, pp. 28631–28640, Aug. 2019, doi: 10.1021/acsami.9b07564.

[77] P. Mazurek, B. E. F. Ekbrant, F. B. Madsen, L. Yu, and A. L. Skov, “Glycerol-silicone foams – Tunable 3-phase elastomeric porous materials,” *Eur. Polym. J.*, vol. 113, pp. 107–114, Apr. 2019, doi: 10.1016/j.eurpolymj.2019.01.051.

[78] S. Shukla and K. W. Koelling, “Classical Nucleation Theory Applied to Homogeneous Bubble Nucleation in the Continuous Microcellular Foaming of the Polystyrene−CO_2 System,” *Ind. Eng. Chem. Res.*, vol. 48, no. 16, pp. 7603–7615, Aug. 2009, doi: 10.1021/ie8011243.

[79] A. Davis, S. Surdo, G. Caputo, I. S. Bayer, and A. Athanassiou, “Environmentally Benign Production of Stretchable and Robust Superhydrophobic Silicone Monoliths,” *ACS Appl. Mater. Interfaces*, vol. 10, no. 3, pp. 2907–2917, Jan. 2018, doi: 10.1021/acsami.7b15088.

[80] X. Jiang, K. A. Whitehead, N. Arneborg, Y. Fang, and J. Risbo, “Understanding bacterial surface and adhesion properties and the implications for Pickering stabilization of colloidal structures,” *Current Opinion in Colloid & Interface Science*, vol. 69, p. 101767, Feb. 2024, doi: 10.1016/j.cocis.2023.101767.

[81] S. L. Arias, J. Devorkin, A. Civantos, and J. P. Allain, “*Escherichia coli* Adhesion and Biofilm Formation on Polydimethylsiloxane are Independent of Substrate Stiffness,” *Langmuir*, vol. 37, no. 1, pp. 16–25, Jan. 2021, doi: 10.1021/acs.langmuir.0c00130.

[82] S. L. Arias, J. Devorkin, J. C. Spear, A. Civantos, and J. P. Allain, “Bacterial envelope damage inflicted by bioinspired nanospikes grown in a hydrogel,” Bioengineering, preprint, Mar. 2020. doi: 10.1101/2020.03.28.013797.

[83] C. Beloin, A. Roux, and J.-M. Ghigo, “Escherichia coli Biofilms,” in *Bacterial Biofilms*, vol. 322, T. Romeo, Ed., in Current Topics in Microbiology and Immunology, vol. 322. , Berlin, Heidelberg: Springer Berlin Heidelberg, 2008, pp. 249–289. doi: 10.1007/978-3-540-75418-3_12.

[84] F. Ghilini, D. E. Pissinis, A. Miñán, P. L. Schilardi, and C. Diaz, “How Functionalized Surfaces Can Inhibit Bacterial Adhesion and Viability,” *ACS Biomater. Sci. Eng.*, vol. 5, no. 10, pp. 4920–4936, Oct. 2019, doi: 10.1021/acsbiomaterials.9b00849.

[85] V. Kochkodan, S. Tsarenko, N. Potapchenko, V. Kosinova, and V. Goncharuk, “Adhesion of microorganisms to polymer membranes: a photobactericidal effect of surface treatment with TiO2,” *Desalination*, vol. 220, no. 1–3, pp. 380–385, Mar. 2008, doi: 10.1016/j.desal.2007.01.042.

[86] A. J. Paula, G. Hwang, and H. Koo, “Dynamics of bacterial population growth in biofilms resemble spatial and structural aspects of urbanization,” *Nat Commun*, vol. 11, no. 1, p. 1354, Mar. 2020, doi: 10.1038/s41467-020-15165-4.

[87] Y. Yuan, M. P. Hays, P. R. Hardwidge, and J. Kim, “Surface characteristics influencing bacterial adhesion to polymeric substrates,” *RSC Adv.*, vol. 7, no. 23, pp. 14254–14261, 2017, doi: 10.1039/C7RA01571B.

[88] H. J. Busscher, G. I. Geertsema-Doornbusch, and H. C. van der Mei, “Adhesion to silicone rubber of yeasts and bacteria isolated from voice prostheses: Influence of salivary conditioning films,” *J. Biomed. Mater. Res.*, vol. 34, no. 2, pp. 201–209, Feb. 1997, doi: 10.1002/(SICI)1097-4636(199702)34:2<201::AID-JBM9>3.0.CO;2-U.

[89] B. McVerry *et al.*, “A Readily Scalable, Clinically Demonstrated, Antibiofouling Zwitterionic Surface Treatment for Implantable Medical Devices,” *Adv. Mater.*, vol. 34, no. 20, p. 2200254, May 2022, doi: 10.1002/adma.202200254.

[90] R. Wang, K. G. Neoh, Z. Shi, E.-T. Kang, P. A. Tambyah, and E. Chiong, "Inhibition of escherichia coli and proteus mirabilis adhesion and biofilm formation on medical grade silicone surface," *Biotechnol. Bioeng.*, vol. 109, no. 2, pp. 336–345, Feb. 2012, doi: 10.1002/bit.23342.

[91] A. Armugam *et al.*, "Broad spectrum antimicrobial PDMS-based biomaterial for catheter fabrication," *Biomater Res*, vol. 25, no. 1, p. 33, Dec. 2021, doi: 10.1186/s40824-021-00235-5.

[92] H. Chen, C. Yin, X. Zhang, and Y. Zhu, "Preparation and characterisation of bi-functional surface-modified silicone catheter in lumen," *Journal of Global Antimicrobial Resistance*, vol. 23, pp. 46–54, Dec. 2020, doi: 10.1016/j.jgar.2020.07.019.

[93] M. Zare, E. R. Ghomi, P. D. Venkatraman, and S. Ramakrishna, "Silicone-based biomaterials for biomedical applications: Antimicrobial strategies and 3D printing technologies," *J of Applied Polymer Sci*, vol. 138, no. 38, p. 50969, Oct. 2021, doi: 10.1002/app.50969.

[94] S. Pinto *et al.*, "Poly(dimethyl siloxane) surface modification by low pressure plasma to improve its characteristics towards biomedical applications," *Colloids and Surfaces B: Biointerfaces*, vol. 81, no. 1, pp. 20–26, Nov. 2010, doi: 10.1016/j.colsurfb.2010.06.014.

[95] A. Krasowska and K. Sigler, "How microorganisms use hydrophobicity and what does this mean for human needs?," *Front. Cell. Infect. Microbiol.*, vol. 4, no. 2014, Aug. 2014, doi: 10.3389/fcimb.2014.00112.

[96] M. Mu *et al.*, "Influence of Surface Roughness, Nanostructure, and Wetting on Bacterial Adhesion," *Langmuir*, vol. 39, no. 15, pp. 5426–5439, Apr. 2023, doi: 10.1021/acs.langmuir.3c00091.

[97] L. C. Gomes, L. N. Silva, M. Simões, L. F. Melo, and F. J. Mergulhão, "*Escherichia coli* adhesion, biofilm development and antibiotic susceptibility on biomedical materials: *E. coli* ADHESION, BIOFILM DEVELOPMENT AND ANTIBIOTIC SUSCEPTIBILITY," *J. Biomed. Mater. Res.*, vol. 103, no. 4, pp. 1414–1423, Apr. 2015, doi: 10.1002/jbm.a.35277.

[98] M. K. Chug and E. J. Brisbois, "Recent Developments in Multifunctional Antimicrobial Surfaces and Applications toward Advanced Nitric Oxide-Based Biomaterials," *ACS Mater. Au*, vol. 2, no. 5, pp. 525–551, Sep. 2022, doi: 10.1021/acsmaterialsau.2c00040.

[99] P. Shivapooja *et al.*, "Modification of Silicone Elastomer Surfaces with Zwitterionic Polymers: Short-Term Fouling Resistance and Triggered Biofouling Release," *ACS Appl. Mater. Interfaces*, vol. 7, no. 46, pp. 25586–25591, Nov. 2015, doi: 10.1021/acsami.5b09199.

[100] T. J. Gutiérrez, Ed., *Reactive and Functional Polymers Volume One: Biopolymers, Polyesters, Polyurethanes, Resins and Silicones*. Cham: Springer International Publishing, 2020. doi: 10.1007/978-3-030-43403-8.

[101] T. R. Garrett, M. Bhakoo, and Z. Zhang, "Bacterial adhesion and biofilms on surfaces," *Progress in Natural Science*, vol. 18, no. 9, pp. 1049–1056, Sep. 2008, doi: 10.1016/j.pnsc.2008.04.001.

[102] "ISO 23641:2021, 'Flexible cellular polymeric materials – Determination of antibacterial effectiveness,'" International Organization of Standardization, Geneva, Switzerland, 2021. [Online]. Available: https://www.iso.org/standard/76511.html

[103] S. Rajendran, S. S. Prabha, R. J. Rathish, G. Singh, and A. Al-Hashem, “Antibacterial activity of platinum nanoparticles,” in *Nanotoxicity*, Elsevier, 2020, pp. 275–281. doi: 10.1016/B978-0-12-819943-5.00012-9.

[104] F. M. Helaly, S. M. El-Sawy, A. I. Hashem, A. A. Khattab, and R. M. Mourad, “Synthesis and characterization of nanosilver-silicone hydrogel composites for inhibition of bacteria growth,” *Contact Lens and Anterior Eye*, vol. 40, no. 1, pp. 59–66, Feb. 2017, doi: 10.1016/j.clae.2016.09.004.

[105] S. Kheiri, M. G. A. Mohamed, M. Amereh, D. Roberts, and K. Kim, “Antibacterial efficiency assessment of polymer-nanoparticle composites using a high-throughput microfluidic platform,” *Materials Science and Engineering: C*, vol. 111, p. 110754, Jun. 2020, doi: 10.1016/j.msec.2020.110754.

[106] M. Firoozbahr, P. Kingshott, E. A. Palombo, and B. Zaferanloo, “Recent Advances in Using Natural Antibacterial Additives in Bioactive Wound Dressings,” *Pharmaceutics*, vol. 15, no. 2, p. 644, Feb. 2023, doi: 10.3390/pharmaceutics 15020644.

[107] E. Lukevics and M. Dzintara, “The alcoholysis of hydrosilanes,” *Journal of Organometallic Chemistry*, vol. 295, no. 3, pp. 265–315, Nov. 1985, doi: 10.1016/ 0022-328X(85)80314-4.

[108] K. D. Safa, S. Tofangdarzadeh, and A. Hassanpour, “Facile route to synthesis of functionalised poly(methylalkoxy)siloxane under mild and aerobic conditions in the presence of platinum catalysts,” *Journal of Organometallic Chemistry*, vol. 694, no. 25, pp. 4107–4115, detsember 2009, doi: 10.1016/j.jorganchem.2009. 08.018.

[109] O. Mukbaniani, G. Gurgenidze, L. Khananashvili, and S. Meladze, “Dehydrocondensation and hydrosilylation reactions of methylhydridesiloxane with allyl alcohol,” *International Journal of Polymeric Materials and Polymeric Biomaterials*, vol. 52, no. 10, pp. 861–876, Jan. 2003, doi: 10.1080/713743644.

[110] D. R. Burfield and R. H. Smithers, “Desiccant efficiency in solvent and reagent drying. 7. Alcohols,” *J. Org. Chem.*, vol. 48, no. 14, pp. 2420–2422, Jul. 1983, doi: 10.1021/jo00162a026.

[111] A. A. Al-Juhni, “Incorporation of less toxic antifouling compounds into silicone coatings to study their release behaviors,” University of Akron, 2006. [Online]. Available: http://rave. ohiolink.edu/etdc/view?acc_num=akron1154974014

[112] J. Sun *et al.*, “Facile fabrication of self-healing silicone-based poly(urea-thiourea)/ tannic acid composite for anti-biofouling,” *Journal of Materials Science & Technology*, vol. 124, pp. 1–13, Oct. 2022, doi: 10.1016/j.jmst.2022.01.026.

[113] C. Qin, H. Li, Q. Xiao, Y. Liu, J. Zhu, and Y. Du, “Water-solubility of chitosan and its antimicrobial activity,” *Carbohydrate Polymers*, vol. 63, no. 3, pp. 367–374, Mar. 2006, doi: 10.1016/j.carbpol.2005.09.023.

[114] S. Türk, T. Tamm, H. Mändar, A. Raal, P. Laurson, and U. Mäeorg, “Microbiological and chemical properties of shungite water,” *PEAS*, vol. 71, no. 4, p. 361, 2022, doi: 10.3176/proc.2022.4.06.

[115] T. Seifi and A. R. Kamali, “Enhanced dispersion and antibacterial activity of mechanically exfoliated graphite flakes in the presence of n-hexane and NaCl,” *Materials Letters*, vol. 304, p. 130730, Dec. 2021, doi: 10.1016/j.matlet.2021. 130730.

[116] E. S. Kravchenko, P. I. Anzhaurov, E. E. Potapov, B. A. Maizelis, A. P. Bobrov, and V. V. Belkovskii, “Highly filled composite materials based on natural rubber latex and shungite,” *International Polymer Science and Technology*, vol. 40, no. 3,

p. T/15+, Mar. 2013, Accessed: Nov. 16, 2022. [Online]. Available: https://link.gale.com/apps/doc/A325491127/AONE?u=anon~4da675b4&sid=googleScholar&xid=40d31c42
[117] J. Schindelin *et al.*, "Fiji: an open-source platform for biological-image analysis," *Nat. Methods*, vol. 9, no. 7, pp. 676–682, Jul. 2012, doi: 10.1038/nmeth.2019.
[118] *Surftens Version 4.6*. OEG, Germany. [Online]. Available: https://www.oeggmbh.com/?k=35&l=1
[119] *ASTM D 3574-17, Standard Test Methods for Flexible Cellular Materials—Slab, Bonded, and Molded Urethane Foams*, Mar. 01, 2017. doi: 10.1520/D3574-17.
[120] B. E. Obi, "Foaming Processes," in *Polymeric Foams Structure-Property-Performance*, Elsevier, 2018, pp. 131–188. doi: 10.1016/B978-1-4557-7755-6.00006-9.
[121] M. Dong *et al.*, "An overview of polymer foaming assisted by supercritical fluid," *Adv Compos Hybrid Mater*, vol. 6, no. 6, p. 207, Dec. 2023, doi: 10.1007/s42114-023-00790-6.
[122] A. Harinath, J. Bhattacharjee, S. Anga, and T. K. Panda, "Dehydrogenative Coupling of Hydrosilanes and Alcohols by Alkali Metal Catalysts for Facile Synthesis of Silyl Ethers," *Aust. J. Chem.*, vol. 70, no. 6, p. 724, 2017, doi: 10.1071/CH16537.
[123] B. P. S. Chauhan, J. S. Rathore, and N. Glloxhani, "First example of ?palladium-nanoparticle?-catalyzed selective alcoholysis of polyhydrosiloxane: a new approach to macromolecular grafting," *Appl. Organometal. Chem.*, vol. 19, no. 4, pp. 542–550, Apr. 2005, doi: 10.1002/aoc.867.
[124] A. Jurásková, A. L. Skov, and M. A. Brook, "Mild Route To Convert SiH Compounds to Their Alkoxy Analogues," *Ind. Eng. Chem. Res.*, vol. 59, no. 41, pp. 18412–18418, Oct. 2020, doi: 10.1021/acs.iecr.0c03555.
[125] H. Schüler Dr. et al, "Low density silicone foam," EP0334125A2, Mar. 10, 1989
[126] Therese M. Bauman and John E. Dietlein, "Water-blown silicone foam," US4613630A, 1985
[127] V. Consonni and R. Todeschini, "Molecular Descriptors," in *Recent Advances in QSAR Studies*, vol. 8, T. Puzyn, J. Leszczynski, and M. T. Cronin, Eds., in Challenges and Advances in Computational Chemistry and Physics, vol. 8. , Dordrecht: Springer Netherlands, 2010, pp. 29–102. doi: 10.1007/978-1-4020-9783-6_3.
[128] D. P. White, J. C. Anthony, and A. O. Oyefeso, "Computational Measurement of Steric Effects: the Size of Organic Substituents Computed by Ligand Repulsive Energies," *J. Org. Chem.*, vol. 64, no. 21, pp. 7707–7716, Oct. 1999, doi: 10.1021/jo982405w.
[129] C. Reichardt and T. Welton, *Solvents and solvent effects in organic chemistry*, 4th, updated and enl. ed ed. Weinheim, Germany: Wiley-VCH, 2011.
[130] H. Bahrmann, H.-D. Hahn, D. Mayer, and G. D. Frey, "2-Ethylhexanol," in *Ullmann's Encyclopedia of Industrial Chemistry*, Wiley-VCH Verlag GmbH & Co. KGaA, Ed., Weinheim, Germany: Wiley-VCH Verlag GmbH & Co. KGaA, 2013, p. a10_137.pub3. doi: 10.1002/14356007.a10_137.pub3.
[131] E. S. Souza, L. Zaramello, C. A. Kuhnen, B. da S. Junkes, R. A. Yunes, and V. E. F. Heinzen, "Estimating the Octanol/Water Partition Coefficient for Aliphatic Organic Compounds Using Semi-Empirical Electrotopological Index," *IJMS*, vol. 12, no. 10, pp. 7250–7264, Oct. 2011, doi: 10.3390/ijms12107250.

[132] I. Rebane, U. Mäeorg, U. Johanson, M. Ilisson, P. Piirimägi, and T. Tamm, "Kinetics of catalyzed dehydrocondensation of hydrogen functionalized siloxane," *J of Applied Polymer Sci*, vol. 139, no. 23, p. 52304, Jun. 2022, doi: 10.1002/app.52304.

[133] F. G. Bordwell, "Equilibrium acidities in dimethyl sulfoxide solution," *Acc. Chem. Res.*, vol. 21, no. 12, pp. 456–463, Dec. 1988, doi: 10.1021/ar00156a004.

[134] T. Sato and R. Buchner, "The cooperative dynamics of the H-bond system in 2-propanol/water mixtures: Steric hindrance effects of nonpolar head group," *J. Chem. Phys.*, vol. 119, no. 20, pp. 10789–10800, Nov. 2003, doi: 10.1063/1.1620996.

[135] S. Nakagawa, J. Xia, and N. Yoshie, "Quantifying the effects of cooperative hydrogen bonds between vicinal diols on polymer dynamics," *Soft Matter*, vol. 18, no. 6, pp. 1275–1286, 2022, doi: 10.1039/D1SM01747K.

[136] X.-Q. Dou, D. Zhang, C. Feng, and L. Jiang, "Bioinspired Hierarchical Surface Structures with Tunable Wettability for Regulating Bacteria Adhesion," *ACS Nano*, vol. 9, no. 11, pp. 10664–10672, Nov. 2015, doi: 10.1021/acsnano.5b04231.

[137] Y. Liu, S.-F. Yang, Y. Li, H. Xu, L. Qin, and J.-H. Tay, "The influence of cell and substratum surface hydrophobicities on microbial attachment," *Journal of Biotechnology*, vol. 110, no. 3, pp. 251–256, Jun. 2004, doi: 10.1016/j.jbiotec.2004.02.012.

[138] H. Ma, W. Qin, B. Guo, and P. Li, "Effect of plant tannin and glycerol on thermoplastic starch: Mechanical, structural, antimicrobial and biodegradable properties," *Carbohydrate Polymers*, vol. 295, p. 119869, Nov. 2022, doi: 10.1016/j.carbpol.2022.119869.

[139] W. Mussard, N. Kebir, I. Kriegel, M. Estève, and V. Semetey, "Facile and Efficient Control of Bioadhesion on Poly(dimethylsiloxane) by Using a Biomimetic Approach," *Angew. Chem. Int. Ed.*, vol. 50, no. 46, pp. 10871–10874, Nov. 2011, doi: 10.1002/anie.201101029.

[140] H. Honarkar, "Waterborne polyurethanes: A review," *Journal of Dispersion Science and Technology*, vol. 39, no. 4, pp. 507–516, Apr. 2018, doi: 10.1080/01932691.2017.1327818.

[141] F. Rodríguez-Reinoso, "Activated Carbon and Adsorption," in *Encyclopedia of Materials: Science and Technology*, Elsevier, 2001, pp. 22–34. doi: 10.1016/B0-08-043152-6/00005-X.

[142] L. Mivehi, S. Hajir Bahrami, and R. M. A. Malek, "Properties of polyacrylonitrile-*N* -(2-hydroxy) propyl-3-trimethylammonium chitosan chloride blend films and fibers," *J of Applied Polymer Sci*, vol. 109, no. 1, pp. 545–554, Jul. 2008, doi: 10.1002/app.28133.

[143] D. Hu, H. Wang, and L. Wang, "Physical properties and antibacterial activity of quaternized chitosan/carboxymethyl cellulose blend films," *LWT – Food Science and Technology*, vol. 65, pp. 398–405, Jan. 2016, doi: 10.1016/j.lwt.2015.08.033.

[144] A. Ahmad, S.-H. Li, and Z.-P. Zhao, "Insight of organic molecule dissolution and diffusion in cross-linked polydimethylsiloxane using molecular simulation," *Journal of Membrane Science*, vol. 620, p. 118863, Feb. 2021, doi: 10.1016/j.memsci.2020.118863.

ACKNOWLEDGMENTS

I hope this dissertation will not be my last lengthy writing endeavor. Only those who have written and completed a doctoral dissertation understand how valuable this process can be for both professional and personal development. Throughout this journey, there are companions who guide you and help you overcome challenges.

I would like to express my deepest gratitude to my principal supervisor, Prof. Tarmo Tamm, for granting me the freedom to experiment and write, placing immense trust in me, and allowing me to navigate the research world independently while continuously supporting and guiding me throughout these years. I am also profoundly thankful to my co-supervisor, Uno Mäeorg, for his generous support, warmth, and vast reservoir of ideas, opportunities, contacts, and infrastructure, along with his infectious enthusiasm and plan B-s. My academic journey at the Institute of Technology was greatly enhanced by supportive colleagues, both scientists and administrative staff, contributing to a stronger and more innovative institution. I am grateful to Karl Jakob Levin for sharing my journey with silicones, always being willing to help and experiment, and being truly collaborative. To Urmas Johanson for exemplary analytical thinking and discussions on the importance of details (and how some details can be completely irrelevant), and for teaching me clarity in writing. My sincere gratitude to our head of the IMS Lab, Professor Alvo Aabloo, for letting me decide my mode of action (simulations vs hands-on) therefore defining my first experience in academia, and his trust in me to tackle non-research-related activities from time to time enriched my perspectives in the academic and entrepreneurial world. I thank Mihkel Ilisson for guidance in kinetics and formulation, Artur Kaljo from the Institute of Chemistry for ^{1}H-NMR analysis and UT Chair of Analytical Chemistry for calculations in COSMO-RS. I would also like to express my gratitude to the scientists who have offered me assistance in exploring another scientific field: Prof. Tanel Tenson, İsmail Sarıgül, and *Viia Kõiv* for warmth, guidance, and exciting and fruitful discussions on microbiology and other life-related matters.

My supervisors and colleagues are an example of an impeccable way of doing science and supporting students around them, and I am grateful for the opportunity to have spent several years as their supervisee.

While we spend a significant portion of our days with colleagues, my family remains my foundation. I am thankful to my partner and our children for their unwavering support throughout my studies, encouraging me to give my best and to let go of the rest.

The topic of my research would not have emerged without the initiative and trust of Estelaxe OÜ in our research group, for which I am forever appreciative.

PUBLICATIONS

CURRICULUM VITAE

Name	Ingrid Rebane
Date of birth	31.03.1987
Citizenship	Estonian
Contact	ingrid.rebane@ut.ee, rebaneingrid@gmail.com

Education

2019–…	University of Tartu, doctoral studies in Engineering and Technology
2012–2019	University of Tartu, MSc in Materials Science, *cum laude*
2007–2012	University of Tartu, BSc in Materials Science
2003–2006	Pärnu Sütevaka Humanitaagümnaasium

Additional studies

2023	EIT Manufacturing STRADA (digitalization, innovation, entrepreneurship, sustainability)
04/2023	Intellectual property in Ph.D. Studies: Industrial Property
11–12/2023	EIT Manufacturing Doctoral School Winter School, 'Innovation Ecosystem & Business Design'

Employment in Academic Institutions

2019–2024	Junior Research Fellow in Materials Science Institute of Technology, University of Tartu
2019–2021	Project Assistant, Institute of Technology, Intelligent Materials and Systems Laboratory (IMS Lab)
03-11/2013, 2017–2023	Project-based Graduate Researcher, Institute of Technology, IMS Lab

Scholarships

2022	Dora Plus Short-term Mobility Scholarship
2023	Kristjan Jaagu Short Study Visits Scholarship
2023	EITM STRADA Women in Manufacturing Program

ELULOOKIRJELDUS

Nimi	Ingrid Rebane
Sünnikuupäev	31.03.1987
Kodakondsus	Eesti
Kontaktinfo	ingrid.rebane@ut.ee, rebaneingrid@gmail.com

Haridus

2019–…	Tartu Ülikool, doktoriõpe erialal ‘Tehnika ja tehnoloogia’
2012–2019	Tartu Ülikool, materjaliteadus, MSc *cum laude*
2007–2012	Tartu Ülikool, materjaliteaduses, BSc
2003–2006	Pärnu Sütevaka Humanitaagümnaasium

Täiendõpe

2023EIT	Manufacturing STRADA (tööstuse digitaliseerimine, jätkusuutlikkus, innovatsioon, ettevõtlus)
04/2023	Intellektuaalomand doktoriõppes: tööstusomand
11–12/2023	EIT Manufacturing Doktorikooli Talvekool, ‘Innovation Ecosystem & Business Design’

Töökogemus haridus- ja teadusasutustes

2019–2024	Materjaliteaduse nooremteadur, Tehnoloogiainstituut, Tartu Ülikool
2019–2021	Projektiassistent, Arukate materjalide ja seadmete labor (IMS Lab), Tehnoloogiainstituut, Tartu Ülikool
03–11/2013, 2017–2023	Project-based Graduate Researcher, IMS Lab

Stipendiumid

2022	DoRa Pluss lühiajalise õpirände stipendium
2023	Kristjan Jaagu nimeline õpirände stipendium
2023	EITM STRADA Women in Manufacturing stipendium

DISSERTATIONES TECHNOLOGIAE UNIVERSITATIS TARTUENSIS

1. **Imre Mäger**. Characterization of cell-penetrating peptides: Assessment of cellular internalization kinetics, mechanisms and bioactivity. Tartu 2011, 132 p.
2. **Taavi Lehto**. Delivery of nucleic acids by cell-penetrating peptides: application in modulation of gene expression. Tartu 2011, 155 p.
3. **Hannes Luidalepp**. Studies on the antibiotic susceptibility of *Escherichia coli*. Tartu 2012, 111 p.
4. **Vahur Zadin**. Modelling the 3D-microbattery. Tartu 2012, 149 p.
5. **Janno Torop**. Carbide-derived carbon-based electromechanical actuators. Tartu 2012, 113 p.
6. **Julia Suhorutšenko**. Cell-penetrating peptides: cytotoxicity, immunogenicity and application for tumor targeting. Tartu 2012, 139 p.
7. **Viktoryia Shyp**. G nucleotide regulation of translational GTPases and the stringent response factor RelA. Tartu 2012, 105 p.
8. **Mardo Kõivomägi**. Studies on the substrate specificity and multisite phosphorylation mechanisms of cyclin-dependent kinase Cdk1 in *Saccharomyces cerevisiae*. Tartu, 2013, 157 p.
9. **Liis Karo-Astover**. Studies on the Semliki Forest virus replicase protein nsP1. Tartu, 2013, 113 p.
10. **Piret Arukuusk**. NickFects–novel cell-penetrating peptides. Design and uptake mechanism. Tartu, 2013, 124 p.
11. **Piret Villo**. Synthesis of acetogenin analogues. Asymmetric transfer hydrogenation coupled with dynamic kinetic resolution of α-amido-β-keto esters. Tartu, 2013, 151 p.
12. **Villu Kasari**. Bacterial toxin-antitoxin systems: transcriptional cross-activation and characterization of a novel *mqsRA* system. Tartu, 2013, 108 p.
13. **Margus Varjak**. Functional analysis of viral and host components of alphavirus replicase complexes. Tartu, 2013, 151 p.
14. **Liane Viru**. Development and analysis of novel alphavirus-based multifunctional gene therapy and expression systems. Tartu, 2013, 113 p.
15. **Kent Langel**. Cell-penetrating peptide mechanism studies: from peptides to cargo delivery. Tartu, 2014, 115 p.
16. **Rauno Temmer**. Electrochemistry and novel applications of chemically synthesized conductive polymer electrodes. Tartu, 2014, 206 p.
17. **Indrek Must**. Ionic and capacitive electroactive laminates with carbonaceous electrodes as sensors and energy harvesters. Tartu, 2014, 133 p.
18. **Veiko Voolaid**. Aquatic environment: primary reservoir, link, or sink of antibiotic resistance? Tartu, 2014, 79 p.
19. **Kristiina Laanemets**. The role of SLAC1 anion channel and its upstream regulators in stomatal opening and closure of *Arabidopsis thaliana.* Tartu, 2015, 115 p.

20. **Kalle Pärn**. Studies on inducible alphavirus-based antitumour strategy mediated by site-specific delivery with activatable cell-penetrating peptides. Tartu, 2015, 139 p.
21. **Anastasia Selyutina**. When biologist meets chemist: a search for HIV-1 inhibitors. Tartu, 2015, 172 p.
22. **Sirle Saul**. Towards understanding the neurovirulence of Semliki Forest virus. Tartu, 2015, 136 p.
23. **Marit Orav**. Study of the initial amplification of the human papillomavirus genome. Tartu, 2015, 132 p.
24. **Tormi Reinson**. Studies on the Genome Replication of Human Papillomaviruses. Tartu, 2016, 110 p.
25. **Mart Ustav Jr**. Molecular Studies of HPV-18 Genome Segregation and Stable Replication. Tartu, 2016, 152 p.
26. **Margit Mutso**. Different Approaches to Counteracting Hepatitis C Virus and Chikungunya Virus Infections. Tartu, 2016, 184 p.
27. **Jelizaveta Geimanen**. Study of the Papillomavirus Genome Replication and Segregation. Tartu, 2016, 168 p.
28. **Mart Toots**. Novel Means to Target Human Papillomavirus Infection. Tartu, 2016, 173 p.
29. **Kadi-Liis Veiman**. Development of cell-penetrating peptides for gene delivery: from transfection in cell cultures to induction of gene expression *in vivo*. Tartu, 2016, 136 p.
30. **Ly Pärnaste**. How, why, what and where: Mechanisms behind CPP/cargo nanocomplexes. Tartu, 2016, 147 p.
31. **Age Utt**. Role of alphavirus replicase in viral RNA synthesis, virus-induced cytotoxicity and recognition of viral infections in host cells. Tartu, 2016, 183 p.
32. **Veiko Vunder**. Modeling and characterization of back-relaxation of ionic electroactive polymer actuators. Tartu, 2016, 154 p.
33. **Piia Kivipõld**. Studies on the Role of Papillomavirus E2 Proteins in Virus DNA Replication. Tartu, 2016, 118 p.
34. **Liina Jakobson**. The roles of abscisic acid, CO_2, and the cuticle in the regulation of plant transpiration. Tartu, 2017, 162 p.
35. **Helen Isok-Paas**. Viral-host interactions in the life cycle of human papillomaviruses. Tartu, 2017, 158 p.
36. **Hanna Hõrak**. Identification of key regulators of stomatal CO_2 signalling via O_3-sensitivity. Tartu, 2017, 260 p.
37. **Jekaterina Jevtuševskaja**. Application of isothermal amplification methods for detection of *Chlamydia trachomatis* directly from biological samples. Tartu, 2017, 96 p.
38. **Ülar Allas**. Ribosome-targeting antibiotics and mechanisms of antibiotic resistance. Tartu, 2017, 152 p.
39. **Anton Paier**. Ribosome Degradation in Living Bacteria. Tartu, 2017, 108 p.
40. **Vallo Varik**. Stringent Response in Bacterial Growth and Survival. Tartu, 2017, 101 p.

41. **Pavel Kudrin**. In search for the inhibitors of *Escherichia coli* stringent response factor RelA. Tartu, 2017, 138 p.
42. **Liisi Henno**. Study of the human papillomavirus genome replication and oligomer generation. Tartu, 2017, 144 p.
43. **Katrin Krõlov**. Nucleic acid amplification from crude clinical samples exemplified by *Chlamydia trachomatis* detection in urine. Tartu, 2018, 118 p.
44. **Eve Sankovski**. Studies on papillomavirus transcription and regulatory protein E2. Tartu, 2018, 113 p.
45. **Morteza Daneshmand**. Realistic 3D Virtual Fitting Room. Tartu, 2018, 233 p.
46. **Fatemeh Noroozi**. Multimodal Emotion Recognition Based Human-Robot Interaction Enhancement. Tartu, 2018, 113 p.
47. **Krista Freimann**. Design of peptide-based vector for nucleic acid delivery in vivo. Tartu, 2018, 103 p.
48. **Rainis Venta**. Studies on signal processing by multisite phosphorylation pathways of the *S. cerevisiae* cyclin-dependent kinase inhibitor Sic1. Tartu, 2018, 155 p.
49. **Inga Põldsalu**. Soft actuators with ink-jet printed electrodes. Tartu, 2018, 85 p.
50. **Kadri Künnapuu**. Modification of the cell-penetrating peptide PepFect14 for targeted tumor gene delivery and reduced toxicity. Tartu, 2018, 114 p.
51. **Toomas Mets**. RNA fragmentation by MazF and MqsR toxins of *Escherichia coli.* Tartu, 2019, 119 p.
52. **Kadri Tõldsepp**. The role of mitogen-activated protein kinases MPK4 and MPK12 in CO_2-induced stomatal movements. Tartu, 2019, 259 p.
53. **Pirko Jalakas**. Unravelling signalling pathways contributing to stomatal conductance and responsiveness. Tartu, 2019, 120 p.
54. **S. Sunjai Nakshatharan**. Electromechanical modelling and control of ionic electroactive polymer actuators. Tartu, 2019, 165 p.
55. **Eva-Maria Tombak**. Molecular studies of the initial amplification of the oncogenic human papillomavirus and closely related nonhuman primate papillomavirus genomes. Tartu, 2019, 150 p.
56. **Meeri Visnapuu**. Design and physico-chemical characterization of metal-containing nanoparticles for antimicrobial coatings. Tartu, 2019, 138 p.
57. **Jelena Beljantseva**. Small fine-tuners of the bacterial stringent response – a glimpse into the working principles of Small Alarmone Synthetases. Tartu, 2020, 104 p.
58. **Egon Urgard**. Potential therapeutic approaches for modulation of inflammatory response pathways. Tartu, 2020, 120 p.
59. **Sofia Raquel Alves Oliveira**. HPLC analysis of bacterial alarmone nucleotide (p)ppGpp and its toxic analogue ppApp. Tartu, 2020, 122 p.
60. **Mihkel Örd**. Ordering the phosphorylation of cyclin-dependent kinase Cdk1 substrates in the cell cycle. Tartu, 2021, 228 p.
61. **Fred Elhi**. Biocompatible ionic electromechanically active polymer actuator based on biopolymers and non-toxic ionic liquids. Tartu, 2021, 140 p.

62. **Liisi Talas**. Reconstructing paleo-diversity, dynamics and response of eukaryotes to environmental change over the Late-Glacial and Holocene period in lake Lielais Svētiņu using sedaDNA. Tartu, 2021, 118 p.
63. **Livia Matt**. Novel isosorbide-based polymers. Tartu, 2021, 118 p.
64. **Koit Aasumets**. The dynamics of human mitochondrial nucleoids within the mitochondrial network. Tartu, 2021, 104 p.
65. **Faiza Summer**. Development and optimization of flow electrode capacitor technology. Tartu, 2022, 109 p.
66. **Olavi Reinsalu**. Cancer-testis antigen MAGE-A4 is incorporated into extracellular vesiclesand is exposed to the surface. Tartu, 2022, 130 p.
67. **Tetiana Brodiazhenko**. RelA-SpoT Homolog enzymes as effectors of Toxin-Antitoxin systems. Tartu, 2022, 132 p.
68. **Georg-Marten Lanno**. Development of novel antibacterial drug delivery systems as wound scaffolds using electrospinning technology. Tartu, 2022, 175 p.
69. **Liubov Cherkashchenko**. New insights into alphaviral nsP2 functions. Tartu, 2023, 171 p.
70. **Kristina Kiisholts**. Peptide-based drug carriers and preclinical nanomedicine applications for endometriosis treatment. Tartu, 2023, 138 p.
71. **Kai Rausalu**. Alphaviral nsP2 protease: From requirements for functionality to inhibition. Tartu, 2023, 175 p.
72. **Laura Sandra Lello**. Unraveling the intricate nature of the alphavirus RNA replicase. Tartu, 2023, 219 p.
73. **Houman Masnavi**. Visibility Aware Navigation. Tartu, 2023, 180 p.
74. **Kadir Aktas**. Cosmic Ray Tomography based Object Reconstruction and Recognition. Tartu, 2023, 104 p.
75. **Egils Avots**. Brain abnormality detection using statistical analysis of individual structural connectivity networks and EEG signals. Tartu, 2023, 223 p.
76. **Sainan Wang**. Structure-guided insights into the functions of CHIKV nsP2. Tartu, 2024, 154 p.
77. **Anneli Samel**. Unveiling the characteristics of cancer-testis antigen MAGEA10. Tartu, 2024, 136 p.
78. **Ikechukwu Ofodile**. Fault tolerant attitude control for nanosatellites: ESTCube-2 case. Tartu, 2024, 130 p.
79. **Olena Zamora**. Impacts of plant hormones on controlling stomatal conductance. Tartu, 2024, 166 p.
80. **Mariliis Hinnu**. *In vitro* methods for studying the mechanisms of ribosome-targeting antibiotics. Tartu, 2024, 143 p.
81. **Chung-Yueh Yeh**. Characterization of MPK and HT1 kinases in CO_2-induced stomatal movements. Tartu, 2024, 118 p.
82. **Iman Dadras**. Low power neural network-based control and actuation solutions for insect-scale robots. Tartu, 2024, 149 p.
83. **Fatemeh Rastgar**. Towards reliable real-time trajectory optimization. Tartu, 2024, 158 p.

84. **Maria Maloverjan**. Optimizing cell-penetrating peptide-based nanoparticles for delivery of nucleic acid therapeutics. Tartu, 2024, 172 p.
85. **Joonas Merisalu**. Resistive switching in memristor structures with multilayer dielectrics. Tartu, 2024, 149 p.
86. **Siim Laanesoo**. Novel high-performance biomass-based polymers. Tartu, 2024, 117 p.
87. **Henri Ingelman**. Systems-level characterisation and improvement of *Clostridium autoethanogenum* metabolism. Tartu, 2024, 164 p.
88. **Mailis Laht**. Using the One Health approach for mapping the spread of antibiotic resistant bacteria in Estonia. Tartu, 2024, 188 p.